



# GRAĐEVINSKI MATERIJALI I KONSTRUKCIJE

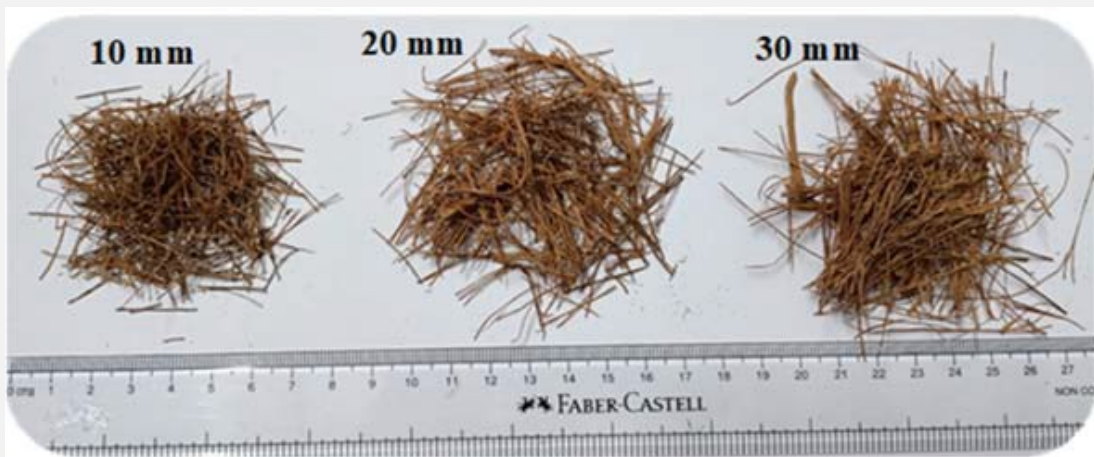
## BUILDING MATERIALS AND STRUCTURES

Volume 65  
March 2022

ISSN 2217-8139 (Print)  
ISSN 2335-0229 (Online)  
UDK: 06.055.2:62-  
03+620.1+624.001.5(49  
7.1)=861

1

Society for Materials and Structures Testing of Serbia  
University of Belgrade Faculty of Civil Engineering  
Association of Structural Engineers of Serbia





**CONTENTS**

Vedran Carević, Ivan Ignjatović <b>Limit values of accelerated carbonation resistance to meet EC2 durability requirements</b> <b>Original scientific paper</b> .....	1
Vijayalakshmi Ramalingam, Keerthika Ramesh, Modhagapriyan Arumugam, Vaishnavi Muralidharan <b>Effect of natural fish tail palm fiber on the workability and mechanical properties of fiber reinforced concrete</b> <b>Original scientific paper</b> .....	7
Nemanja Miljković, Mladen Milićević, Svetlana Ristić, Darko Popović, Vanja Alendar <b>Kula Belgrade – Part 2 - Specifics of construction of Kula structure</b> <b>Technical paper</b> .....	23
Dr. Jochen Buhler, Danijel Vilotijević <b>Improving the punching shear and shear capacity of reinforced concrete elements with a new post-installed retrofitting system</b> <b>Technical paper</b> .....	37
Instructions for authors .....	46

**EDITORIAL BOARD**

**Editor-in-Chief**

Professor **Snežana Marinković**  
University of Belgrade, Faculty of Civil Engineering, Institute  
for Materials and Structures, Belgrade, Serbia  
e-mail: [sneska@imk.grf.bg.ac.rs](mailto:sneska@imk.grf.bg.ac.rs)

**Deputy Editor-in-Chief**

Professor **Mirjana Malešev**  
University of Novi Sad, Faculty of Technical Sciences,  
Department of Civil Engineering, Novi Sad, Serbia  
e-mail: [miram@uns.ac.rs](mailto:miram@uns.ac.rs)

**Members**

Professor **Jose M. Adam**  
ICITECH, Universitat Politècnica de Valencia, Valencia,  
Spain

Dr **Ksenija Janković**  
Institute for Testing Materials – Institute IMS, Belgrade,  
Serbia

Professor Emerita **Dubravka Bjegović**  
University of Zagreb, Faculty of Civil Engineering,  
Department of materials, Zagreb, Croatia

Professor Academician **Yatchko P. Ivanov**  
Bulgarian Academy of Sciences, Institute of Mechanics,  
Sofia, Bulgaria

Professor **Tatjana Isaković**  
University of Ljubljana, Faculty of Civil and Geodetic  
Engineering, Ljubljana, Slovenia

Professor **Michael Forde**  
University of Edinburgh, Institute for Infrastructure and  
Environment, School of Engineering, Edinburgh, United  
Kingdom

Professor **Vlastimir Radonjanin**  
University of Novi Sad, Faculty of Technical Sciences,  
Department of Civil Engineering, Novi Sad, Serbia

**Predrag L. Popovic**  
Vice President, Wiss, Janney, Elstner Associates, Inc.,  
Northbrook, Illinois, USA

Professor **Zlatko Marković**  
University of Belgrade, Faculty of Civil Engineering,  
Institute for Materials and Structures, Belgrade, Serbia

Professor **Vladan Kuzmanović**  
University of Belgrade, Faculty of Civil Engineering,  
Belgrade, Serbia

Professor Emeritus **Valeriu A. Stoian**  
University Politehnica of Timisoara, Department of Civil  
Engineering, Research Center for Construction  
Rehabilitation, Timisoara, Romania

Dr **Vilma Ducman**  
Head of Laboratory for Cements, Mortars and  
Ceramics, Slovenian National Building and Civil  
Engineering Institute, Ljubljana, Slovenia

Assistant Professor **Ildiko Merta**  
TU Wien, Faculty of Civil Engineering, Institute of  
Material Technology, Building Physics, and Building  
Ecology, Vienna, Austria

Associate Professor **Ivan Ignjatović**  
University of Belgrade, Faculty of Civil Engineering,  
Institute for Materials and Structures, Belgrade, Serbia

Professor **Meri Cvetkovska**  
University "St. Kiril and Metodij", Faculty of Civil  
Engineering, Skopje, Macedonia

Dr **Anamaria Feier**  
University Politehnica of Timisoara, Department for  
Materials and Manufacturing Engineering, Timisoara,  
Romania

Associate Professor **Jelena Dobrić**  
University of Belgrade, Faculty of Civil Engineering,  
Institute for Materials and Structures, Belgrade, Serbia

Dr **Vladimir Gocevski**  
Hydro-Quebec, Mécanique, structures et architecture,  
Ingénierie de production, Montréal (Québec), Canada

Dr **Nikola Tošić**  
MSCA Individual Fellow, Civil and Environmental  
Engineering Department, Universitat Politècnica de  
Catalunya (UPC), Barcelona, Spain

Assistant Professor **Ehsan Noroozinejad Farsangi**  
Earthquake Engineering Department, Graduate  
University of Advanced Technology, Iran

Secretary:

**Slavica Živković**, Master of Economics  
Society for Materials and Structures Testing of Serbia, 11000 Belgrade, Kneza Milosa 9  
Telephone: 381 11/3242-589; e-mail: [office@dimk.rs](mailto:office@dimk.rs), web sajt: [www.dimk.rs](http://www.dimk.rs)

English editing:

Professor **Jelisaveta Šafranč**, University of Novi Sad, Faculty of Technical Sciences, Novi Sad, Serbia

Technical support:

**Stoja Todorović**, e-mail: [saska@imk.grf.bg.ac.rs](mailto:saska@imk.grf.bg.ac.rs)

## Aims and scope

Building Materials and Structures aims at providing an international forum for communication and dissemination of innovative research and application in the field of building materials and structures. Journal publishes papers on the characterization of building materials properties, their technologies and modeling. In the area of structural engineering Journal publishes papers dealing with new developments in application of structural mechanics principles and digital technologies for the analysis and design of structures, as well as on the application and skillful use of novel building materials and technologies.

The scope of Building Materials and Structures encompasses, but is not restricted to, the following areas: conventional and non-conventional building materials, recycled materials, smart materials such as nanomaterials and bio-inspired materials, infrastructure engineering, earthquake engineering, wind engineering, fire engineering, blast engineering, structural reliability and integrity, life cycle assessment, structural optimization, structural health monitoring, digital design methods, data-driven analysis methods, experimental methods, performance-based design, innovative construction technologies, and value engineering.

<b>Publishers</b>	Society for Materials and Structures Testing of Serbia, Belgrade, Serbia, veb sajt: <a href="http://www.dimk.rs">www.dimk.rs</a> University of Belgrade Faculty of Civil Engineering, Belgrade, Serbia, <a href="http://www.grf.bg.ac.rs">www.grf.bg.ac.rs</a> Association of Structural Engineers of Serbia, Belgrade, Serbia, <a href="http://dgks.grf.bg.ac.rs">dgks.grf.bg.ac.rs</a>
<b>Print</b>	Razvojno istraživački centar grafičkog inženjerstva, Belgrade, Serbia
<b>Edition</b>	quarterly
<b>Peer reviewed journal</b>	
<b>Journal homepage</b>	<a href="http://www.dimk.rs">www.dimk.rs</a>
<b>Cover</b>	<b>Cut fish tail palm fibers of different length (up), Failure pattern of fiber reinforced cylinder and beam specimen (down)</b> , from <i>Effect of natural fish tail palm fiber on the workability and mechanical properties of fiber reinforced concrete</i> by Vijayalakshmi Ramalingam, Keerthika Ramesh, Modhagapriyan Arumugam and Vaishnavi Muralidharan
<b>Financial support</b>	Ministry of Education, Science and Technological Development of Republic of Serbia University of Belgrade Faculty of Civil Engineering Institute for testing of materials-IMS Institute, Belgrade Faculty of Technical Sciences, University of Novi Sad, Department of Civil Engineering Serbian Chamber of Engineers

CIP - Каталогизacija y publikaciji  
Narodna biblioteka Srbije, Beograd

620.1

**GRAĐEVINSKI materijali i konstrukcije** = Building materials and structures / editor-in-chief Snežana Marinković  
. - God. 54, br. 3 (2011)- . - Belgrade : Society for Materials and Structures Testing of Serbia : University of Belgrade, Faculty of Civil Engineering : Association of Structural Engineers of Serbia, 2011- (Belgrade : Razvojno istraživački centar grafičkog inženjerstva). - 30 cm

Tromesečno. - Je nastavak: Materijali i konstrukcije  
= ISSN 0543-0798. - Drugo izdanje na drugom medijumu:  
Građevinski materijali i konstrukcije (Online) = ISSN 2335-0229  
ISSN 2217-8139 = Građevinski materijali i konstrukcije  
COBISS.SR-ID 188695820



Original scientific paper

## Limit values of accelerated carbonation resistance to meet EC2 durability requirements

Vedran Carević<sup>\*1)</sup>, Ivan Ignjatović<sup>1)</sup><sup>1)</sup> University of Belgrade, Faculty of Civil Engineering, Department for Materials and Structures, Bulevar kralja Aleksandra 73, 11000 Belgrade, Serbia

### Article history

Received: 21 January 2022

Received in revised form:

22 February 2022

Accepted: 28 February 2022

Available online: 31 March 2022

### Keywords

durability,  
exposure classes,  
carbonation resistance,  
concrete cover,  
service life

### ABSTRACT

Although accelerated carbonation resistance has been extensively tested, there are no recommendations for the application of test results in codes of practice. The main objective of this study was to determine the limit values of accelerated carbonation resistance to satisfy the required service life of reinforced concrete structures with concrete covers as prescribed in EN 1992-1-1. The service life of 50 years was considered, as well as all carbonation exposure classes (from XC1 to XC4). A full probabilistic analysis was conducted using the fib-Bulletin 34 carbonation prediction model. Using the limit state function and a defined reliability index, the upper limits of the inverse effective carbonation resistance ( $R^{-1}_{ACC}$ ) for all exposure classes and in a function of concrete cover depth were determined. The determined values of  $R^{-1}_{ACC}$  presented in this study represent the upper limit of the average value, as well as the maximum deviation of one sample in relation to this average value. Thus, a simple assessment of concrete quality is allowed in terms of carbonation resistance based on the accelerated carbonation depth measurements.

## 1 Introduction

Concrete is considered a building material with good durability properties. However, cases of insufficient service life are not uncommon [1]. The main reason for the deterioration of reinforced concrete (RC) structures is the corrosion of steel reinforcement. Reinforcement is protected by the surrounding concrete, which is a highly alkaline environment with a pH value of approximately 13 [2]. This ensures chemical protection of steel reinforcement with a thin oxide (passivation) layer. Carbonation-induced corrosion has been reported as a major durability problem in the urban environment, considering the large number of buildings that are exposed to a CO<sub>2</sub>-rich environment [3]. Carbonation is the process by which CO<sub>2</sub> from the atmosphere enters concrete pores and reacts with the alkalis in the concrete matrix (Ca(OH)<sub>2</sub>), lowering the pH of the concrete. When the pH value of concrete drops below 9, the chemical protection of the reinforcement will be degraded, and reinforcement corrosion can start [2].

The carbonation depth in natural conditions directly influences the concrete cover depth required for the desired service life [4]. Since natural carbonation is a very slow process, measured in years, carbonation resistance is usually determined based on accelerated carbonation tests. There are several ways to accelerate the carbonation process (increase in air pressure or temperature), but the most commonly used method is to increase the CO<sub>2</sub> concentration. This increase is done in specialized chambers, where the concentration of CO<sub>2</sub> can be up to a

thousand times higher than in natural conditions. In different standards and technical recommendations, a great variety of CO<sub>2</sub> concentrations are prescribed, ranging from 1% to 50% [5]. It has been shown that under a CO<sub>2</sub> concentration of 2%, as proposed by the fib-Bulletin 34 [6], there will be no significant difference between the natural and accelerated carbonation processes [7,8]. There will be a difference in carbonation depth when comparing natural and accelerated carbonation, but the kinetics of the process will not change (there will be no increase in humidity and the formation of different compounds). This is important because fib-Bulletin 34 [6] allows the use of accelerated carbonation depth for the prediction of natural carbonation depth over time using the proposed prediction model.

Although accelerated carbonation resistance has been extensively tested, there are no recommendations for the application of test results in codes of practice, such as EN 1992-1-1 [9]. In current codes, the durability of concrete is ensured by a sufficient concrete cover and prescribed composition or compressive strength [10]. A concrete cover is defined for each exposure class to carbonation and service life duration. Also, the minimum concrete strength classes that can be used for certain exposure classes are defined. The prescribed composition (minimum amount of cement and maximum water-cement ratio) of concrete is only a recommendation in SRPS U.M1 206-1 [10]. Having in mind the increasing use of concrete with recycled and waste materials, pozzolanic cements, as well as the use of fillers that reduce the amount of cement in concrete, this recommendation is not adequate. Different concrete types,

<sup>\*</sup> Corresponding author:E-mail address: [vedran@imk.grf.bg.ac.rs](mailto:vedran@imk.grf.bg.ac.rs)

although belonging to the same strength classes, do not have the same durability properties, and vice versa [4]. Also, prescribing the minimum amount of cement is not in line with the agenda of reducing CO<sub>2</sub> emissions in the construction industry [11]. The cement industry causes approximately 7–10% of all anthropogenic origin CO<sub>2</sub> emissions [12], which impacts the environment and causes significant greenhouse gas emissions.

On the other hand, there is no carbonation resistance criteria defined in SRPS U.M1 206-1 [10], as defined for other durability related properties such as chloride ingress, freeze-thaw effect, and water permeability. Therefore, the limit values of characteristic parameters should be defined so that each concrete must satisfy these requirements during the accelerated testing in order to meet the requirements of the prescribed service life with the prescribed concrete covers.

## 2 Objectives and Methodology

Concrete carbonation resistance has already been the topic of many studies, but the use of test results to determine concrete cover depth according to EN 1992-1-1 [9] is still unknown. Therefore, the objective of this study was to determine the limit values of accelerated carbonation resistance to satisfy the required service life of RC structures for different exposure classes prescribed in EN 1992-1-1 [9]. The standard S4 structural class defined in EN 1992-1-1 [9] was considered corresponding to a service life of 50 years, as well as all exposure classes to carbonation (from XC1 to XC4).

In order to define the concrete resistance that corresponds to prescribe concrete cover, it is necessary to know the development of carbonation depth over time under natural exposure conditions. For that purpose, *fib*-Bulletin 34 [6] was used:

$$x_c(t) = \sqrt{2 \cdot k_e \cdot k_c \cdot (k_t \cdot R_{ACC}^{-1} + \varepsilon_t) \cdot C_s \cdot t \cdot W(t)} \quad (1)$$

where,  $x_c(t)$  is carbonation depth at the time  $t$  [mm],  $k_e$  is environmental function [-],  $k_c$  is execution transfer parameter [-],  $k_t$  is regression parameter with average value of 1.25 [-],  $R_{ACC}^{-1}$  is inverse effective carbonation resistance of concrete [(mm<sup>2</sup>/year)/(kg/m<sup>3</sup>)],  $\varepsilon_t$  is error term with average value of 315.5 [(mm<sup>2</sup>/year)/(kg/m<sup>3</sup>)],  $C_s$  is CO<sub>2</sub> concentration [kg/m<sup>3</sup>] and  $W(t)$  is weather function [-].

The *fib*-Bulletin 34 [6] was chosen because it allows the carbonation depth to be obtained while taking into account both the environment and curing conditions and concrete properties. A previously formed database [4] was used. *Fib*-Bulletin 34 [6] proposed an accelerated test with a CO<sub>2</sub> concentration of 2% for 28 days. If a different CO<sub>2</sub> concentration is used, for example, the new European standard for accelerated carbonation resistance EN 12390-12 [14] specifies a CO<sub>2</sub> concentration of 3% for 70 days,  $R_{ACC}^{-1}$  values can be calculated using the expression defined in the LIFECON D 3.2 Service Life Models project [13]:

$$R_{ACC}^{-1} = \left( \frac{x_c}{\sqrt{2 \cdot C_s \cdot t}} \right)^2 \quad (2)$$

where,  $x_c$  is the average carbonation depth (m),  $C_s$  is CO<sub>2</sub> concentration (kg/m<sup>3</sup>) and  $t$  is the duration (s) of the accelerated carbonation test. The use of Eq. (2) enables the

use of the results of any accelerated carbonation test for calculation of  $R_{ACC}^{-1}$  [8].

## 3 Definition of parameters for the probabilistic approach of service life design

The important aspect in selecting the prediction model (*fib* model) is the nature of the input data. If parameters are treated as continuous stochastic variables, defined by mean values, standard deviations, and probabilistic density functions, the model is probabilistic. A fully probabilistic approach makes it possible to determine the service life that is characterized by a defined probability of failure. Therefore, it was decided to apply the fully probabilistic approach in this study. Based on this, it is possible to define the limit state function of reinforcement depassivation caused by carbonation as follows:

$$g(c, x_c(t)) = c - x_c(t) = c - \sqrt{2 \cdot k_e \cdot k_c \cdot (k_t \cdot R_{ACC}^{-1} + \varepsilon_t) \cdot C_s \cdot t \cdot W(t)} \quad (3)$$

where  $c$  is concrete cover (mm).

The value of the nominal concrete cover is usually chosen in terms of the environment in which the concrete will be used. The corresponding design value for different exposure classes is defined in EN 1992-1-1 [9]. Although strictly determined, its actual value in practice varies due to the inevitable irregularities that occur during the construction phase. Therefore, this parameter should be considered as a stochastic variable instead of a constant value. However, for the calculation of service life from a durability point of view, instead of nominal concrete cover, which is a stochastic variable, the minimum concrete cover from durability conditions ( $c_{min,dur}$ ) should be used. This depth is a deterministic value and represents the minimum concrete cover depth necessary in order to achieve the desired service life. In EN 1992-1-1 [9] a minimum concrete cover in the range of 15 to 30 mm is prescribed for exposure classes from XC1 to XC4, for a standard S4 structural class corresponding to a service life of 50 years. The final (nominal) value of the concrete cover ( $c_{nom}$ ) will be increased by a typical standard deviation for concrete covers ( $\Delta c_{dev}$ ), which depends on the type and quality of execution works:

$$c_{nom} = c_{min,dur} + \Delta c_{dev} \quad (4)$$

To solve the limit state function, it is necessary to define certain parameters, first of all the exposure conditions. The mean atmospheric CO<sub>2</sub> concentration ( $C_s$ ) was estimated by the *fib*-Bulletin 34 [6] as 0.00082 kg/m<sup>3</sup> or 0.05% by volume, taking into account that the current value will increase even more (due to the greenhouse gas effect). According to some data [13], the standard deviation is fairly constant at 0.0001 kg/m<sup>3</sup>.

The execution transfer parameter ( $k_c$ ) takes into account the influence of concrete curing conditions on the carbonation resistance. All measures taken to prevent premature concrete drying (water treatment, air conditioning while the surface of the concrete is covered, etc.) are considered to guarantee proper curing. The execution transfer parameter is defined as:

$$k_{cur} = \left( \frac{t_c}{7} \right)^{b_c} \quad (5)$$

where,  $t_c$  is period of curing (days), and  $b_c$  is regression exponent (-).

It should be emphasized that the value of the exponent  $b_c$  in Eq. (5) can vary depending on the type of concrete. For instance, a slow pozzolanic reaction of fly ash may require longer curing time in order to achieve the highest possible carbonation resistance. Van Den Heede [16] noted that, for concrete with fly ash, the recommended values proposed in *fib*-Bulletin 34 [6] can still be used. The mean value (-0.567), standard deviation (0.024) and normal distribution have been adopted for the  $b_c$  exponent. The curing period ( $t_c$ ) of 7 days was adopted because it is assumed that this is the standard time of curing on site, as well as the curing time prescribed in *fib*-Bulletin 34 [6] for the accelerated carbonation test.

The environmental function ( $k_e$ ) takes into account the influence of natural relative humidity ( $RH_{real}$ ) on carbonation depth:

$$k_e = \left( \frac{1 - (RH_{real} / 100)^{f_c}}{1 - (RH_{ref} / 100)^{f_c}} \right)^{g_c} \quad (6)$$

where,  $RH_{real}$  is environment relative humidity (%),  $RH_{ref}$  is referent relative humidity (%),  $f_c$  is exponent (-) and  $g_c$  is exponent (-).

As proposed in the *fib*-Bulletin 34 [6], parameter  $k_e$  represent the relative humidity of the carbonated concrete, instead of the environmental humidity. Due to the fact that these data are not easily available and that the carbonation process takes place only in the concrete surface layer, it is reasonable to use the values of environmental relative humidity. Such data for  $RH_{real}$  is usually collected from the meteorological stations near the site location. Since the lower relative humidity limit is significantly different from zero and the upper limit is 100%, it is appropriate to assume that these parameters are beta-distributed with the upper and lower limits. In this study, a lower limit of 40% and an upper

limit of 100% were adopted. An assessment of relative humidity and distribution parameters for particular exposure classes, has been carried out in accordance with the descriptions that can be found in EN 1992-1-1 [9] and relevant studies [13]. Adopted values are presented in Table 1.

Certain specificities existed only within the classes XC1 and XC4. For the XC4 class, wetting and drying cycles were presented through a large standard deviation (16%), where as the mean value was taken based on recommendations from the literature [6,13,17]. The XC1 class represents two opposite exposure conditions: completely wet or completely dry. The relationship between the carbonation depth and relative humidity is a parabolic curve, with a maximum of 50% to 60% RH [18–20]. In other words, the carbonation depth under dry or extremely high humidity conditions should be similar. This is based on a physical model of the carbonation process. Under dry conditions, the CO<sub>2</sub> available in the air cannot be dissolved in pores (due to a lack of humidity), which slows down the carbonation process. On the other hand, under extremely high humidity, CO<sub>2</sub> cannot diffuse through the saturated pore solution, which also slows down the carbonation process. The environmental function should reflect the nature of the process. However, parameter  $k_e$ , as already emphasized, represents the relative humidity of the carbonated concrete layer rather than the relative humidity of the environment. According to Eq. (6), the value of the parameter  $k_e$  under dry conditions is up to 36% higher compared with conditions of moderate humidity ( $RH = 65\%$ ). This causes a problem in determining the service life under dry conditions. Since the XC1 class defines structures under dry or extremely high humidity conditions, a high relative humidity of 92% [13] was used to determine the concrete service life for this class. This will lead to more reliable results for the XC1 exposure class. The adopted beta distribution functions for all exposure classes are presented in Figure 1.

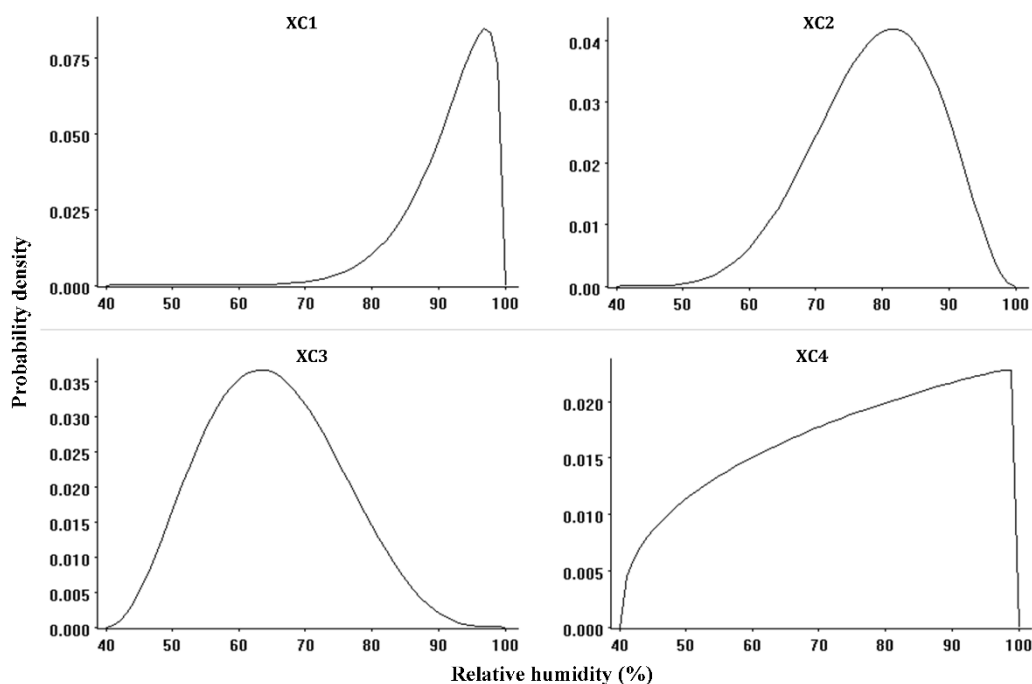


Figure 1. The beta distributions with adopted parameters for all exposure classes [21]

Table 1. Input parameters of the limit state function for service life prediction

Parameter	Distribution	$\mu$	$\sigma$	Unit
$C_{min,dur}$	XC1	Constant	15	–
	XC2	Constant	25	–
	XC3	Constant	25	–
	XC4	Constant	30	–
$RH_{real}$	XC1	Beta	92 (40*)	6 (100*)
	XC2	Beta	79 (40*)	9 (100*)
	XC3	Beta	65 (40*)	10 (100*)
	XC4	Beta	75 (40*)	16 (100*)
$RH_{ref}$	Constant	65	–	%
$f_c$	Constant	5.0	–	–
$g_c$	Constant	2.5	–	–
$t_c$	Constant	7	–	days
$b_c$	Normal	–0.567	0.024	–
$C_s$	Normal	0.0008	0.0001	kg/m <sup>3</sup>
$t$	Constant	50	–	year
$k_t$	Normal	1.25	0.35	–
$\varepsilon_t$	Normal	315.5	48	(mm <sup>2</sup> /year)/(kg/m <sup>3</sup> )
$R^{-1}_{ACC}$	Normal	variable	CoV 10%	(mm <sup>2</sup> /year)/(kg/m <sup>3</sup> )

\* Lower and upper limit of the beta distribution

The mean values for  $k_t$  and  $\varepsilon_t$  and their distribution functions are proposed in the *fib*-Bulletin 34 [6]. For the weather function, it was adopted that the concrete was sheltered from rain in order to obtain the maximum carbonation depth (the most unfavourable case). The only unknown parameter in this limit state function is the inverse effective carbonation resistance ( $R^{-1}_{ACC}$ ). Since the determination of the limit value was the subject of this study, the value of  $R^{-1}_{ACC}$  was varied. A normal distribution with a coefficient of variation (CoV) of 10% was used.

Overviews of the applied distributions (mean value, standard deviation, lower and upper bound) for each of the input parameters of the limit state function are shown in Table 1.

The reliability index ( $\beta$ ) and the probability of failure ( $P_f$ ) associated with the limit state function (Eq. (3)) was calculated using the *First Order Reliability Method* (FORM). According to the *fib*-Bulletin 34[6], in order to qualify concrete for use, the reliability index must meet the requirements for the depassivation limit state ( $\beta \geq 1.3$ ), which corresponds to  $P_f \leq 0.10$ .

#### 4 Results and discussions

The relationship between the reliability index and  $R^{-1}_{ACC}$  is shown in Figure 2 for all carbonation exposure classes.

Using a defined reliability index ( $\beta \geq 1.3$ ), the maximum values of the inverse effective carbonation resistance for all exposure classes were determined, assuming the minimum concrete cover for each exposure class given in [9]. Since  $R^{-1}_{ACC}$  represents the inverse carbonation resistance, an increase in the coefficient represents a decrease in the resistance and vice versa. Therefore, the upper limit of the  $R^{-1}_{ACC}$  value was determined. The relationship between exposure classes and the inverse effective carbonation resistance for the service life of 50 years is shown in Table 2. The values in Table 2 represent the average value of the

upper limit that needs to be achieved, as well as the maximum deviation of the individual sample. The maximum deviation of an individual sample was determined based on CoV of 10%.

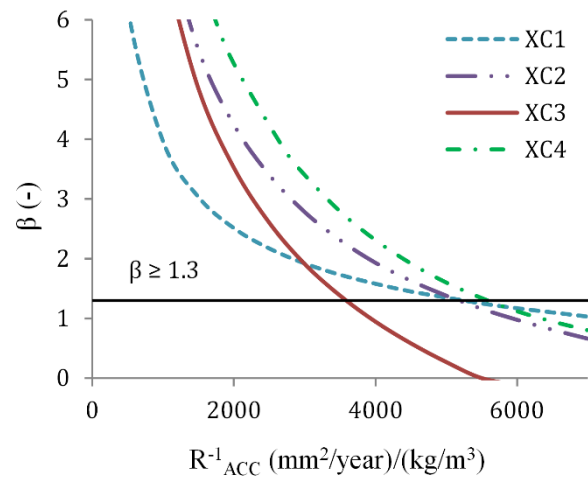


Figure 2. The relationship between reliability index and  $R^{-1}_{ACC}$

As previously mentioned, extreme environments (very high or low humidity) slow down the carbonation reaction considerably. For the exposure class XC1, which represents a very dry or humid environment, the allowed average value is 5200 (mm<sup>2</sup>/year)/(kg/m<sup>3</sup>). Although the exposure class XC2 represents a more aggressive carbonation environment, a similar value (5150 (mm<sup>2</sup>/year)/(kg/m<sup>3</sup>)) was determined. The reason was the higher concrete cover depth prescribed in EN 1992-1-1 [9] for exposure class XC2 compared to XC1 (see Table 1). Exposure class XC3 represents a moderate humidity environment, and as such,

is most suitable for carbonation development. It is therefore not surprising that the lowest value of the inverse effective carbonation resistance is obtained for the XC3 exposure class. Also, the prescribed concrete cover depth (25 mm) is the same as for exposure class XC2, which represents a less harsh environment.

Table 2. Average and maximum values of  $R^{-1}_{ACC}$  for different carbonation exposure classes

Exposure class	$R^{-1}_{ACC}(\text{mm}^2/\text{year})/(\text{kg}/\text{m}^3)$	
	Average	Maximum
XC1	< 5200	5700
XC2	< 5150	5650
XC3	< 3600	3950
XC4	< 5600	6150

Although wet and dry cycles prolong the depassivation time, the constant change in relative humidity leads to an increase in the corrosion rate during the propagation phase [21] and therefore the highest inverse effective carbonation resistance for XC4 exposure class. However, EN 1992-1-1 [9] as well as the fib-Bulletin 34 [6] define service life only through the depassivation phase, not taking into account the propagation period in the service life calculation. The question arises as to whether this concept of prescribing a concrete cover depth for this exposure class (wet and dry cycles) has potentially considered the propagation period. This could open the possibility of considering one part of the propagation period in defining the service life of RC structures.

In addition to the upper limits of  $R^{-1}_{ACC}$  for concrete covers defined in EN 1992-1-1 [9], an analysis was also performed for concrete covers in a range of 10-40 mm, Table 3. This allows the determination of the required concrete cover depth for a defined exposure class based on the concrete carbonation resistance tested by accelerated carbonation tests. On the contrary, for the determined carbonation resistance, the table provides the necessary

concrete cover. The higher the concrete carbonation resistance, the smaller the concrete cover is required and vice versa. This is in line with the service life design concept.

When comparing values within the same concrete cover depth ( $c_{min}$ ), the highest values of  $R^{-1}_{ACC}$  were obtained for exposure class XC1. These values are several times higher compared to other exposure classes, regardless of the concrete cover depth. This was expected, given that this exposure class represents the least aggressive environment.  $R^{-1}_{ACC}$  values for exposure class XC2 were approximately three times lower than those for exposure class XC1. For exposure classes XC3 and XC4, the values were similar regardless of the concrete cover depth. The values of  $R^{-1}_{ACC}$  for exposure class XC3 were up to 8% lower compared to XC4. Having this in mind, the concrete cover depth for these two exposure classes should be the same.

As already mentioned, the  $R^{-1}_{ACC}$  values presented in Table 3 are calculated based on the measured carbonation depth under accelerated conditions. For practical application, the expected average values of accelerated carbonation depth ( $x_c$ ) after 28 days under 2% CO<sub>2</sub> were calculated and shown in Table 4. These values are indicative because they are the result of probabilistic analysis, which implies certain assumptions, especially in terms of relative humidity and their distribution functions. However, this approach enables us to have an indication of the concrete quality in terms of carbonation resistance as well as suitability for the designed exposure class and concrete cover immediately after the measurement of carbonation depth after the accelerated test.

Expected values of carbonation depth after 28 days of exposure to 2% CO<sub>2</sub> range between 1.5 mm and 15 mm, depending on the exposure class and the concrete cover depth. The use of other accelerated tests, such as EN 12390-12 [14], is also possible, but values in Table 4 must be recalculated using Eq. (2) according to the exposure conditions defined in that test (CO<sub>2</sub> concentration and test duration).

Table 3. Average values of  $R^{-1}_{ACC}$  ((mm<sup>2</sup>/year)/(kg/m<sup>3</sup>)) for different exposure classes and concrete covers ( $c_{min}$ )

Exposure class	$c_{min}$ (mm)						
	10	15	20	25	30	35	40
XC1	< 2100	< 5200	< 9500	< 15000	< 21500	< 29500	< 38500
XC2	< 650	< 1700	< 3200	< 5150	< 7500	< 10200	< 13500
XC3	< 400	< 1150	< 2200	< 3600	< 5200	< 7200	< 9500
XC4	< 430	< 1250	< 2350	< 3800	< 5600	< 7600	< 10000

Table 4. Expected average values of accelerated carbonation depth  $x_c$  (mm) after 28 days under 2% of CO<sub>2</sub> for different carbonation exposure classes and concrete covers

Exposure class	$c_{min}$ (mm)						
	10	15	20	25	30	35	40
XC1	< 3.4	< 5.4	< 7.3	< 9.2	< 11.0	< 12.8	< 14.7
XC2	< 1.9	< 3.1	< 4.2	< 5.4	< 6.5	< 7.6	< 8.7
XC3	< 1.5	< 2.5	< 3.5	< 4.5	< 5.4	< 6.3	< 7.3
XC4	< 1.6	< 2.6	< 3.6	< 4.6	< 5.6	< 6.5	< 7.5

## 5 Conclusions

Since carbonation has become an important issue in the durability analysis of RC structures, it was necessary to find a simple way in which the results of the accelerated carbonation test could be used in service life design. Therefore, the objective of this study was to determine the limit values of accelerated carbonation resistance to satisfy the required service life of RC structures with concrete covers as prescribed in EN 1992-1-1. The service life of 50 years was considered, as well as all carbonation exposure classes (from XC1 to XC4). A full probabilistic analysis was conducted using the *fib*-Bulletin 34 carbonation prediction model and FORM analysis. For the defined reliability index and minimum concrete cover depth defined by EN 1992-1-1, the upper limits of the inverse effective carbonation resistance for all exposure classes were determined (Table 2).

Also, values of  $R_{ACC}^{-1}$  for different exposure classes and for concrete covers in a range of 10-40 mm are calculated in Table 3. In this way, it is possible to adopt the required concrete cover depth for a defined exposure class, based on the concrete carbonation resistance, which is in line with the service life design concept. In addition to this, and taking the values of  $R_{ACC}^{-1}$  from Table 3, the carbonation depths after conducting accelerated tests were determined, which gives an early indication of concrete quality in terms of carbonation resistance (Table 4).

## Funding

This work was supported by the Ministry for Education, Science and Technology, Republic of Serbia [grant number 200092].

## References

- [1] B. Pailles, Effect of Cracking on Reinforced Concrete Corrosion, ACI Spring 2018 Conv. (2018). <https://www.concrete.org/education/freewebsessions/completelecturing/coursepreviews.aspx?ID=51713407> (accessed March 10, 2019).
- [2] V.G. Papadakis, M.N. Fardis, A reaction engineering approach to the problem of concrete carbonation, *Am. Inst. Chem. Eng.* 35 (1989) 1639–1651.
- [3] V. Carević, Ignjatović Ivan, Influence of Cracks on the Carbonation Resistance of Recycled Aggregate Concrete, in: E. Júlio, J. Valença, A.S. Louro (Eds.), *Proc. Fib Symp. Concr. Struct. New Trends Eco-Efficiency Perform.*, International Federation for Structural Concrete (fib), Lisbon, Portugal, 2021: pp. 422–431.
- [4] V. Carević, I. Ignjatović, Evaluation of concrete cover depth for green concretes exposed to carbonation, *Struct. Concr.* (2020). doi:10.1002/suco.202000086.
- [5] T.A. Harrison, G. Khanna, S. Kandasami, M.D. Newlands, M.R. Jones, Experience of using the prTS 12390-12 accelerated carbonation test to assess the relative performance of concrete, *Mag. Concr. Res.* 64 (2012) 737–747. doi:10.1680/mac.11.00162.
- [6] *fib*-Bulletin 34, Model Code for Service Life Design, 1st ed., International Federation for Structural Concrete (fib), Lausanne, Switzerland, 2006.
- [7] V. Carević, I. Ignjatović, Carbonation resistance of high volume fly ash concrete with accelerated tests (in Serbian), in: XXVII Congr. Int. Symp. Res. Appl. Contemp. Achiev. Civ. Eng. F. Mater. Struct., Society for materials and structures testing of Serbia, Vrsac, Serbia, 2017: pp. 211–220.
- [8] V. Carević, I. Ignjatović, J. Dragaš, Model for practical carbonation depth prediction for high volume fly ash concrete and recycled aggregate concrete, *Constr. Build. Mater.* 213 (2019) 194–208. doi:10.1016/j.conbuildmat.2019.03.267.
- [9] CEN, EN 1992-1-1, in: CEN (Ed.), 1st ed., ISS, Belgrade, 2015.
- [10] CEN, SRPS U.M1 206-1. Beton - Deo 1: Specifikacija, performanse, proizvodnja i usaglašenost, (2011) 81.
- [11] IEA, Technology Roadmap: Low-Carbon Transition in the Cement Industry, in: OECD/IEA.; WBCSD, France, 2018.
- [12] K.L. Scrivener, V.M. John, E.M. Gartner, Eco-efficient cements: Potential, economically viable solutions for a low-CO<sub>2</sub>, cement-based materials industry, Paris, 2016.
- [13] S. Lay, P. Schießl, J. Cairns, Probabilistic service life models for reinforced concrete structures, *Life Cycle Manag. Concr. Infrastructures Improv. Sustain.* (2003) 169.
- [14] CEN, EN 12390-12 Testing hardened concrete - Part 12: Determination of the carbonation resistance of concrete - Accelerated carbonation method, (2020) 18.
- [15] DuraCrete, Probabilistic Performance based Durability Design of Concrete Structures DuraCrete, 2000.
- [16] P. Van Den Heede, Durability and Sustainability of Concrete with High Volumes of Fly Ash, University of Ghent, Belgium, 2014. doi:10.1017/CBO9781107415324.004.
- [17] P. Van den Heede, Durability and Sustainability of Concrete with High Volumes of Fly Ash, Ghent University, Belgium, 2014.
- [18] I. Galan, C. Andrade, M. Castellote, Natural and accelerated CO<sub>2</sub> binding kinetics in cement paste at different relative humidities, *Cem. Concr. Res.* 49 (2013) 21–28. doi:10.1016/j.cemconres.2013.03.009.
- [19] C. feng Lu, W. Wang, Q. tao Li, M. Hao, Y. Xu, Effects of micro-environmental climate on the carbonation depth and the pH value in fly ash concrete, *J. Clean. Prod.* 181 (2018) 309–317. doi:10.1016/j.jclepro.2018.01.155.
- [20] S.K. Roy, K.B. Poh, D.O. Nortwood, Durability of Concrete-Accelerated Carbonation and Weathering Studies, *Build. Environ.* 34 (1999) 597–606.
- [21] V. Carević, Uticaj Prslina na Mehanizme Deterioracije i Trajnost Armiranobetonskih Konstrukcija, PhD Thesis, University of Belgrade, Faculty of Civil Engineering, 2020.



Original scientific paper

## Effect of natural fish tail palm fiber on the workability and mechanical properties of fiber reinforced concrete

Vijayalakshmi Ramalingam<sup>\*1)</sup>, Keerthika Ramesh<sup>2)</sup>, Modhagapriyan Arumugam<sup>2)</sup>,  
Vaishnavi Muralidharan<sup>2)</sup><sup>1)</sup> Associate Professor, Department of Civil Engineering, Sri Sivasubramaniya Nadar College of Engineering, Kalavakkam Chennai-603110, Tamil Nadu, India. <https://orcid.org/0000-0003-4678-2020><sup>2)</sup> UG Student, Department of Civil Engineering, Sri Sivasubramaniya Nadar College of Engineering, Kalavakkam Chennai-603110, Tamil Nadu, India

### Article history

Received: 23 December 2021

Received in revised form:

14 February 2022

Accepted: 21 February 2022

Available online: 31 March 2022

### Keywords

Fish Tail Palm Fiber;  
natural fibers;  
fiber reinforced concrete;  
impact strength;  
workability

### ABSTRACT

To improve the pre-cracking behavior and post peak strength of concrete composites, a new variety of natural fiber called Fish Tail Palm Fibers was used as micro reinforcement in concrete. Fish Tail Palm Fibers (FTPF) are completely renewable natural resources and are available in abundance, in many parts of the country including India. Three different volume fractions, (0.1%, 0.2% and 0.3%), and three different lengths of fibers (10 mm, 20 mm and 30 mm) were chosen as the parameters for investigation. Silane treated FTPF was added to concrete and the fresh and mechanical properties were studied. The slump values were slightly affected by the increase in volume fraction of fibers, as the viscosity of concrete increases with fiber content. The compressive strength of the control specimen was 30 MPa (M30). The maximum compressive strength, splitting tensile strength, and flexural strength of Fish Tail Palm Fiber Reinforced Concrete (FTPFRC) specimens are 36 MPa, 2.82 MPa and 4.2 MPa respectively, which were recorded for specimens with 0.2 Volume Fraction (VF) and 30 mm Fiber Length (FL). The increase in the compressive strength, splitting tensile strength and flexure strength is about 20 %, 22% and 30 % with the addition of 0.2 VF of fibers. The findings indicate that the incorporation of fish tail palm fibers reduced the workability of concrete. But the mechanical characteristics such as compressive strength, splitting tensile strength, flexural strength, and impact resistance were enhanced with the increase in fiber content and fiber length.

## 1 Introduction

Nowadays, natural fibers are in the foreground due to the need to turn to alternative materials with low environmental footprints. Natural fibers are used to control cracks developed in concrete structures due to plastic and drying shrinkage, increase the tensile strength, toughness, and durability. The functionality of fibers depends on the geometric properties of fibers, fiber content, orientation and interaction with binders [1]. Many studies have been conducted to investigate the effects of fibers as a crack arresting medium in concrete [2]. Different natural fibers such as jute, hemp, flax, banana, bamboo, roselle, basalt, palm, sisal, abaca. etc. have been used by many researchers in the recent past to study the mechanical properties, fracture energy, impact strength, shrinkage characteristics, and durability properties of concrete elements [3]. In some of the developing southeast Asian countries, natural fibers such as hemp cotton and jute are used to produce fiber reinforced polymers that can be used as an alternative to carbon fiber

reinforced polymers (CFRP) and glass fiber reinforced polymers (GFRP)[4] Combinations of synthetic and natural fibers are also used to increase the strength properties and flow characteristics of self-compacting concrete [5]. Even though the mechanical property of natural fiber is less than that of synthetic fiber, it is always within the acceptable limit and suitable for concrete and other related applications [6].

Natural fibers are non-uniform with an irregular cross-section, which makes them unique and different from man-made fibers such as polypropylene, polyolefin, glass fibers etc. This property of fibers attracts more researchers to using natural fibers as reinforcement [7]. Many new plant fibers are identified, and their properties are studied in detail so they find their application in concrete as fiber reinforcement. Fish Tail Palm Fiber (FTPF) is also one of its kind, FTPF is a unique type of cellulosic fiber obtained from the peduncle portion of the fish tail palm tree. Those fibers were tested for chemical composition, mechanical strength, surface property

<sup>\*</sup> Corresponding author:E-mail address: [vijayalakshmir@ssn.edu.in](mailto:vijayalakshmir@ssn.edu.in)

and it was proved that this fiber can be used as a novel plant based natural fiber for improving the strength of polymer composites and concrete elements [8].

The FTPF used in this study is obtained from the Toddy palm tree, also known as the Fish Tail Palm Tree, which is a renewable resource with low production cost and wide availability in India. Toddy palm is a fast-growing feather palm that makes a beautiful addition to the landscape. It belongs to the family of *Aceraceae* and the fiber is also called *Caryota Urens* fiber [9]. Most automotive industries are supplanting synthetic fibers such as carbon and glass with cellulose fibers (FTPF) in polymer matrix reinforcement [10]. Much research work has been carried out using FTP fibers as fiber reinforcement in polyester composites [11]. It also finds its application in the production of non-asbestos free break pad applications [12]. The application of caryota fibers in polymer composites is developing vigorously after 2019, but its application in concrete as fiber reinforcement has not been studied in detail. Therefore, the main aim of this study is to study the effect of FTPF on the workability characteristics and mechanical properties such as compressive strength, splitting tensile strength, flexural strength, and impact resistance of concrete.

## 2 Literature review

Many researchers studied the fresh and mechanical properties of cement concrete, the strength of fiber-reinforced composites (FRC), and the thermal and acoustic properties of FRC using various natural fibers. When banana fiber stem is used as reinforcement in concrete, it increases flexural strength and spalling resistance [13]. Fiber length, fiber content, and chemical treatment of banana pseudo stems have a major influence on the flexural strength of banana pseudo stem-epoxy polymer composites [2]. Maximum stress transfer between the fibers and matrix was observed for a combination of banana-sisal (3:1) hybrid fiber reinforced polyester composites [14]. Cellulosic fiber chemical composition, mechanical strength, and micro-structure all play a significant role in the compressive, flexural, and impact strength of fabric reinforced cementitious polymers and geopolymer composites [15]. Cellulosic fibers such as jute and kelp are more suitable for soft natural mortars such as lime, but coconut fiber, which is rich in lignin is more suitable for cement mortar [16]. The addition of Indian mellow fiber and roselle fiber mat in a polymer matrix with saw dust as fillers resulted in the fabrication of automobile rear view mirrors, fan blades, and auto wheel hubs [17]. Coconut fiber reinforced concrete along with coconut rope in the column has better seismic performance and results in the development of low cost housing in seismic zones [18]. When compared to most of the natural fibers coconut fiber has the highest toughness value, which helps to improve the ductile behavior of concrete elements and their composites [19]. Coconut fiber when used as insulation for concrete roof slabs helps to reduce the energy consumption of the building by a maximum of 9% and helps in the cost reduction [20]. Wheat straw is another plant fiber that contributes to the flexural strength, energy absorption and increases the toughness indices of concrete pavement [21].

Jute is an easily available plant fiber that has excellent crack arresting behavior and high tensile strength [22]. Increasing the dosage of fibers beyond 0.5% has a negative

impact on the fresh properties of concrete. Alkali and polymer modification is the technique in which the durability of plant fibers can be increased in fiber reinforced concrete composites [23]. Tannin modified jute fiber along with mild alkali and diluted polymer emulsion are used to make paver blocks to meet the global demand for sustainable infrastructure development [24]. Kenaf fiber, being the outstanding renewable resource for the fabrication of composites, in combination with sisal and jute is used to produce fiber reinforced polymer composites [25]; [26]. Natural plant fibers (sisal, abaca, jute, etc.) are also used in combination with steel fibers and synthetic polypropylene fibers to improve the mechanical and durability characteristics of concrete elements [27].

*Prosopis Juliflora* bark used as reinforcement along with banana and coconut fibers with epoxy resulted in FRP composites with increased flexural attributes and better mechanical strength and toughness indices. High density polyethylene composites reinforced with another unique fiber, curaua fiber, tend to improve the interfacial, mechanical, and morphological properties of composites [28]. The use of giant reed fibers and date palm fibers as fiber reinforcement for cement-based mortar significantly improves fracture toughness [29], impact strength, and flexure strength [30]. The mechanical properties and thermal behavior of concrete [31] improve with the addition of a very small amount of (0.05%) of water hyacinth fiber, along with banana fiber and bio-filler egg shell powder. Details of some research work carried out using natural plant fiber are listed in Table 1. From the previous literature study, it can be concluded that the characteristics of this unique FTPF in concrete have not been extensively studied. Therefore, the main aim of this work is to study the fresh properties, mechanical strength, and durability characteristics of M30 (30 Mpa) concrete, using FTPF as fiber reinforcement in the concrete mix. The two main parameters of investigation are, fiber length and volume fraction.

## 3 Experimental investigations

### 3.1 Materials

Concrete specimens were prepared by using ordinary Portland cement as a binder, gravel of a maximum size 20 mm as coarse aggregate and river sand as fine aggregate. The materials selection was based on the Indian standard code specification IS-456:2000[37]. To improve the mechanical strength and crack resistance characteristics of concrete, natural fibers, namely Fish Tail Palm Fibers (FTPF) were added to the concrete in different lengths and volume fractions. Fish tail palm fiber was obtained from the palm trees grown at Sri sivasubramaniya Nadar College of Engineering Campus, Chennai, India. The peduncle portion, which is shown in Figure. 1, was cut from the Fish Tail Palm tree (FTP) and the fiber was extracted. Fully matured fibers have fruits on the surface (Figure. 2). Each strand was separated from the main stem, and the impurities and fruits present on the surface were cleaned. After proper chemical treatment, the Fish Tail Palm Fibers (FTPF) of a strand length of 2 m were obtained from the stem. The step-by-step process of extraction of FTPF is shown in Figure. 3. The physical and chemical properties of FTPF are given in Table 2. The SEM image of the silane treated fiber is shown in Figure. 4.

Table 1. Few studies of fiber reinforced concrete using natural plant fibers

S.No	Author/Year	Type of fiber	Fiber Content	Parameter of study	Conclusion
1	Farooqi and Ali (2018) [21]	Wheat straw	1% of mass of concrete, 25 mm length	To improve flexural strength, toughness indices and energy absorption capacity	Delayed crack initiation and enhanced load capacity up to 7.5%
2	Islam &Ahamed (2018) [22]	Jute Fiber	lengths -10 mm & 20 mm. Volumes of 0 %, 0.25%, 0.50%, & 1.00%	Study of compressive and flexural strength @ 7,28 and 90days	addition of 0.50% jute fiber had an adverse impact on the fresh properties of concrete
3	Kundun et al (2020) [32]	Jute fiber	1% by weight of paver block (3-5 mm length)	surface modified jute fiber in controlling the physical and mechanical properties of concrete paver blocks.	30%, 49% and 166% higher compressive strength, flexural strength, and flexural toughness respectively
4	Pirmohammad et al (2020) [25]	Kenaf & goat wool	lengths (4, 8 and 12 mm) and contents (i.e., 0.1, 0.2 and 0.3% by weight of total asphalt mixture	Influence of kenaf and goat wool on mixed mode fracture strength of asphalt mixtures.	asphalt mixtures reinforced by 0.3% kenaf fibers with 8 mm & 0.3% goat wool fibers with 4 mm length demonstrate the best results
5	Alam&Riami (2018) [26]	kenaf, jute and jute rope fiber	Polymer composites	natural fiber reinforced polymer laminates for shear strengthening of reinforced concrete beam.	shear strengthened beams with kenaf, jute and jute rope composite plates higher failure load as compared to control beam
6	Qamaar et al (2018) [33]	Sisal+Rice straw	2% fibres by weight of cement	effectiveness of natural fibrous plaster for improving the out of plane lateral resistance of mortarless interlocked masonry walling was evaluated	The use of natural fibres within plaster did more to enhance the wall strength than fibres within blocks or mortar
7	Badagliacco et al (2020) [29]	Giant reed fiber	4cm, 8 cm and 12 cm fiber	investigate the bio-lime based mortar flexural toughness improvement due to the addition of common reed fiber	effectiveness of giant reed fibers in the manufacturing of green building materials, as bricks or laying mortars.
8	Niyasom&Tangboriboon (2021) [31]	Water hyacinth + banana fiber+ egg shell powder	3-13 cm long banana fiber and hyacinth fibers	The bulk density, true density, water absorption, compressive strength, tensile strength, flexural strength, and maximum load	Adding eggshell powder can reinforce and enhance physical and mechanical properties of concrete composites
9	Wongsa et al (2020) [34]	Sisal + Coconut	0.25-1%	Mechanical, thermal, and physical properties of geopolymer mortar reinforced with fibers were tested	Fibers improves the flexural and tensile strength, but reduces the workability, dry density.
10	Comak et al (2018) [35]	Hemp	Volume- 0%, 1%, 2%, 3% lengths - 6 mm, 12 mm & 18 mm	Durability and mechanical property of cement mortar	cement mortars with 2–3% amount and 12 mm length of hemp fiber give optimum results.
11	Tidarat et al (2019) [36]	Cotton,Jute,hemp	Jute hemp cotton polymer composites	compressive behavior of concrete confined with low-cost natural fiber reinforced polymer (NFRP)	NFRP is effective and suitable to enhance the confinement effect of concrete, especially Jute-NFRP.

### 3.2 Methodology



Figure 1. Fish Tail Palm Fiber



Figure 2..Fully matured fibers with fruits on the surface

The effect of FTPF on the fresh and hardened properties of normal strength concrete was investigated. Fiber length and volume fraction were considered as the parameters of investigation. Because short fibers have higher flexural strength, toughness, and energy absorption than long fibers [38], three short lengths of fiber (10 mm, 20 mm, and 30 mm) were chosen at three different Volume Fractions (VF), namely 0.1%, 0.2%, and 0.3%. The addition of fibers beyond 0.5% has a negative impact on the workability, air content and fiber distribution in fresh concrete [39]. Therefore, the VF was restricted to 0.1-0.3%. To arrive at the mix proportioning of control concrete with a compressive strength of 30 MPa, three trial mixes were prepared. From the trial mix, the ratio of cement, sand, gravel, and water required to prepare the concrete mix was decided as 1:1.98:2.77:0.54:0.007. The superplasticizer content was slightly increased with the increase in fiber content. In total, ten concrete mixes were prepared, including the control mix. The quantity of material used for each mix is listed in Table 3. The FTPF was cut into 10 mm, 20 mm, and 30 mm lengths as shown in Figure. 5 and used as fiber reinforcement in concrete. The specimens were identified based on the presence of fibers, volume fraction and fiber length. For example, NSC-CM represents normal strength concrete-control mix with no fibers, and FRC-0.1-20 represents fiber reinforced concrete with a fiber volume fraction of 0.1% and a fiber length of 20 mm. For batching, coarse aggregate, fine aggregate, cement, and mineral additives were mixed in a concrete mixer for 5-8 minutes. The concrete-fiber mix compositions were prepared by adding FTPF fibers to the fresh concrete in the concrete mixer. Fibers were added gradually and slowly to avoid a balling effect due to fiber content, and were allowed to mix for another three minutes to ensure that the fibers were uniformly distributed in the concrete.

The fresh properties of normal and FRC were determined using the slump cone test, and for the hardened properties of concrete, compressive strength, splitting tensile strength, flexural strength, modulus of elasticity, and impact resistance tests were done. Cubes of size 150 mm were prepared to determine the compressive strength. Cylinder specimens of dimension 150 mm × 300 mm were prepared to determine the splitting tensile strength and modulus of elasticity. A beam specimen of size 100 mm × 100 mm × 500 mm was prepared for modulus of rupture and a 150 mm × 65 mm disc was used for measuring the impact resistance. The fresh and hardened concrete tests carried out for FTPF reinforced concrete are shown in Figure. 6.

Table 2. Physical and chemical properties of FTPF

Chemical Composition	Cellulose (%)	Hemicellulose (%)	Lignin (%)	Extractives (%)	Crystallinity index (%)
	72.51	8.97	11.75	6.77	51.2
Physical and Mechanical property	Length (m)	Diameter (µm)	Tensile strength (MPa)	Modulus of elasticity (GPa)	Density (g/cm <sup>3</sup> )
	2-3	210-240	476	2.8	1.3



(a) Raw fibers from palm tree (b) Fiber stems immersed in water (c) Beaten fibers to remove outer skin (d) Fibers extracted from outer skin (e) Silane chemical treatment (f) Fibers washed in ethanol (g) Oven dried fibers (h) Fibers cut into different length

Figure 3. Step by step process of extraction of fish tail palm fibers

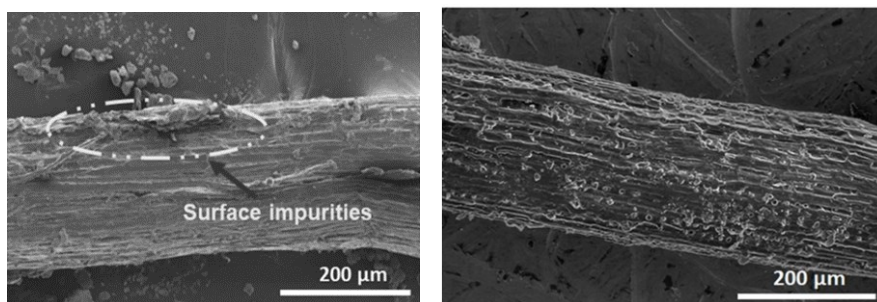


Figure 4. SEM image of (a) untreated and (b) silane treated FTPF [8]



Figure 5. Cut fish tail palm fibers of different length

Table 3. Mix proportion

Specimen ID	Cement (kg/m <sup>3</sup> )	Sand (kg/m <sup>3</sup> )	Aggregate (kg/m <sup>3</sup> )	Fiber length (mm)	Fiber Content (kg/m <sup>3</sup> )	Super plasticizer (kg/m <sup>3</sup> )	Water (kg/m <sup>3</sup> )
NSC-CM	470	930	1300	-	-	3.6	256
FRC-0.1-10	470	930	1300	10	1.02	3.6	256
FRC-0.1-20	470	930	1300	10	1.02	3.6	256
FRC-0.1-30	470	930	1300	10	1.02	3.6	256
FRC-0.2-10	470	930	1300	20	2.04	3.8	256
FRC-0.2-20	470	930	1300	20	2.04	3.8	256
FRC-0.2-30	470	930	1300	20	2.04	3.8	256
FRC-0.3-10	470	930	1300	30	3.07	4.0	256
FRC-0.3-20	470	930	1300	30	3.07	4.0	256
FRC-0.3-30	470	930	1300	30	3.07	4.0	256



Figure 6. Experimental test procedure for FTPF reinforced concrete(a) Slump test (b) Compression test (c) Splitting tensile strength test (d) Modulus of elasticity (e) Flexural strength

## 4 Result and Discussion

An experimental study was carried out to study the fresh and hardened properties of FTPFRC for three different fiber lengths and three volume fractions of fibers. The slump value, compressive strength, split tensile strength, modulus of elasticity, and flexural strength values are tabulated in Table 4. Three specimens were tested for each case, and the mean values are listed along with the coefficient of variation.

### 4.1 Fresh property of FTPF reinforced concrete

The slump flow test was carried out to determine the workability of concrete. Workability is an important parameter for concrete construction, in addition to the quality of ingredients used in concrete. The addition of fibers to concrete increases the viscosity of concrete and restricts the distribution of the cement matrix, thereby reducing the slump value [40]. Natural fibers tend to absorb moisture from the wet concrete, which again influences the slump value [5]. The presence of fibers increases the surface area of concrete, which reduces the amount of free water available for the mobility of cement particles [41]. In addition, the fibers also affect the relative mobility of coarse aggregate and the

free flow of concrete. Wang et al. [42] studied the effect of fiber length and volume fraction on the slump value of concrete. The lowest slump value of 15.8 mm was recorded for a volume fraction of 0.4% basalt fiber, and it was concluded that with the increase in volume fraction of fibers, the slump values decreased. Prakash et al. [43] studied the influence of sisal fiber on the lightweight coconut shell aggregate concrete and concluded that the increase in fiber content from 1% to 4% reduces the slump value by 50%. Short fibers improve the workability compared to long fibers, because the latter have a large surface area that provides interference and blockage to aggregate, thereby reducing the workability [44]. The conclusion from previous research work supports our present study of FTPFRC. The density of concrete slightly decreases with the increase in fiber content. For control mix, the density is about 2450 kg/m<sup>3</sup>, which reduces to 2435 kg/m<sup>3</sup>, 2410 kg/m<sup>3</sup> and 2390 Kg/m<sup>3</sup> for concrete with 0.1%, 0.2% and 0.3% fiber content,

respectively. A very minimal change in density was observed for the change in length of fibers.

The plot showing the variation of slump value with respect to fiber length (FL) and volume fraction (VF) is shown in Figure. 7. For the volume fraction of 0.1% the slump value decreased from 80 to 77 for a change in fiber length from 10 mm to 30 mm. With the increase in volume fraction from 0.1 to 0.2% the slump value slightly decreases. With a constant slump value, the increase in fiber length also affects the slump value. The lowest slump value of 65 mm was recorded for FRC with 0.3% VF and 30 mm FL. The empirical correlation between the slump value (S) and fiber volume fraction was obtained through linear regression analysis, which is shown in Figure. 8. Three empirical equations were developed for three fiber lengths. All three-regression analyses showed a high coefficient of determination (R<sup>2</sup> = 0.95-0.98).

Table 4. Fresh and hardened properties of FTPF reinforced concrete

Specimen ID	Slump value (mm) (CoV %)	Compressive Strength (MPa) (CoV %)	Splitting tensile strength (MPa) (CoV %)	Modulus of elasticity (GPa) (CoV %)	Flexural strength (MPa) (CoV %)
NSC-CM	83 (1.21)	30.1 (1.2)	2.3 (0.67)	27 (.123)	3.5 (0.21)
FRC-0.1-10	80 (1.9)	30.2 (1.02)	2.59 (0.67)	27.56 (1.34)	3.80 (0.32)
FRC-0.1-20	78 (1.42)	30.33 (1.5)	2.60 (0.45)	27.9 (1.32)	3.81 (0.11)
FRC-0.1-30	77 (0.45)	30.92 (1.34)	2.62 (0.32)	28.2 (1.02)	3.89 (0.12)
FRC-0.2-10	76 (.135)	32 (0.91)	2.61 (0.12)	27.92 (1.12)	3.90 (0.23)
FRC-0.2-20	75 (1.11)	33.3 (1.32)	2.63 (0.34)	28.5 (1.05)	3.91 (0.11)
FRC-0.2-30	73 (.120)	36 (1.1)	2.82 (0.05)	30 (1.11)	4.20 (0.21)
FRC-0.3-10	72 (0.56)	32.9(1.03)	2.66 (0.21)	28.4 (.136)	3.95 (0.23)
FRC-0.3-20	68 (1.32)	33.8(1.24)	2.70 (0.42)	28.72 (1.45)	4.02 (0.14)
FRC-0.3-30	65 (1.08)	35 (1.42)	2.75 (0.12)	29.98 (1.03)	4.10 (0.16)

Note: Three specimens tested for each hardened concrete test and the coefficient of variation percentage are shown in bracket

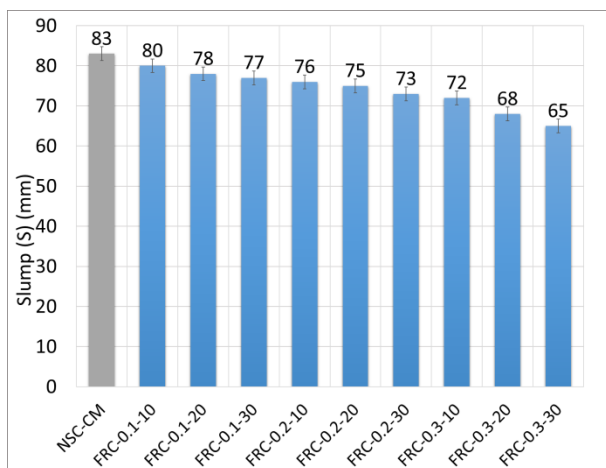


Figure 7. Slump values of FTPFRC

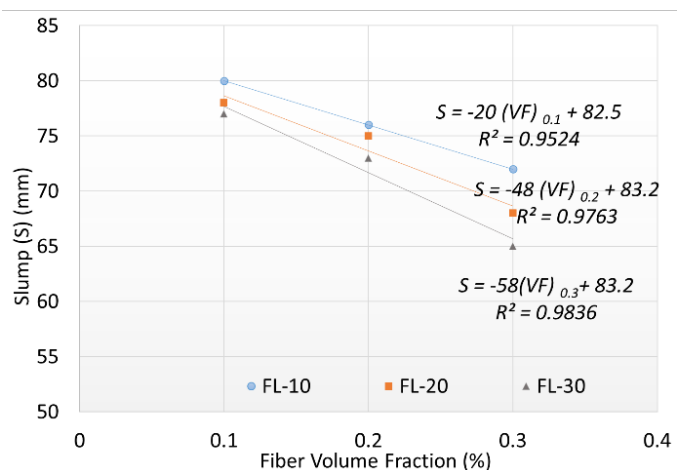


Figure 8. Linear correlation between slump and fiber volume fraction

## 4.2 Compressive Strength

The compressive strength of FTPFRC with different volume fractions and fiber lengths is shown in Figure. 9. The compressive strength does not show a significant increase with a volume fraction of 0.1%- at 10-mm fiber length. The strength gradually increases to 0.2% volume fraction. A maximum of 19% increase in compressive strength was obtained for 0.2 VF with 30 mm FL. For 0.3% VF, the increase in strength is about 9%, 12% and 16% for 10 mm, 20 mm, and 30 mm long fibers, respectively. Compared to the strength of specimen with 0.3%VF, only 30 mm FL showed a reasonable increase in strength of about 16%. As the fiber content increases, the concrete becomes more porous due to fiber clustering and interaction with large particles, which reduces the strength of the concrete specimen with 0.3 VF of fibers. Improper compaction and packing of concrete materials may also contribute to the reduction in strength. When comparing short and long fibers, the contribution of short fiber is minimal when compared to long fibers (30 mm). Compared to all the three-volume fractions, FRC with 0.2%VF and 30 mm FL showed a better performance in compression.

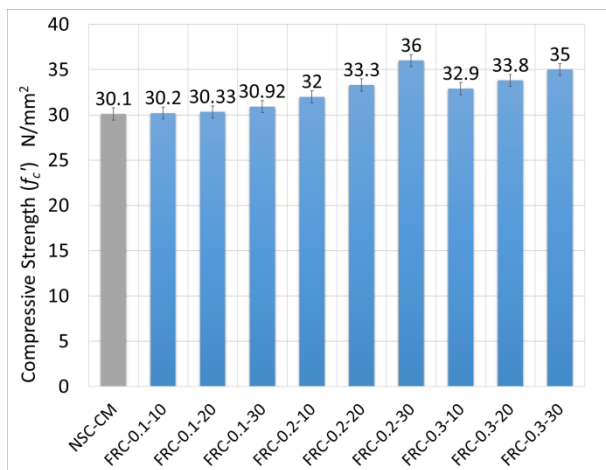


Figure 9. Compressive strength of FTPERC with different fiber length and volume fraction

The work done by Chakraborty et al. [23] proved that the fiber length plays a major role in improving the compressive strength of mortar, but only up to a certain volume fraction (1% wt. of cement). Prakash et al. [45] reported that the addition of sisal fiber and polypropylene fibers to concrete increases the compressive strength of coconut shell aggregate concrete. They reported a maximum compressive strength of 35 MPa for light weight concrete. The increase in compressive strength with the fiber length can be attributed to the fact that the stress transfer from matrix to the fiber is insufficient for short length fiber. On the other hand, stress is completely transferred from the matrix to the fibers in the case of long length fibers [46]. Use of fibers in concrete results in closely spaced cracks with reduced crack width. Fibers also help to bridge the crack, which increases the strength of FRC [19]. It can be clearly stated that, previous research work on FRC supports our present experimental results.

## 4.3 Splitting tensile strength

The addition of fibers enhances the tensile strength and fracture energy of concrete specimens [47]. The fibers not only act as micro reinforcement, but also contribute to the strength of the concrete. The failure pattern of a cylinder specimen reinforced with 0.3% VF of fibers is shown in Figure. 10. From the figure, it is clearly visible that the fibers play an important role in reducing the stress concentration in concrete matrix. Once a crack develops in concrete, the fibers distribute the stress in different directions and prevent the formation of wider cracks. In the case of a control specimen with no fibers, the failure of the specimen was a single explicit crack. The cement matrix glues all the reinforcing fibers into shape and transfers the stress through them along their longitudinal direction [48]. Prakash et al [50] reported that the addition of steel and polypropylene fiber increased the tensile strength of concrete. Wahyuni et al. [51] reported that the addition of bamboo fibers resulted in a splitting tensile strength of 3.9 MPa. Islam et al. [22] reported an increasing trend in the splitting tensile strength of jute FRC for an aspect ratio of 100-200 and fiber content of 0.5%. The splitting tensile strength obtained from the present study is shown in Figure.11. The plot is similar to the compression strength variation. The tensile strength increases with the addition of fibers from 2.3 to 2.5 MPa for 0.1 F and 10 mm FL. For the same VF, the length of fibers does not have major impact. FRC with 0.2%VF and 30 mm FL showed a maximum tensile strength. Again, comparing the specimen with 0.3% VF, only 30 mm FL showed a significant increase in tensile strength. As the fiber content increases, the concrete becomes more porous due to fiber clustering and interaction with large particles, which reduces the strength of the concrete specimen with 0.3 VF of fibers. Improper compaction and packing of concrete materials may also contribute to the reduction in strength. From the experimental observations, it can be concluded that the mechanical properties of FRC show a maximum value of 0.2 VF and 30 mm FL.



Figure 10. Failure pattern of fiber reinforced cylinder specimen

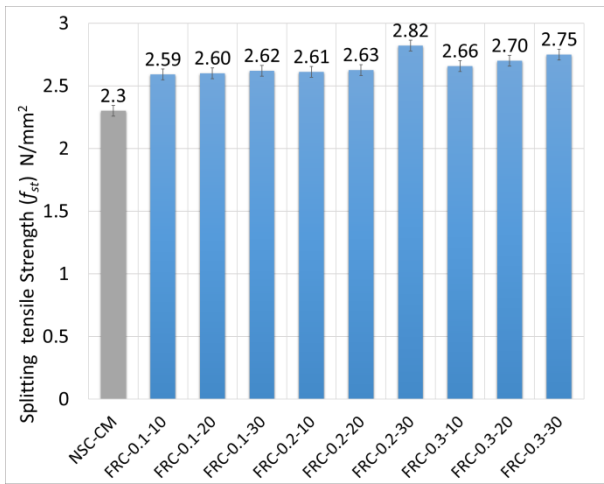


Figure 11. Splitting tensile strength of FTPERC with different fiber length and volume fraction

The regression analysis was carried out to develop an empirical equation to relate the split tensile strength ( $f_{st}$ ) with the compressive strength ( $f_c'$ ). The correlation between split tensile strength and compressive strength with a high regression value ( $R^2 = 0.94$ ) is shown in Figure. 12. The American Concrete Institute code [52] suggests equ (1) to correlate the splitting tensile strength with the compressive strength

$$f_{st} = 0.53\sqrt{f_c'} \quad (1)$$

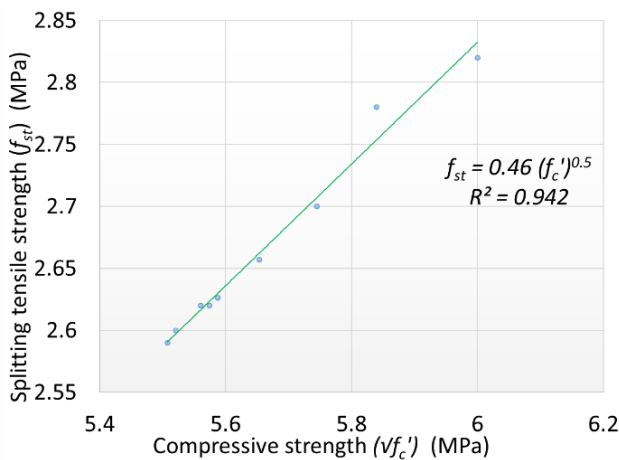


Figure 12. Regression plot of splitting tensile strength and compressive strength

According to European standards [53] the correlation between splitting tensile strength and compressive strength is given by equ (2)

$$f_{st} = 0.3(f_c')^{2/3} \quad (2)$$

The correlation between splitting tensile strength and compressive strength according to the Japanese Concrete Institute code [54] and the New Zealand code [55] is given by equ (3) and equ (4)

$$f_{st} = 0.13(f_c')^{0.85} \quad (3)$$

$$f_{st} = 0.44\sqrt{f_c'} \quad (4)$$

The comparison between the present experimental result and the standard codal correlation equation for splitting tensile strength and compressive strength is shown in Figure. 13. From the plot, it is clearly visible that the experimental results agree well with the correlation predicted by standard codes. The proposed equation for correlating splitting tensile strength with compressive strength of fish tail palm fiber reinforced concrete is given by equ (5)

$$f_{st} = 0.46\sqrt{f_c'} \quad (5)$$

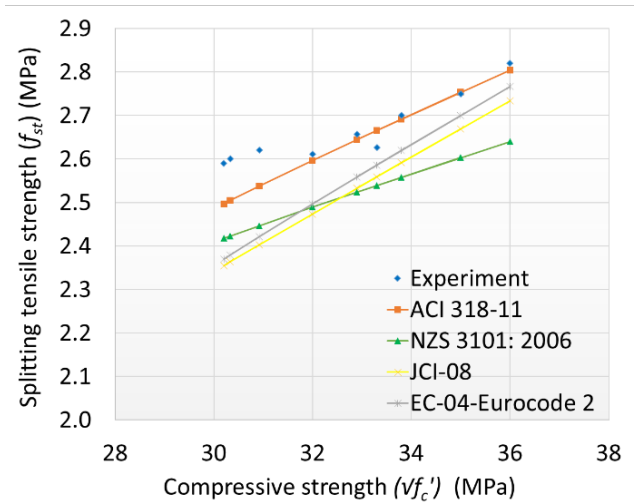


Figure 13. Comparison of experimental splitting tensile strength value Vs standard codal values

#### 4.4 Flexural strength

The failure of the specimen started in the tension zone with the development of tension cracks, as the maximum tensile capacity of the specimen was reached. The failure of the beam was ductile in nature, which can be explained by the fact that the fibers bridge the crack within the concrete and improve the post cracking behavior of FRC [56]. The failure pattern of the beam along with the bridging of micro cracks by the fibers is shown in Figure. 14. Failure of the specimen occurs once the maximum tensile capacity of the fiber is reached. Awwad et al. [57] studied that the flexural strength of hemp FRC is increased by fiber content and resulted in a ductile post-cracking behavior of FRC. It has been demonstrated that the addition of roselle fiber [58], flax fibers [59], jute [26], and sisal fiber [60] improves concrete flexural strength while also increasing toughness and residual strength. In the present study also, the flexural strength increased with the VF of fibers. Flexural strength increased from 3.5 MPa for the control specimen to 4.2 MPa and 4.1 MPa for the 0.2VF and 0.3VF with 30 mm FL, respectively. The maximum flexural strength is about 12% of its corresponding compressive strength. The variation of flexural strength with FL and VF is shown in Figure. 15. The length of fibers does not have a major influence on the flexural strength for lower volume fractions. But for higher VF, the fiber length plays a crucial role and improves the flexural strength.

The ratio of splitting tensile strength to compressive strength varies from 0.076, 0.084, 0.078, and 0.078 for control specimens and specimens with 0.1 VF, 0.2 VF, 0.3

VF of fiber reinforced specimens, respectively. From the ratio, it is clear that the addition of fibers equally contributes to the tensile strength and compressive strength of concrete. The ratio of flexural strength to compressive strength varies from 0.11, 0.125, 0.117 and 0.117 for control specimens and specimens with 0.1 VF, 0.2 VF, 0.3 VF of fiber reinforced specimens with 30 mm fiber length, respectively. From the ratios, it is much clear that the contribution of fibers to the flexural strength is much greater than the splitting tensile strength.



Figure 14. Failure pattern of fiber reinforced beam specimen

A linear regression analysis was carried out to develop an empirical equation to relate the flexural strength ( $f_r$ ) with the compressive strength ( $f_c'$ ). Figure.16 depicts the regression analysis correlation developed between flexural strength ( $f_r$ ) and compressive strength ( $f_c'$ ), and the developed equation has a high regression value ( $R^2 = 0.98$ ). The American Concrete Institute code [52] suggests equ (6) to correlate the flexural strength with the compressive strength

$$f_r = 0.62\sqrt{f_c'} \quad (6)$$

According to European standards [53] the correlation between flexural strength and compressive strength is given by equ. (7)

$$f_r = 0.435(f_c')^{2/3} \quad (7)$$

The correlation between flexural strength and compressive strength according to and the New Zealand code [55] is given by equ. (8)

$$f_r = 0.6\sqrt{f_c'} \quad (8)$$

The comparison between the present experimental result and the standard codal correlation equation between flexural strength and compressive strength is shown in Figure. 17. From the plot, it is clearly visible that the experimental results agree well with the correlation predicted by standard codes. The proposed correlation equation for flexural strength and compressive strength of fish tail palm fiber reinforced concrete is given by equ. (9)

$$f_r = 0.5771\sqrt{f_c} \quad (9)$$

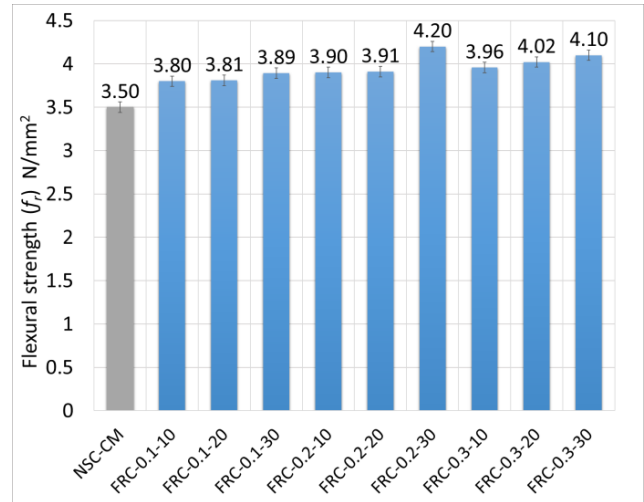


Figure 15. Flexural strength of FTRC with different fiber length and volume fraction

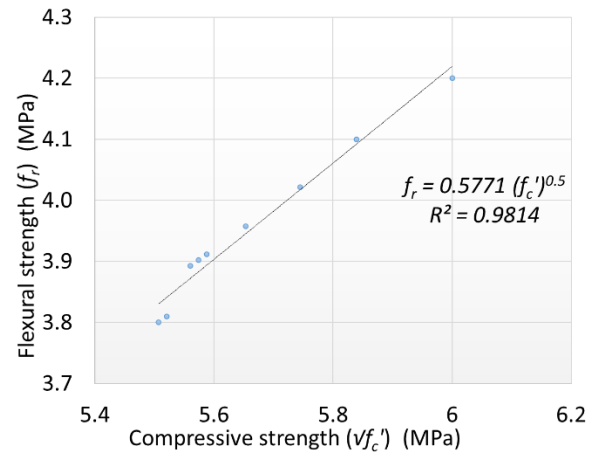


Figure 16. Regression plot of flexural strength and compressive strength

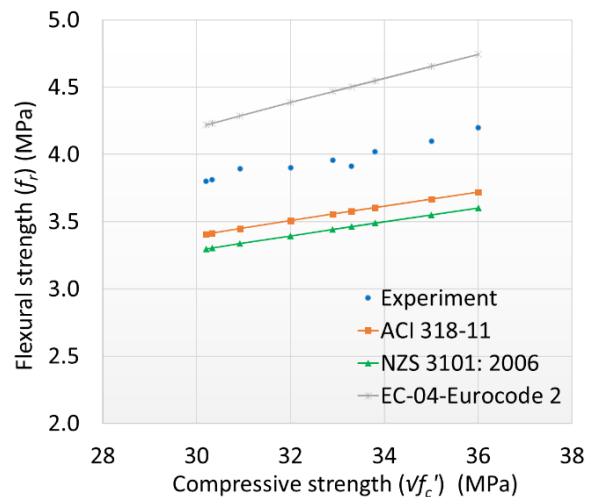


Figure 17. Comparison of experimental flexural strength with standard codal values

4.5 Modulus of elasticity

The modulus of elasticity is the ratio of stress to the corresponding strain of a concrete specimen within the elastic zone. Fiber tensile strength governs the modulus of elasticity (MoE) of concrete [61], which plays a major role in the pre-cracking behavior of concrete specimens. The addition of fibers helps improve the mechanical properties of concrete and composites [62]. As the fiber content increases, the ductility of the concrete specimen is also increased, and the MoE also increases. Addition of fibers increases the stress redistribution and reduces the strain localization within the concrete. The fibers restrain the crack at the beginning, reducing stress concentration and preventing crack growth in the post-cracking region [47]. Prakash et al. [50] reported that the addition of steel fibers increases the elasticity of coconut shell aggregate concrete by 17%. The addition of sisal fibers also tends to increase the MoE by 6% for the addition of 3% volume of fibers [45]. The MoE increases up to a maximum of 9% with the addition of sisal fiber in self-compacting concrete, but beyond 4% volume of fibers, the MoE decreases [58]. The MoE of the FTPFRC with different VF and fiber lengths is shown in Figure. 18. As the fiber content increases, the elasticity of concrete increases as a greater number of fibers are involved in the crack arresting mechanism, which prevents the development of new cracks and also reduces the stress concentration. For the VF of 0.1 %, the increase in MoE value is about 4% for the FL of 30 mm. For 30 mm fiber length, the MoE increases by 11% for VF of 0.2% and 0.30%. From the result, it is clearly visible that the length of fibers also plays a minor role in increasing the elasticity of fiber reinforced concrete.

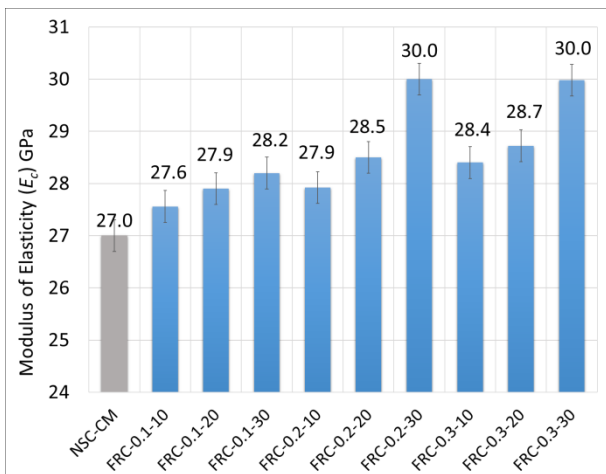


Figure 18. Modulus of elasticity of FTPFRC

The linear regression analysis was carried out to develop an empirical equation to relate the modulus of elasticity ( $E_c$ ) with the compressive strength ( $f_c'$ ). The correlation obtained between modulus of elasticity ( $E_c$ ) and compressive strength ( $f_c'$ ) with a high regression value ( $R^2 = 0.93$ ) is shown in Figure. 19. The American Concrete Institute (ACI) code [52] suggests equ (10) to correlate the MoE with the compressive strength

$$E_c = 4.73\sqrt{f_c'} \tag{10}$$

According to European standards [53] the correlation between flexural strength and compressive strength is given by equ (11)

$$E_c = 22(f_c'/10)^{0.3} \tag{11}$$

The correlation between modulus of elasticity and compressive strength according to the Japanese Concrete Institute code [54] and the New Zealand code [55] is given by equ (12) and equ (13)

$$E_c = 0.63(f_c')^{0.45} \tag{12}$$

$$E_c = 3.32\sqrt{f_c'} + 6.9 \tag{13}$$

The comparison between the present experimental result and the standard codal correlation equation for MoE and compressive strength is shown in Figure. 20. From the plot, it is clearly visible that the experimental results agree well with the correlation predicted by standard codes. The proposed equation for correlating modulus of elasticity with the compressive strength of fish tail palm fiber reinforced concrete is given by equ (14)

$$E_c = 4.233\sqrt{f_c'} \tag{14}$$

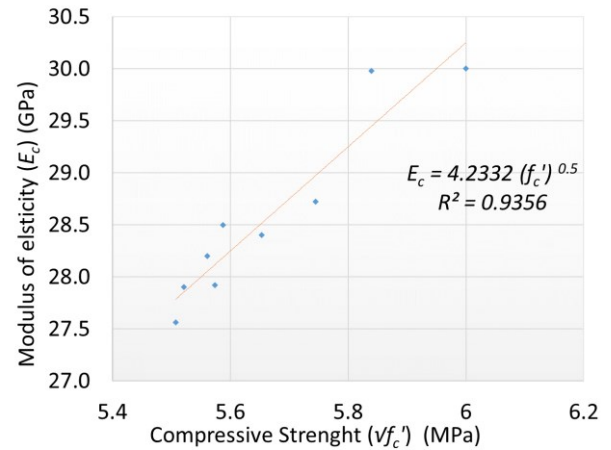


Figure 19. Correlation relation between MoE and compressive strength

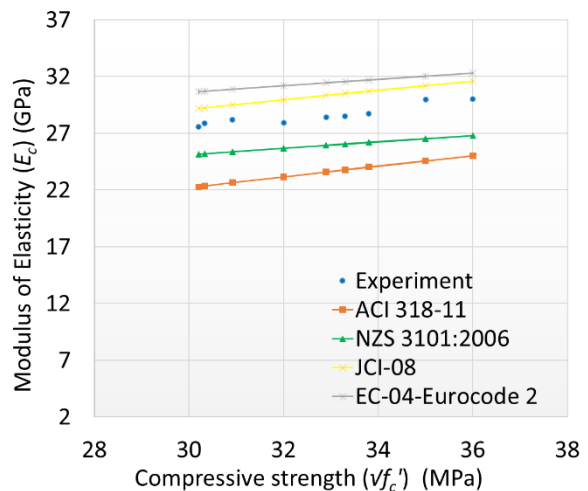


Figure 20. Comparison of experimental MoE with the standard codal prediction

4.6 Impact resistance

The repeated dropping weight test method was used to measure the impact strength and energy absorption capacity of FRC. The addition of natural fibers helps to improve the fracture properties and impact resistance of FRC [63]. When compared to plain cement mortar panels, the impact resistance of mortar panels reinforced with coir, sisal, jute, and hibiscus increases by 3-18 [64]. Hybridization of synthetic fibers with natural fibers not only makes the environment friendly but also increases the impact resistance and load carrying capacity of composites [65]. Wang et al. [66] studied the impact resistance of coconut

fiber reinforced concrete cylinders and reported that fiber reinforcement results in the formation of tiny microcracks at the initial stage of impact load, which propagates through different fiber lengths across the cylinder and results in the ultimate failure of the specimen. Prakash et al. [58] showed that the addition of 4% of roselle fiber increases the impact resistance by about 100%. Thus, fibers prevent the sudden failure of a concrete specimen and play an important role in the post cracking behavior of concrete. The addition of 4% of sisal fiber increases the impact strength by 91 % for coconut shell aggregate light weight FRC [50]. In the present study the number of blows recorded for the First Crack, Ultimate Crack and the impact energy is listed in Table 5.

Table 5. Impact energy of fish tail palm fiber reinforced concrete

Specimen ID	Number of blows for first crack (N <sub>1</sub> )	Number of blows for ultimate crack (N <sub>2</sub> )	Impact energy (N <sub>2</sub> -N <sub>1</sub> ) *mv <sup>2</sup> /2 N-m
NSC-CM	6	10	81.38
FRC-0.1-10	7	12	101.725
FRC-0.1-20	8	14	122.07
FRC-0.1-30	9	18	183.105
FRC-0.2-10	8	13	101.725
FRC-0.2-20	9	16	142.415
FRC-0.2-30	10	21	223.795
FRC-0.3-10	9	14	101.725
FRC-0.3-20	10	20	203.45
FRC-0.3-30	12	24	244.14

The impact energy plotted with respect to fiber volume fraction is shown in Figure. 21. From the plot, it can be concluded that for low VF (0.1) the increase in impact energy is not prominent. But for 0.2VF and 0.3VF of fibers, the impact energy shows a considerable increase for 20 mm and 30 mm of the fiber length. Thus, in addition to fiber volume fraction, fiber length also plays a role in the post cracking behavior of concrete. When compared to a control specimen, the increase in impact energy is about 175% and 200 % for 0.2VF and 0.3 VF with 30 mm fiber length. All the FTPFRC showed improved performance in arresting the micro cracks and resulted in higher impact resistance compared to the unreinforced control specimen. Out of all the nine FRC mixes, the specimen with 0.2 VF-20 mm FL and the 0.3VF with 30 mm FL specimen show better mechanical properties and impact resistance. Linear regression analysis was carried out to correlate the number of blows between the first crack and the ultimate crack for FL 10, FL20, and FL 30 mm and the plot is shown in Figure. 22. The equation developed showed a high regression value (R<sup>2</sup> = 0.96-1). The three-equation developed between Ultimate Crack (UC) and First Crack (FC) for 10 mm, 20 mm, and 30 mm fiber lengths is given by equ. (15), equ. (16), and equ. (17) respectively.

$$UC_{20} = 3(FC_{20}) - 10.33 \tag{16}$$

$$UC_{30} = 2.57(FC_{30}) - 4.57 \tag{17}$$

$$UC_{10} = FC_{10} + 5 \tag{15}$$

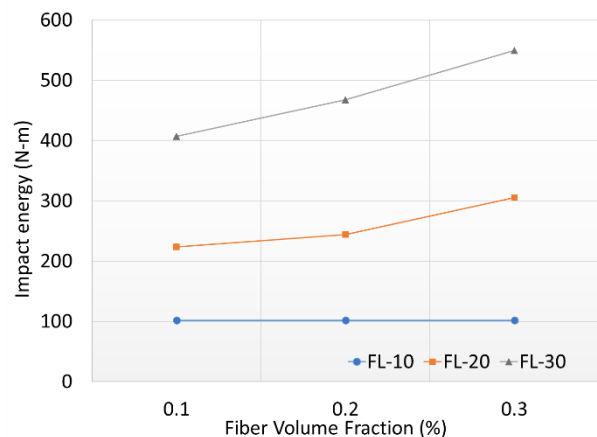


Figure 21. Relation between impact energy and fiber volume fraction

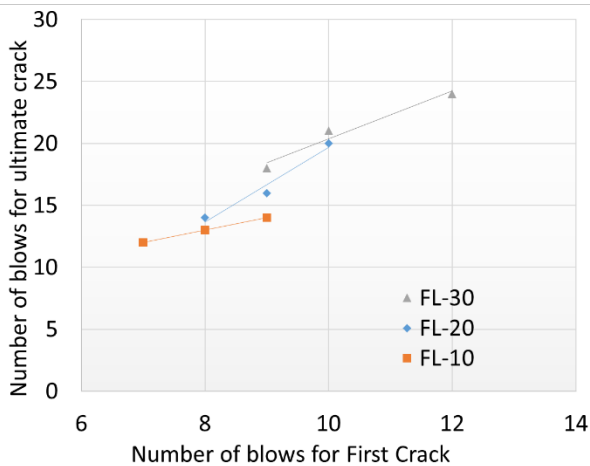


Figure 22. Correlation between number of blows for first and ultimate crack for different FL and VF

## 5. Conclusion

The experimental investigation was carried out on concrete with a 28-day compressive strength of 30 MPa that was reinforced with natural fish tail palm fiber for three different volume fractions and three different fiber lengths. The following conclusion can be drawn:

- For a fiber volume fraction of 0.3%, the slump value decreases and reduces the workability. The viscosity of the concrete matrix is increased by 0.3 VF, and the fibers prevent the even distribution of the cement matrix, which is more prominent for 30 mm fiber length.

- The contribution of fibers to the compressive strength of concrete is a minimum of 2%, for 0.1 VF of fiber addition. The maximum increase in compressive strength of 20% was recorded for a concrete specimen with 0.2% VF and a 30 mm fiber length, followed by a specimen with 0.3VF and a 30 mm FL, which showed a strength increase of 16%.

- The tensile strength of fibers contributes mainly to improving the crack arresting mechanism of concrete in the pre cracking as well as in the post peak region. Once cracks develop in concrete, the fibers share the stress and distribute the stress across the cross section, which reduces the stress concentration and prevents the formation of wider cracks. The maximum increase in splitting tensile strength and flexural strength is about 22% and 20%, which was observed for mix with 0.2VF and 30 mm FL.

- The impact energy of all the FTPFRC specimens increases with the addition of fibers. The maximum increase in impact energy of 175% and 200% was recorded for 0.2 VF with 20 mm and 30 mm FL. Thus, the fiber length also contributes to absorbing the impact load and increasing the impact resistance.

- These micro fibers prevent crack formation at the micro level and improve the strength properties and impact resistance of concrete elements. Due to the study of the residual strength and strain energy properties of fish tail palm fiber reinforced concrete, a detailed investigation has to be carried out.

### Declarations:

**Funding:** No funds was received for this research work.

**Conflicts of interest/Competing interests:** The authors state that the work disclosed in this study was not influenced

by any conflicting financial interests or personal relationships.

### Authors' contributions:

Vijayalakshmi Ramalingam: Investigation, Data curation, Writing – original draft

Keerthika Ramesh: Investigation and data curation

Modhagapriyan Arumugam: Investigation and data curation

Vaishnavi Muralidharan: Investigation and data curation

### Acknowledgements

The authors are appreciative to the Sri Sivasubramaniya Nadar College of Engineering for enabling them to perform this research in the lab and for allowing them to use the fish tail palm fibres available on the college campus for research purposes.

### Reference

- [1] V. Mahesh, S. Joladarashi, and S. M. Kulkarni, "A comprehensive review on material selection for polymer matrix composites subjected to impact load," *Def. Technol.*, vol. 17, no. 1, pp. 257–277, 2021, doi: 10.1016/j.dt.2020.04.002.
- [2] M. Z. Hassan, S. M. Sapuan, S. A. Roslan, S. A. Aziz, and S. Sarip, "Optimization of tensile behavior of banana pseudo-stem (*Musa acuminata*) fiber reinforced epoxy composites using response surface methodology," *J. Mater. Res. Technol.*, vol. 8, no. 4, pp. 3517–3528, 2019, doi: 10.1016/j.jmrt.2019.06.026.
- [3] S. S. Kumar and V. M. Raja, "Processing and determination of mechanical properties of Prosopis juliflora bark, banana and coconut fiber reinforced hybrid bio composites for an engineering field," *Compos. Sci. Technol.*, vol. 208, no. March, p. 108695, 2021, doi: 10.1016/j.compscitech.2021.108695.
- [4] K. tak Lau, P. yan Hung, M. H. Zhu, and D. Hui, "Properties of natural fibre composites for structural engineering applications," *Compos. Part B Eng.*, vol. 136, no. September 2017, pp. 222–233, 2018, doi: 10.1016/j.compositesb.2017.10.038.
- [5] P. Kumar and R. Roy, "Study and experimental investigation of flow and flexural properties of natural fiber reinforced self compacting concrete," *Procedia Comput. Sci.*, vol. 125, pp. 598–608, 2018, doi: 10.1016/j.procs.2017.12.077.
- [6] N. Ranjbar and M. Zhang, "Fiber-reinforced geopolymer composites: A review," *Cem. Concr. Compos.*, vol. 107, no. February 2019, p. 103498, 2020, doi: 10.1016/j.cemconcomp.2019.103498.
- [7] J. G. Teng, T. Yu, and D. Fernando, "Strengthening of steel structures with fiber-reinforced polymer composites," *J. Constr. Steel Res.*, vol. 78, pp. 131–143, 2012, doi: 10.1016/j.jcsr.2012.06.011.
- [8] P. Sabarinathan, K. Rajkumar, V. E. Annamalai, and K. Vishal, "Characterization on chemical and mechanical properties of silane treated fish tail palm fibres," *Int. J. Biol. Macromol.*, vol. 163, pp. 2457–2464, 2020, doi: 10.1016/j.ijbiomac.2020.09.159.
- [9] K. Ramanaiah, A. V. R. Prasad, and K. H. C. Reddy, "Fire properties of elephant grass fiber and glass fiber reinforced polyester composites," *Appl. Mech. Mater.*, vol. 592–594, no. July, pp. 380–384, 2014, doi: 10.4028/www.scientific.net/AMM.592-594.380.

- [10] M. M. Kabir, H. Wang, K. T. Lau, and F. Cardona, "Chemical treatments on plant-based natural fibre reinforced polymer composites: An overview," *Compos. Part B Eng.*, vol. 43, no. 7, pp. 2883–2892, 2012, doi: 10.1016/j.compositesb.2012.04.053.
- [11] Ganesh Babu L, "Investigation on the Mechanical and Morphological Characteristics of Caryota Urens Spadix Fibre Reinforced With Polyester Composites," *J. Balk. Tribol. Assoc.*, vol. 26, no. 8, pp. 128–169, 2020.
- [12] G. Sai Krishnan, L. Ganesh Babu, P. Kumaran, G. Yoganjaneyulu, and J. Sudhan Raj, "investigation of caryota urens fibers on physical, chemical, mechanical and tribological properties for brake pad applications," *Mater. Res. express*, vol. 2, pp. 1–15, 2019.
- [13] A. Elbehiry, O. Elnawawy, M. Kassem, A. Zaher, and M. Mostafa, "FEM evaluation of reinforced concrete beams by hybrid and banana fiber bars (BFB)," *Case Stud. Constr. Mater.*, vol. 14, p. e00479, 2021, doi: 10.1016/j.cscm.2020.e00479.
- [14] M. Idicula, S. K. Malhotra, K. Joseph, and S. Thomas, "Dynamic mechanical analysis of randomly oriented intimately mixed short banana/sisal hybrid fibre reinforced polyester composites," *Compos. Sci. Technol.*, vol. 65, no. 7–8, pp. 1077–1087, 2005, doi: 10.1016/j.compscitech.2004.10.023.
- [15] L. Yan, B. Kasal, and L. Huang, "A review of recent research on the use of cellulosic fibres, their fibre fabric reinforced cementitious, geo-polymer and polymer composites in civil engineering," *Compos. Part B Eng.*, vol. 92, pp. 94–132, 2016, doi: 10.1016/j.compositesb.2016.02.002.
- [16] F. Kesikidou and M. Stefanidou, "Natural fiber-reinforced mortars," *J. Build. Eng.*, vol. 25, no. April, p. 100786, 2019, doi: 10.1016/j.job.2019.100786.
- [17] V. Vignesh *et al.*, "Cellulosic fiber based hybrid composites: A comparative investigation into their structurally influencing mechanical properties," *Constr. Build. Mater.*, vol. 271, p. 121587, 2021, doi: 10.1016/j.conbuildmat.2020.121587.
- [18] M. Ali, "Seismic performance of coconut-fibre-reinforced-concrete columns with different reinforcement configurations of coconut-fibre ropes," *Constr. Build. Mater.*, vol. 70, pp. 226–230, 2014, doi: 10.1016/j.conbuildmat.2014.07.086.
- [19] A. Zia and M. Ali, "Behavior of fiber reinforced concrete for controlling the rate of cracking in canal-lining," *Constr. Build. Mater.*, vol. 155, pp. 726–739, 2017, doi: 10.1016/j.conbuildmat.2017.08.078.
- [20] D. S. Mintonogo, W. K. Widigdo, and A. Juniwati, "Application of coconut fibres as outer eco-insulation to control solar heat radiation on horizontal concrete slab rooftop," *Procedia Eng.*, vol. 125, pp. 765–772, 2015, doi: 10.1016/j.proeng.2015.11.129.
- [21] M. U. Farooqi and M. Ali, "Contribution of plant fibers in improving the behavior and capacity of reinforced concrete for structural applications," *Constr. Build. Mater.*, vol. 182, pp. 94–107, 2018, doi: 10.1016/j.conbuildmat.2018.06.041.
- [22] M. S. Islam and S. J. Ahmed, "Influence of jute fiber on concrete properties," *Constr. Build. Mater.*, vol. 189, pp. 768–776, 2018, doi: 10.1016/j.conbuildmat.2018.09.048.
- [23] S. Chakraborty, S. P. Kundu, A. Roy, R. K. Basak, B. Adhikari, and S. B. Majumder, "Improvement of the mechanical properties of jute fibre reinforced cement mortar: A statistical approach," *Constr. Build. Mater.*, vol. 38, pp. 776–784, 2013, doi: 10.1016/j.conbuildmat.2012.09.067.
- [24] S. P. Kundu, S. Chakraborty, S. B. Majumder, and B. Adhikari, "Effectiveness of the mild alkali and dilute polymer modification in controlling the durability of jute fibre in alkaline cement medium," *Constr. Build. Mater.*, vol. 174, pp. 330–342, 2018, doi: 10.1016/j.conbuildmat.2018.04.134.
- [25] S. Pirmohammad, Y. Majd Shokorlou, and B. Amani, "Influence of natural fibers (kenaf and goat wool) on mixed mode I/II fracture strength of asphalt mixtures," *Constr. Build. Mater.*, vol. 239, p. 117850, 2020, doi: 10.1016/j.conbuildmat.2019.117850.
- [26] M. A. Alam and K. Al Riyami, "Shear strengthening of reinforced concrete beam using natural fibre reinforced polymer laminates," *Constr. Build. Mater.*, vol. 162, pp. 683–696, 2018, doi: 10.1016/j.conbuildmat.2017.12.011.
- [27] G. Silva, S. Kim, B. Bertolotti, J. Nakamatsu, and R. Aguilar, "Optimization of a reinforced geopolymer composite using natural fibers and construction wastes," *Constr. Build. Mater.*, vol. 258, p. 119697, 2020, doi: 10.1016/j.conbuildmat.2020.119697.
- [28] J. R. Araujo, B. Mano, G. M. Teixeira, M. A. S. Spinacé, and M. A. De Paoli, "Biomicrofibrillar composites of high density polyethylene reinforced with curauá fibers: Mechanical, interfacial and morphological properties," *Compos. Sci. Technol.*, vol. 70, no. 11, pp. 1637–1644, 2010, doi: 10.1016/j.compscitech.2010.06.006.
- [29] D. Badagliacco, B. Megna, and A. Valenza, "Induced Modification of Flexural Toughness of Natural Hydraulic Lime Based Mortars by Addition of Giant Reed Fibers," *Case Stud. Constr. Mater.*, vol. 13, p. e00425, 2020, doi: 10.1016/j.cscm.2020.e00425.
- [30] O. Benaimeche, A. Carpinteri, M. Mellas, C. Ronchei, D. Scorza, and S. Vantadori, "The influence of date palm mesh fibre reinforcement on flexural and fracture behaviour of a cement-based mortar," *Compos. Part B Eng.*, vol. 152, no. July, pp. 292–299, 2018, doi: 10.1016/j.compositesb.2018.07.017.
- [31] S. Niyasom and N. Tangboriboon, "Development of biomaterial fillers using eggshells, water hyacinth fibers, and banana fibers for green concrete construction," *Constr. Build. Mater.*, vol. 283, no. March, p. 122627, 2021, doi: 10.1016/j.conbuildmat.2021.122627.
- [32] S. P. Kundu, S. Chakraborty, and S. Chakraborty, "Effectiveness of the surface modified jute fibre as fibre reinforcement in controlling the physical and mechanical properties of concrete paver blocks," *Constr. Build. Mater.*, vol. 191, pp. 554–563, 2018, doi: 10.1016/j.conbuildmat.2018.10.045.
- [33] F. Qamar, T. Thomas, and M. Ali, "Use of natural fibrous plaster for improving the out of plane lateral resistance of mortarless interlocked masonry walling," *Constr. Build. Mater.*, vol. 174, pp. 320–329, 2018, doi: 10.1016/j.conbuildmat.2018.04.064.
- [34] A. Wongsa, R. Kunthawatwong, S. Naenudon, V. Sata, and P. Chindaprasirt, "Natural fiber reinforced high calcium fly ash geopolymer mortar," *Constr. Build. Mater.*, vol. 241, p. 118143, 2020, doi: 10.1016/j.conbuildmat.2020.118143.
- [35] B. Çomak, A. Bideci, and Ö. Salli Bideci, "Effects of hemp fibers on characteristics of cement based mortar," *Constr. Build. Mater.*, vol. 169, pp. 794–799, 2018, doi: 10.1016/j.conbuildmat.2018.03.029.
- [36] T. Jirawattanasomkul *et al.*, "Effect of natural fibre reinforced polymers on confined compressive strength of concrete," *Constr. Build. Mater.*, vol. 223, pp. 156–164, 2019, doi: 10.1016/j.conbuildmat.2019.06.217.

- [37] *Plain and reinforced concrete code of practice (IS-456-2000)*, Indian Standard India, 2000. .
- [38] T. F. Yuan, J. Y. Lee, K. H. Min, and Y. S. Yoon, "Experimental investigation on mechanical properties of hybrid steel and polyethylene fiber-reinforced no-slump high-strength concrete," *Int. J. Polym. Sci.*, vol. 2019, 2019, doi: 10.1155/2019/4737384.
- [39] D. Vafaei, R. Hassanli, X. Ma, J. Duan, and Y. Zhuge, "Sorptivity and mechanical properties of fiber-reinforced concrete made with seawater and dredged sea-sand," *Constr. Build. Mater.*, vol. 270, p. 121436, 2021, doi: 10.1016/j.conbuildmat.2020.121436.
- [40] M. S. Islam and S. J. Ahmed, "Influence of jute fiber on concrete properties," *Construction and Building Materials*, vol. 189, pp. 768–776, 2018, doi: 10.1016/j.conbuildmat.2018.09.048.
- [41] W. Wang, A. Shen, Z. Lyu, Z. He, and K. T. Q. Nguyen, "Fresh and rheological characteristics of fiber reinforced concrete—A review," *Constr. Build. Mater.*, vol. 296, p. 123734, 2021, doi: 10.1016/j.conbuildmat.2021.123734.
- [42] X. Wang, J. He, A. S. Mosallam, C. Li, and H. Xin, "The Effects of Fiber Length and Volume on Material Properties and Crack Resistance of Basalt Fiber Reinforced Concrete (BFRC)," *Adv. Mater. Sci. Eng.*, vol. 2019, 2019, doi: 10.1155/2019/7520549.
- [43] R. Prakash, R. Thenmozhi, S. N. Raman, C. Subramanian, and N. Divyah, "Mechanical characterisation of sustainable fibre-reinforced lightweight concrete incorporating waste coconut shell as coarse aggregate and sisal fibre," *Int. J. Environ. Sci. Technol.*, pp. 1–16, 2020, doi: 10.1007/s13762-020-02900-z.
- [44] B. H. AbdelAleem and A. A. A. Hassan, "Influence of synthetic fibers' type, length, and volume on enhancing the structural performance of rubberized concrete," *Constr. Build. Mater.*, vol. 229, p. 116861, 2019, doi: 10.1016/j.conbuildmat.2019.116861.
- [45] S. N. R. R. Prakash, R. Thenmozhi, "Mechanical characterisation and flexural performance of eco-friendly concrete produced with fly ash as cement replacement and coconut shell coarse aggregate," *Int. J. Environ. Sustain. Dev.*, vol. 18, no. 2, 2019.
- [46] C. Unterweger *et al.*, "Impact of fiber length and fiber content on the mechanical properties and electrical conductivity of short carbon fiber reinforced polypropylene composites," *Compos. Sci. Technol.*, vol. 188, no. January, p. 107998, 2020, doi: 10.1016/j.compscitech.2020.107998.
- [47] A. Razmi and M. M. Mirsayar, "On the mixed mode I/II fracture properties of jute fiber-reinforced concrete," *Constr. Build. Mater.*, vol. 148, pp. 512–520, 2017, doi: 10.1016/j.conbuildmat.2017.05.034.
- [48] G. Silva, S. Kim, R. Aguilar, and J. Nakamatsu, "Natural fibers as reinforcement additives for geopolymers – A review of potential eco-friendly applications to the construction industry," *Sustain. Mater. Technol.*, vol. 23, p. e00132, 2020, doi: 10.1016/j.susmat.2019.e00132.
- [49] R. Prakash, R. Thenmozhi, S. N. Raman, C. Subramanian, and N. Divyah, "Mechanical characterisation of sustainable fibre-reinforced lightweight concrete incorporating waste coconut shell as coarse aggregate and sisal fibre," *Int. J. Environ. Sci. Technol.*, 2020, doi: 10.1007/s13762-020-02900-z.
- [50] C. S. Ramaiah Prakash, Rajagopal Thenmozhi, Sudharshan N. Raman, "Characterization of eco-friendly steel fiber-reinforced concrete containing waste coconut shell as coarse aggregates and fly ash as partial cement replacement," *Int. J. Environ. Sci. Technol.*, vol. 21, no. 1, pp. 437–447, 2020, [Online]. Available: <https://onlinelibrary.wiley.com/doi/epdf/10.1002/suco.201800355>.
- [51] A. S. Wahyuni, F. Supriani, Elhusna, and A. Gunawan, "The performance of concrete with rice husk ash, sea shell ash and bamboo fibre addition," *Procedia Eng.*, vol. 95, no. Scescm, pp. 473–478, 2014, doi: 10.1016/j.proeng.2014.12.207.
- [52] *ACI 318-11, Building Code Requirements for Structural Concrete and Commentary*, American Concrete Institute, USA, 2011. .
- [53] *EC-04, Eurocode 2: Design of concrete structures: Part 1-1: General rules and rules for buildings*, British Standards Institution, 2004. .
- [54] *J.C.I, Guideline for control of cracking of mass concrete*, Japan Concrete Institute, Japan, 2008. .
- [55] *N.Z. Standard, Concrete Structures Standard, NZS 3101: The Design of Concrete Structures*, New Zealand, 2006. .
- [56] F. Iucolano, L. Boccarusso, and A. Langella, "Hemp as eco-friendly substitute of glass fibres for gypsum reinforcement: Impact and flexural behaviour," *Compos. Part B Eng.*, vol. 175, no. March, p. 107073, 2019, doi: 10.1016/j.compositesb.2019.107073.
- [57] E. Awwad, M. Mabsout, B. Hamad, M. T. Farran, and H. Khatib, "Studies on fiber-reinforced concrete using industrial hemp fibers," *Constr. Build. Mater.*, vol. 35, no. 2012, pp. 710–717, 2012, doi: 10.1016/j.conbuildmat.2012.04.119.
- [58] R. Prakash, S. N. Raman, N. Divyah, C. Subramanian, C. Vijayaprabha, and S. Praveenkumar, "Fresh and mechanical characteristics of roselle fibre reinforced self-compacting concrete incorporating fly ash and metakaolin," *Constr. Build. Mater.*, vol. 290, p. 123209, 2021, doi: 10.1016/j.conbuildmat.2021.123209.
- [59] F. A. Almansour, H. N. Dhakal, and Z. Y. Zhang, "Investigation into Mode II interlaminar fracture toughness characteristics of flax/basalt reinforced vinyl ester hybrid composites," *Compos. Sci. Technol.*, vol. 154, pp. 117–127, 2018, doi: 10.1016/j.compscitech.2017.11.016.
- [60] N. Divyah, R. Thenmozhi, and M. Neelamegam, "Strength properties and durability aspects of sintered-fly-ash lightweight aggregate concrete," *Mater. Tehnol.*, vol. 54, no. 3, pp. 301–310, 2020, doi: 10.17222/MIT.2019.101.
- [61] D. Zhang, J. Yu, H. Wu, B. Jaworska, B. R. Ellis, and V. C. Li, "Discontinuous micro-fibers as intrinsic reinforcement for ductile Engineered Cementitious Composites (ECC)," *Compos. Part B Eng.*, vol. 184, no. January, p. 107741, 2020, doi: 10.1016/j.compositesb.2020.107741.
- [62] F. Grzymiski, M. Musiał, and T. Trapko, "Mechanical properties of fibre reinforced concrete with recycled fibres," *Constr. Build. Mater.*, vol. 198, pp. 323–331, 2019, doi: 10.1016/j.conbuildmat.2018.11.183.
- [63] X. Zhou, S. H. Ghaffar, W. Dong, O. Oladiran, and M. Fan, "Fracture and impact properties of short discrete jute fibre-reinforced cementitious composites," *Mater. Des.*, vol. 49, pp. 35–47, 2013, doi: 10.1016/j.matdes.2013.01.029.

- [64] X. Zhou, S. H. Ghaffar, W. Dong, O. Oladiran, and M. Fan, "Fracture and impact properties of short discrete jute fibre-reinforced cementitious composites," *Mater. Des.*, vol. 49, pp. 35–47, 2013, doi: 10.1016/j.matdes.2013.01.029.
- [65] S. N. A. Safri, M. T. H. Sultan, M. Jawaid, and K. Jayakrishna, "Impact behaviour of hybrid composites for structural applications: A review," *Compos. Part B Eng.*, vol. 133, pp. 112–121, 2018, doi: 10.1016/j.compositesb.2017.09.008.
- [66] W. Wang and N. Chouw, "The behaviour of coconut fibre reinforced concrete (CFRC) under impact loading," *Constr. Build. Mater.*, vol. 134, pp. 452–461, 2017, doi: 10.1016/j.conbuildmat.2016.12.092.



## Kula Belgrade – Part 2 - Specifics of construction of Kula structure

Nemanja Miljković<sup>\*1)</sup>, Mladen Milićević<sup>1)</sup>, Svetlana Ristić<sup>1)</sup>, Darko Popović<sup>1)</sup>, Vanja Alendar<sup>1)</sup>

<sup>1)</sup> Company DNEC d.o.o. Belgrade, Serbia

### Article history

Received: 04 February 2022

Received in revised form:

22 February 2022

Accepted: 25 February 2022

Available online: 31 March 2022

### Keywords

Tall building construction  
Piles Ø1200mm,  
Osterberg cell test,  
Raft concreting in volume of 4750m<sup>3</sup>  
Construction of transfer structure  
Construction of PT slabs

### ABSTRACT

Kula Belgrade is the tallest building within the Belgrade Waterfront Project located on the right bank of the Sava River. It is envisaged as the future landmark of Belgrade and the pivotal point of Belgrade Waterfront development. It consists of a 168m high - 42 storey tower, a podium and an eccentric basement. It is one of the rare towers in the world in which the bottom and the top parts are mutually rotated by 90° in plan and where such a transition is achieved through 7 floors - a configuration that imposes significant demands to the structure. While the 1st part of the article addressed specific topics related to design, this 2nd part is about the specific topics related to the construction of Kula Belgrade's structure, including the enabling works, construction, and testing program of piles that comprised various types of tests, including the static compression test by Osterberg cell at two tower piles with a 1200 mm diameter. The article also addresses the construction of foundations, which included the concreting of a raft under the tower in volume of 4750m<sup>3</sup> cast in one turn, the execution of core walls in jump form, the distinctive transfer structure and PT slabs.

## 1 Introduction

While the first part of the article[1] addressed the specifics of the design process, this second part covers the key items related to Kula construction, including: testing and execution of piles, enabling works, concreting of raft (part below the tower – approximately 4750m<sup>3</sup> was concreted in one turn), works on the superstructure, specific transfer structure and PT slabs.

The first works conducted on Kula site, prior to any listed above, were the works on unexploded object detection (UXO) by company PMC Millennium in 2016.

When the Piling Contractor (Novkol) entered the site later that year, they formed a working platform for the execution of testing and working piles at the level of partially excavated terrain by the UXO Contractor. The Investor „BW Kula“, Ltd. awarded supervision on piling works to MACE. First tests of piles were done in 2016., while the construction of working piles took place in 2017. Darko Božić, BSc, CEng was the pile construction's responsible engineer.

Once the building permit for main works was obtained, early in 2019., the main contractor, Pizzarotti MillenniumTeam (PZMT) overtook the site from Novkol and proceeded with further excavations to the final levels. Upon the excavations, the piles were cropped to design cut off levels by Novkol and handed over to the Main Contractor.

Nenad Marković, MSc, CEng, was the responsible engineer for Kula construction.

Only then could the work on Kula structure have started. Supervision at this stage of the project was conducted by DNEC.

## 2 Testing and construction of piles and enabling works

Enabling works were conducted under a separate building permit, which included excavations as well as the testing of two tower test piles by the Osterberg cell method. Additionally, a whole series of pile tests were performed, with the aim of testing geotechnical parameters provided by the Geotech report [2], as a basis for design as well as piling construction methodology, so the overall pile testing process covered the period from the early stages of design up to the completion of pile construction.

In accordance with the Lex Specialis, execution of working piles was also conducted under a separate building permit, actually two of them – one for the tower and podium piles and the other for plaza piles.

\* Corresponding author:  
E-mail address: [nemanja.miljkovic@dnec.com](mailto:nemanja.miljkovic@dnec.com)



Figure 1. Kula Belgrade Progress of Construction– Sept. 2018 (bottom left), May 2019. (top left), May 2020. (bottom middle), January 2021 (top middle), January 2022 (right)

## 2.1 Piles testing

A description of the conducted tests is given below:

### **The Osterberg cell test for static testing of tower piles ( $\varnothing=1200\text{mm}$ )**

This test was conducted as the first in a series of tests while the design of the structure was still in its early stages in 2016. The aim of the test was to confirm the numerical parameters provided by Geotech report [2], as well as the construction methodology. Two test piles with a diameter of 1200 mm in the zone of the tower were tested. After the test, they remained in the ground but were not used as structural supports.

Having in mind the projected bearing capacity of 23.6MN (Geotech report [2]), it was concluded that a conventional experiment with anchor piles would not be economical, so the Osterberg cell method was adopted, which is standard in countries with a large volume of high-rise construction. To the knowledge of the author of this text, this was the first application of the O-cell test in Serbia.

The main advantage of this method is that by the installation of a hydraulic jack in the body of the pile, the parts above and below the jack are in balance with each other, so it is not necessary to make reactive piles and a structure for load transfer.

The tests were performed by Novkol with subcontractors Fugro and Loadtest from England. A force value of 44MN measured on the jack was adopted as a criterion of success for the test. This force corresponded to a pile working load of 22MN (calculated by SOM) with a safety factor of 2.0.

Upon the failure of the first test on two piles in June 2016., it was concluded that the excavation in the upper strata (top 22m) had to be under the protection of casing to prevent the collapse of soil onto the bottom of the borehole. Furthermore, any loose material that remained after the boring had to be removed in order to allow the activation of the base capacity.

At the repeated testing in November 2016, total forces of 55 and 66MN were achieved (Ref.[3]). Subsequent analysis of the test report by the company Terracon from Chicago estimated the load capacity of piles  $\varnothing = 1200\text{mm}$  of 25.8MN with a stiffness of 1100 MN/m, and for piles  $\varnothing = 1000\text{mm}$  of 5.9MN with a stiffness of 300 MN / m (Ref. [4]). The bearing capacity reported in Geotech report [2] of 23.6 / 5.0MN was adopted in the design, for piles  $\varnothing = 1200\text{mm}$  /  $\varnothing = 1000\text{mm}$ , respectively, while the stiffness values were adopted based on Terracon's recommendation. In addition to the fact that these tests confirmed the values of the design parameters, they also confirmed the construction methodology, so the same procedure used during the construction of test piles was applied during the execution of working piles.

### **Static testing of basement structure piles ( $\varnothing=1000\text{mm}$ ) by reactive piles method**

All piles with a diameter of 1000 mm are adopted 25 m long, so that their base is at a depth of at least 8.5 m into a layer of marl. The aim of static tests was to directly confirm the numerical parameters of this type of pile, as well as the methodology of their construction.

The tests were performed by the Novkol company with the subcontractor Geomehanika from Belgrade in April 2017. Two groups of 4 reactive and one test piles were constructed for the purposes of the test.

Measured settlements at a working force of 5MN were 5 and 9 mm, while at a maximum test force of 10MN, they were 13 and 37 mm, respectively on piles TP1\* and TP2\*, or 1.3 and 3.7% of the diameter of the piles (Ref [5]). Both of these were in accordance with the adopted Weltman's criterion (settlements in range of 5-10% of the pile diameter), so it was concluded that both piles have a safety factor greater than two, and that they have the required bearing capacity. Excavation under the protection of the steel casing was adopted for this group of piles, too, for the full length of the pile.

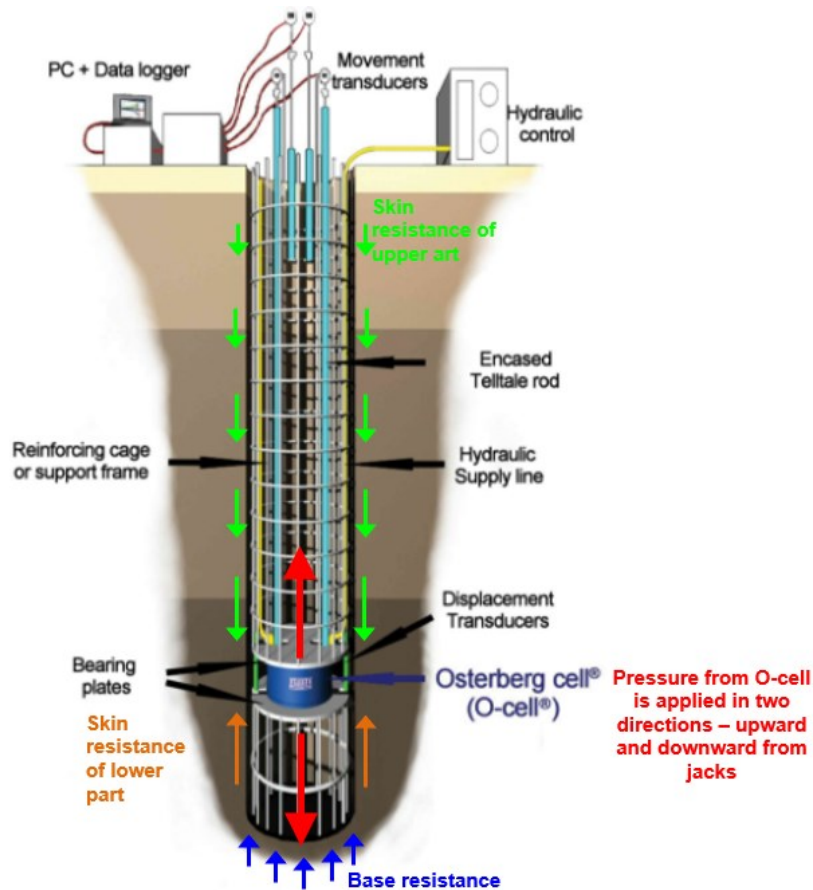


Figure 2. Illustration of principle of O-cell test - Downloaded from <http://www.loadtest.com/services/ocell.htm> - comments in colored text were added by Author



Figure 3. O-cell installed into the pile rebar cage (left) and insertion of rebar cage with O-cell into the borehole (right)

**Cross-hole logging method for pile integrity testing**

The tests were conducted in August 2017. by the Novkol company with a subcontractor, SLP from Slovenia, on working piles in order to check the integrity and continuity of the concrete piles. Four PVC inspection tubes with a diameter of 100 mm were installed in the pile bodies. During the test, probes were inserted into pairs of tubes filled with water - the emitter in one, the signal receiver in the other. The ultrasonic waves were emitted in a combination of pairs - four at the perimeter and two across the diameter, thus

covering the most of the cross section of the pile. 100% of piles  $\varnothing = 1200\text{mm}$  and 20% of piles  $\varnothing = 1000\text{mm}$  were tested. Values in the range of 2700-3300 m/s have been adopted for the minimum acceptable speeds of the ultrasonic wave. On the most of the piles, recorded average speeds were in the range of 3800-3900m/s, which was a very good result, while on 5 piles there was a loss of signal at the top, and on one pile a speed of 3200m/s was measured, at a depth of 25-30m (Ref. [6]). According to the interpretation of the results by the company CSL, the potential reason for such a result was the separation of embedded PVC pipes

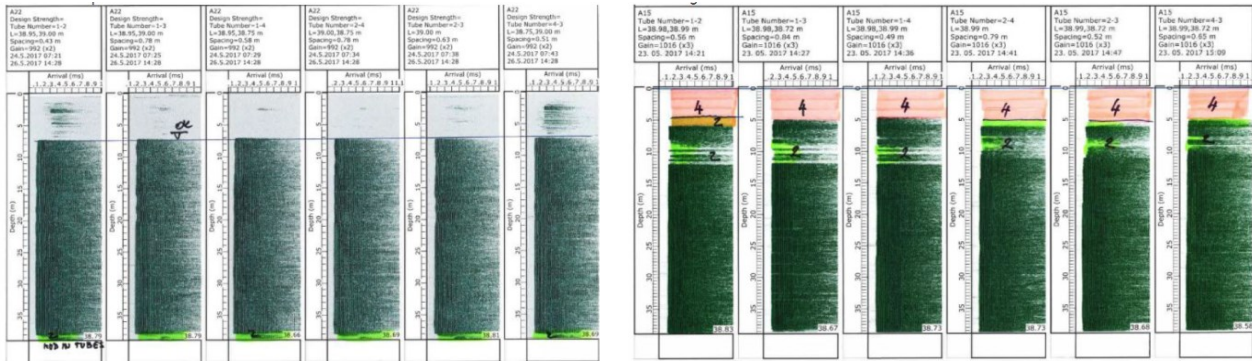


Figure 5. CSL testing records –for a pile with correct record (left) and a pile with a loss of signal at the top of the pile (right) – taken from SLP d.o.o. Ljubljana, report: CHA053-05B-2016 Beograd Waterfront Plot 19.1, August 2017.

from the concrete of the piles. In order to prove this, coring was conducted on all 6 piles, with worse results. Based on the visual inspection of the cores, it was determined that the piles had integrity, and based on the breaking of the cubes conducted in the IMK laboratory at the Faculty of Civil Engineering in Belgrade, it was shown that concrete also had sufficient strength.

**Dynamic pile testing by falling weight and numerical capwap interpretation of results.**

The tests were conducted in August 7 by the Novkol company with the subcontractor SLP from Slovenia in order to check the load-bearing capacity of the working (production) piles. 20% of piles  $\varnothing = 1200\text{mm}$  and 5% of piles  $\varnothing = 1000\text{mm}$  were tested. As a criterion of test success, the force of at least 47.2MN / 10.0MN for piles  $\varnothing = 1200 / 1000\text{mm}$  was adopted, which corresponds to twice the calculated bearing capacity of piles (Geotech report [2]) of 23.6MN / 5.0MN, respectively.

The first part of the test measures the dilatation and acceleration of the shock wave caused by the fall of the weight and the wave bounced off the base, which are converted into wave force and speed and displayed on a graph as a function of time. Then Numerical CAPWAP analysis, which uses the equations of wave motion, determines the static bearing capacity of the pile at the base and shaft.

The results of the CAPWAP analysis were in the range of 48.6 - 68.7MN for piles  $\varnothing = 1200\text{mm}$ , while for piles  $\varnothing = 1000\text{mm}$  they were in the range of 6.7 - 23.4MN. On 5 of the 11 tested piles, which are located on the Northside of the plot, the force estimated by the CAPWAP method was less than the required 10MN, so the bearing capacity was estimated as less than 5.0MN (Ref. [7]).

Based on the additional numerical analysis that compared the calculated forces with the capacities obtained by tests, the following was concluded:

- Pressure: Only on 2 out of 208 piles with diameter  $\varnothing = 1000\text{mm}$  the calculated force was higher than the bearing capacity adopted by averaging the test results by zones. The maximum design force of 3.85MN exceeds the load capacity of 3.5MN (adopted for the zone between the J-L axes) by 9.8%. Based on the diagrams given in the test report, the piles at this level of force are still in the linear range, so that these 2 piles would have a settlement greater than 1 mm compared to the settlement corresponding to the allowable

force value, so there would be no significant consequences for the raft and the rest of the structure.

- tensile: the design forces do not exceed the tensile capacity estimated on the basis of a dynamic test.

According to these results, it was assessed that the piles achieved sufficient capacities.



Figure 6. Testing by 42t falling weight from the elevation of 0.3 to 1.5m

**PIT testing**

This is another type of test that checks the continuity and integrity of the piles. It was conducted in 2019 by MACE, as a part of the procedure of handing over the piles to the Main Contractor (Ref. [8]). All 270 piles were tested.

In addition to the measuring of the speed of the wave caused by the impact of a hand hammer on the top of the



### 3 Construction of raft

The foundation slab, with a total volume of 14000m<sup>3</sup>, was concreted in the multiple pours shown in the picture below. Parts outside the tower zone are divided into more than ten parts.

Part of the slab in the tower zone was divided vertically in two pours (1.1 and 1.2 in the above figure). The deeper one (1.1) was located in the zone of elevator pits. It was 2.8 m thick, about 400m<sup>2</sup> in plan with a volume of 1150m<sup>3</sup> and was cast the first.

The thickness of concrete in pour 1.2 ranged from 2.8 to 4m with an area of about 1600m<sup>2</sup>, so the total volume of concrete was app. 4750m<sup>3</sup>.

Such configuration imposed significant challenges both in terms of reinforcement and concrete works. In the former case, the Contractor had to provide stability of rebar cage. This was achieved by the adoption of two chairs  $\Phi 32$  with 2 legs per square meter. They were horizontally interconnected and braced by inclined bars along the perimeter of the zone.

In terms of concrete works, the volume of 4750m<sup>3</sup> may be regarded as one of the biggest concrete in Belgrade, ever. Decision to cast it in one turn was based on two reasons - division into smaller parts was basically impractical and division by height was discarded as to avoid the formation of cold joints.

This large amount of concrete required careful selection of the components of the concrete mix. This primarily refers to the type of cement - CEM III / B (cement with over 65% slag) was used, which reduced the risk of thermal cracks in mass concrete. The reduced mobility / workability of concrete with such cement was overcome by the use of hyperplasticizers. The large concrete casting area, as well as the logistics of concrete supply from several factories, demanded the provision of a significant time reserve, which was achieved by using retarder admixtures that delayed the starting of the setting of concrete for not less than 16 hours.

This enabled concreting in horizontal layers 40-45 cm thick (in deeper parts with a smaller working area) up to 20 cm (in the upper parts) and to start the casting of the next layer prior to the setting of the previous layer. Adjacent vertical layers were interconnected by vibration.

Concrete grade C40 / 50 was produced by Gradient, Nexe and Karin Komerc factories, in a total of 6 factories with a production capacity of 45 to 77 m<sup>3</sup>/h. Over 30 mixers participated in the delivery of concrete. Three pumps were used simultaneously, and the fourth one was in reserve.

Casting was done in August 2019 and took about 60 hours. Over 70 people participated in the action under the constant control of the contractor's quality team, as well as the constant supervision of DNEC.

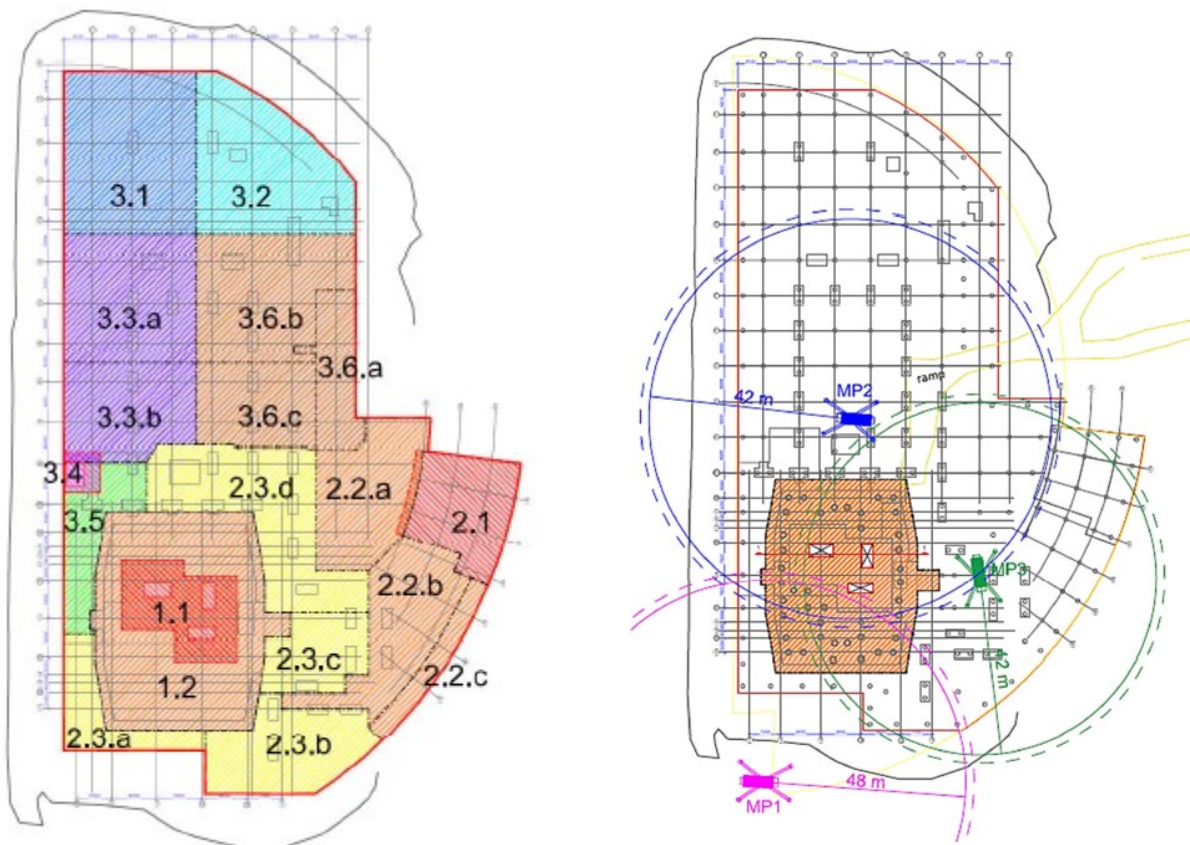


Figure 9. Plan of pours for Kula raft (left) and plan with location of concrete pumps for the pour under the tower (right) – taken from RS\_BW\_P19.1\_C\_025\_PZM\_MST\_0006\_Rev.02\_Site-Specific Method Statement for Raft pouring



Figure 10. Reinforcement works on pour 1.2 – raft pour under the tower

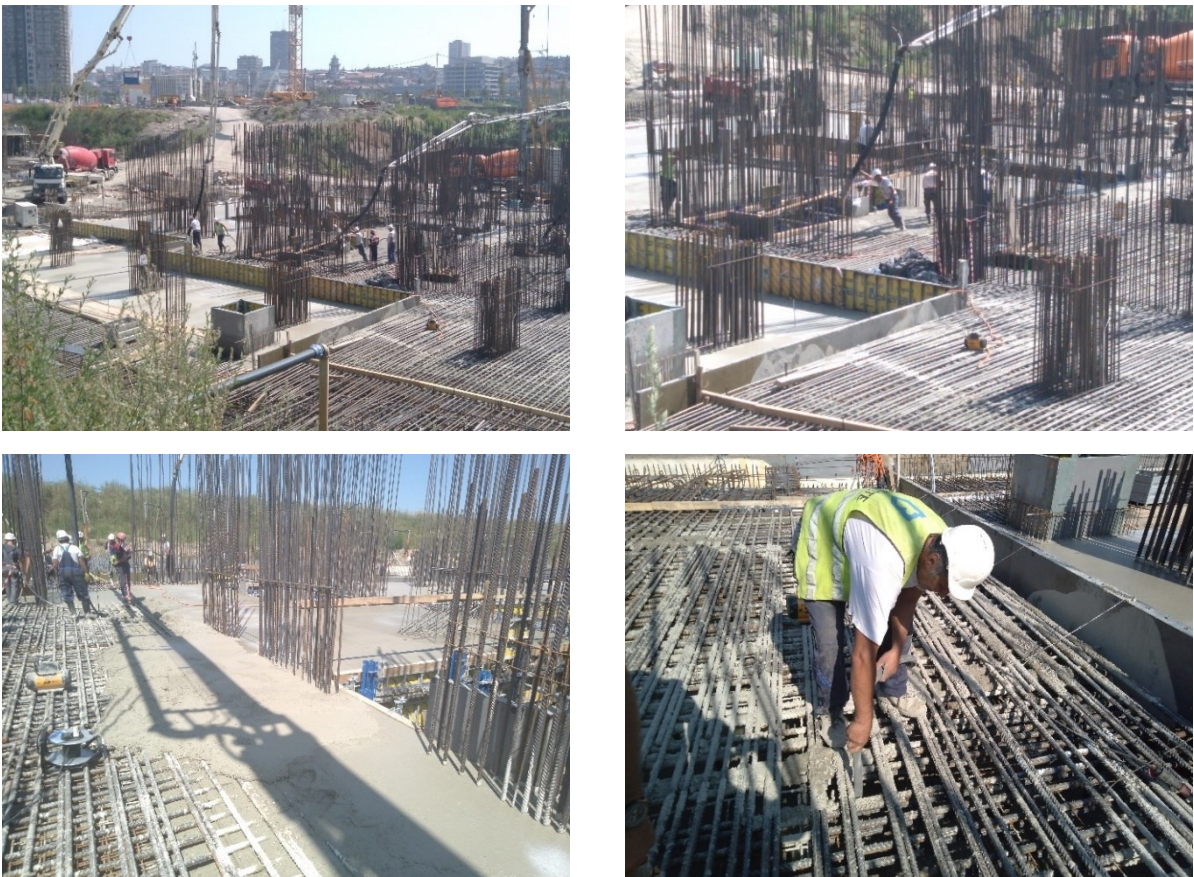


Figure 11. Casting of raft pour 1.2 under the tower

#### 4 Superstructure

During the summer of 2019, it was not only that the raft under the tower was cast, but also several parts of the raft under the basement structure were completed. This enabled simultaneous progress both on the basement and the tower superstructure.

##### 4.1 Corewalls

Kula's core walls were constructed in jump form. Doka's automatic climbing formwork SKE 50 plus was used to jump / climb the core with hydraulic jacks. They were cast in Doka's shuttering system Top 50, which was constructed in height of 4.1m to allow for concreting in one turn of all typical storeys with a height of 3.45m and most of the non-typical storeys. In the case of storeys with a height greater than 4.1m such as GF, Level 2, 11, 12, 19 and 39 to 42, they were cast in two steps. In total, there were 52 castings and 57 climbing steps from B1 level up to the top roof to achieve the cores, starting from level -7.97 and reaching a level of +168m (relative to Architectural zero level).

Reinforcement of wall segments as well as for link beams (described in the 1st part of the article) was prefabricated on the ground, lifted and installed into the shuttering by crane. Horizontal U bars at the wall ends were added.

Reinforcement assembly also included bent out elements by Bindax Company. They were to allow connecting of slabs to core walls.

Based on design requirements, staggered lapping of vertical rebars (50% in one section) was adopted from raft to Level 5 (base of the core, large openings) and from Level 12 to 15 (transfer of forces between central and satellite cores), while on all other levels, 100% of vertical rebars were lapped in one section.

The concrete grade was C50/60. The mix was designed to enable optimum workability with fresh concrete. A concrete placing boom was installed within a core and was jumped together with the formwork. It was used for the concreting of all tower members: core walls, columns, slabs, and beams. Typically, for this construction method, core walls were ahead of slabs for 3-4 storeys. This gap in progress between the walls and slabs was limited by the headroom for the crane above, the jump form and the reach of placing the boom below.

In general, the minimum time for shuttering was 12hours. However this timing was adjusted for concreting in cold weather conditions when thermo couples were built into the walls to provide information about the temperature within a wall that allowed to contractor and engineer to decide on shuttering stripping time.



Figure 12. Construction of core walls in jump form



Figure 13. Link beam reinforcement with Bindax pullout boxes on top - installed into wall rebar cage (left and middle) and core wall reinforcement (right)

## 4.2 Transfer structure

### Transfer columns

As described in the first part of the article, columns located in the corners of the plan are sloped in the transition zone (between Levels 12 and 20), while six central columns (East and West from the central core) branch at Level 14-15 into pairs of columns. The ones closer to the core keep verticality all the way, while the outer ones slope from Level 15 to Level 20 where they turn vertical up to the top of the building. The corner columns are circular, while the branched ones are rectangular.

A very high utility ratio, primarily in terms of axial forces was common to all transfer columns. They were designed as reinforced concrete columns, with a reinforcement percentage of 4% outside lap locations, which corresponded to the maximum percentage of reinforcement defined by Eurocode 2 [9]. Since the column rebar was found to be in compression for all design combinations, 100% of the rebar was lap spliced per section.

Due to the high rebar ratio, as well as the specific geometry of the columns, in addition to high compressive strength, good workability of concrete was required, too. This led to the use of high-performance basic materials such as cement CEM I 52.5R and aggregates of eruptive origin. In order to achieve the required compressive strength, as well

as the time required for transport which took about 1 hour and weather conditions that were an additional unfavourable circumstance (summer), using the appropriate combination of chemical admixtures, concrete of consistency class S5 was delivered to the construction site. For concrete, grade C55/67 was adopted. To the knowledge of the author of this text, such a grade was to be applied for the first time in Serbia by the concrete factories that supplied the Kula site.

Upon the completion of rebar cage, columns of circular cross-section were made in a circular formwork called DOKATop 50, which consisted of two semi-circular parts connected by bolts. Sloped columns of rectangular cross-section were constructed in the DOKA Framax system. At the point of column branching (Levels 14-15), a joint, outer aluminium shuttering, enclosed both branches, while they were internally divided by a wooden partition.

Stability during the construction stage was provided by steel strut stabilizers.

Two days after the casting, the upper part of the formwork was removed. Their surface was covered with geotextile to ensure further curing of concrete. The lower part of the formwork was removed once 70% of the designed strength was reached, but not less than 5 days after concreting. After removal of the formwork, the columns were re-propped for additional 5 days.



Figure 14. Construction of circular transfer columns Level 12-14 (left) and Level 16-17 (right)

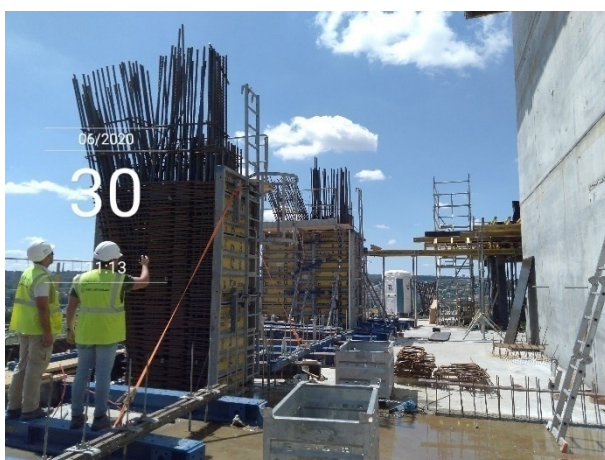


Figure 15. Construction of transfer branching columns Levels 14-15 (left) and Levels 15-16 (right)

**Transfer slabs and beams for lev 12, 14, and 20**

As described in the previous text, kinking of transfer columns at Levels 12, 14 and 20 originated turn forces in horizontal planes, which in some cases acted towards the core and in some away from it, tending to split the slabs on these levels. The tying reinforcement and tendons adopted in prestressed beams restrained these tension forces.

In the case of rebar ties, there were 5 $\Phi$ 32 in the top and bottom zone on Levels 12, 10  $\Phi$ 32 in top and bottom zone on Lev14, and all of  $\Phi$ 32 bars on Level 20 that had to be spliced by mechanical couplers. As the Halfen MBT type, popularly called the „crocodile“ did not require the turning of bars, it was adopted. Instead, the bars are just inserted into a coupler and fixed to it by bolts, tightened until they snap. In case that any of the bolts did not reach the final position, the coupler was discarded and replaced by a new one.



Figure 16. Transfer beams on Level 12 (top row) and on Level 20 (bottom row) – details of coupled bars (bottom left) and discarded coupler (bottom right)

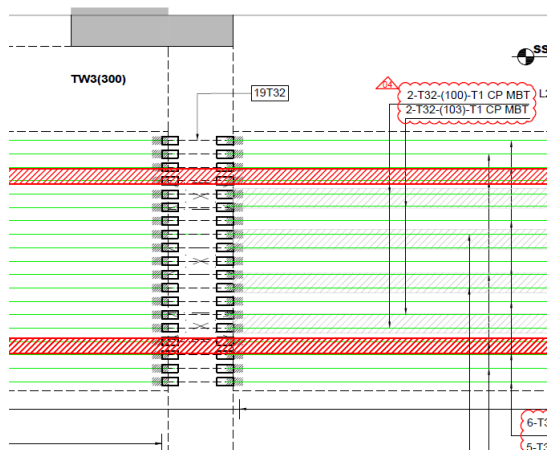


Figure 17. Lenton couplers for Transfer beam on Level 20 at core wall in Contractor's shop drawing (left) and on site (right)

Another type of rebar splicing was adopted at the faces of the core walls where threaded Lenton couplers were used.

Another specific issue was the geometry of transfer slabs. While the slabs were shrinking from Level 12 to 20 in a North-South direction (direction parallel to the Sava River) they expanded in a perpendicular direction. Accordingly, there was an issue of access and supporting shuttering in the East-West direction because the upper slabs were projecting out of the perimeters of the lower ones. The issue was resolved by the application of Doka Staxo towers that were fixed to the structure by a system of anchors and lashing straps.

#### 4.3 Slabs of pt on the hotel and residential levels

As described in the first part of the article, typical slabs on hotel and residential levels were designed as PT slabs. This included slabs from Lev03 to 11 (hotel levels), 16, 18, 19, and 21 to 39 (residential levels), so the great majority of Kula slabs.

The PT works were assigned to PT Subcontractor, company Strong Force Balkans, daughter company of Australian Strong Force, while the reinforcement works were conducted by Construction Centre Manojlović company from

Serbia, while the main contractor coordinated them at all work stages.

Having in mind the dimensions of slabs which extended up to 45m in one direction, each PT slab was divided in the design stage into two pours. This was also practical in terms of the organization of work because it allowed for the parallelization of work. The Contractor achieved casting adjacent horizontal / vertical pours in a 2 / 4-day span, respectively, on some of the residential slabs. The slab under construction was propped and supported by three slabs below. The density of propping on the lowest of three levels was 50% of that of the two upper ones.

The PT system consisted of 12.7mm mono strands. They were inserted by a cable pusher machine into the flat ducts with 3 to 5 slots to form the tendons. A live anchor was mounted at the tendon end at the outer perimeter of the slab, or at the pan box in case it was not designed to reach the slab end. Dead end anchors were formed on site by the onion jack tool and stressing pump. Both ends were supplied by anti-burst spiral reinforcement. Tendon profiling was achieved by fixing the tendons to the plastic chairs at the required height, adopted at approximately 1.0-1.2m spacing, and stapled to the wooden shuttering with a heavy duty stapler to secure their geometry during the concreting.

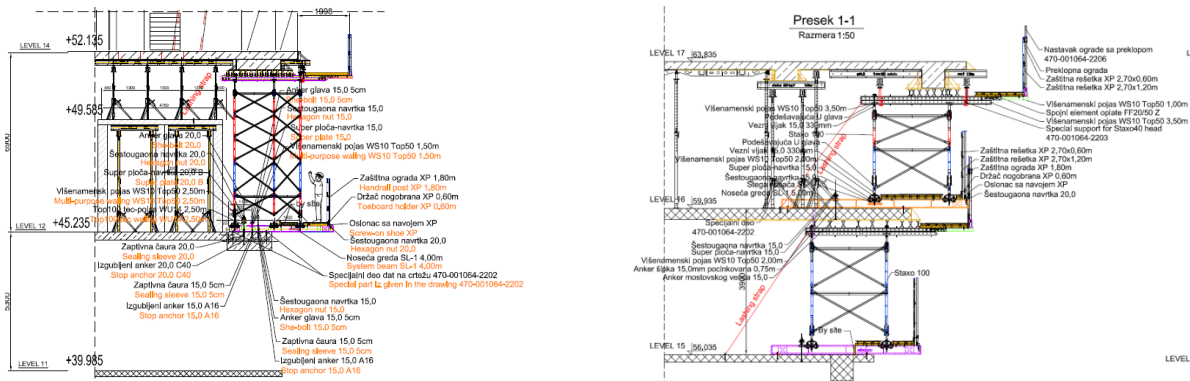


Figure 18. Illustration of extension of slab edges on transfer levels - Levels 12-14 (left) taken from RS\_BW\_P19.1\_C\_025\_PZM\_DDC\_0048\_Rev.00\_Doka Formwork Plans\_L12 formwork Platforms supporting L14 Slab and Levels 15-17 (right) – taken from RS\_BW\_P19.1\_C\_025\_PZM\_DDC\_0058\_Rev.01\_Doka\_Formwork Plans and Platforms supports for L17



Figure 19. Live end with pan box (left) and formation of onion head dead end (right) (both obtained from Contractor's document Method Statement for Post-tensioning works RS\_BW\_P19.1\_C\_025\_PZM\_MST\_0021\_Rev.00\_Post Tensioning Works)

Stressing was conducted in two stages. Stage 1 took place approximately 12 hours after the casting, but not before the concrete cube strength reached 10MPa. It was done to the level of 25% of the total jacking force. The remaining force was applied once the concrete cube strength reached 25MPa (the design concrete grade was C40/50), which was usually less than 48 hours after the casting. The total jacking force was set at 80% of the ultimate tensile strength of the strands, or 1480MPa = 0.8\*1860MPa.

Elongations measured during the stressing were submitted for the engineer's approval in a form of a stressing record report, and only after the approval of the Engineer the cutting of strands was conducted.

The grouting was usually done within a 2-3 week span after the stressing of tendons under the engineer's supervision.

As for the reinforcement works, it is interesting to mention that the slab capacity in terms of punching shear was provided by double headed Halfen studs with a 12mm diameter welded to Halfen HDB shear rails, that were inserted into the installed slab reinforcement. Due to the

requirements in energy efficiency regulations, the balconies had to be completely thermally insulated from the main slab. This was achieved by thermal connectors made by Forbuild Company. The connector consisted of a central part made of thermal insulation, through which two steel plates were embedded to enable the transfer of shear forces, while the moment action was enabled by straight rebars placed on the top of the section and three high strength bearing blocks placed at the bottom to transfer compression forces.

In terms of work related to formwork and shuttering, it is worth mentioning that all the slabs above level 11 had to follow pre-setting schemes adopted during the Value Engineering design by which the perimeter of the slab was supposed to be executed higher than the centre of the slab to allow the slab to achieve horizontal geometry once the differential settlements between the core and columns take place over the years of service. Typically, the difference in levels was 10mm up to level 20 (dark blue hatch on below figure), but it was 20mm on residential levels (21–40) (green hatch on below figure).



Figure 20. Mono strand stressing jack (left) and measurement of achieved elongations (right) (both obtained from Contractor's document Method Statement for Post-tensioning worksRS\_BW\_P19.1\_C\_025\_PZM\_MST\_0021\_Rev.00\_Post Tensioning Works)



Figure 21. Halfen shear rails with double headed studs (left) and thermal connector at balcony location (right)







## Improving the punching shear and shear capacity of reinforced concrete elements with a new post-installed retrofitting system

Dr. Jochen Buhler<sup>\*1)</sup>, Danijel Vilotijevic<sup>2)</sup>

<sup>1)</sup> Adolf Würth GmbH & Co.KG, Germany

<sup>2)</sup> Würth d.o.o. Beograd, Serbia

### Article history

Received: 17 November 2021

Received in revised form:

02 March 2022

Accepted: 05 March 2022

Available online: 31 March 2022

### Keywords

Strengthening method,  
Reinforced concrete,  
Shear resistance,  
Punching shear resistance

### ABSTRACT

Finding appropriate strengthening solutions for existing reinforced concrete (RC) elements is always a challenge for structural engineers. Additional load capacity may be needed as the change of type of occupancy and more restrictive design standards require higher load levels or different detailing of reinforcement.

This paper introduces a post-installed retrofitting system consisting of an adhesive and a concrete screw anchor that can be used to improve either the pure shear capacity or the punching shear capacity of a RC beam or slab. This post-installed retrofitting system acts as shear reinforcement that can be installed with relatively minimal disruption as it is only installed at the soffit of the RC element being strengthened. The system was tested for its suitability and the results were approved by the German Construction Authority with a National Technical Approval. Published parameters are used for the standard methods of detailing shear and punching shear of a RC element according to EN1992-1 and EN1992-2. Calculations and tests have shown that with the use of this post-installed retrofitting system, the shear strength of existing concrete elements can increase by up to 100% and consequently increase the lifetime of a structure. This paper also discusses the test methods employed, the test results, and sample projects that made use of the said system. Another important finding is the substantial savings in project cost attributed to the installation methodology that comes with the system.

## 1 The post-installed retrofitting system

### 1.1 Description of the system

The post-installed retrofitting system employs bonded concrete screw anchors. This system consists of two essential components, a self-tapping concrete screw anchor and a two-component injectable organic adhesive, as shown in Figure 1. The concrete screw anchor transfers forces to the concrete member via a mechanical interlock between the screw anchor thread and the hole cavity. This mechanical interlock is achieved during the installation of the screw anchor, where thread tapping into the wall of a pre-drilled hole occurs. The adhesive, on the other hand, bonds the screw anchor to the hole cavity. Mechanical interlock transfers loads immediately after installation, while the bond effectively adds capacity after the adhesive becomes fully cured. "RELAST" is the proprietary name of this hybrid post-installed retrofitting system.

Although the system is composed of known post-installed anchor components, it is not considered as a post-installed anchor. Its evaluation and force-transfer mechanism is like a

cast-in rebar. As such, the related design approach is therefore not covered in EN 1992-4:2018 "Design of post-installed and cast-in fastenings in concrete". However, EN 1992-1 "Design of concrete structures – Part 1-1: General

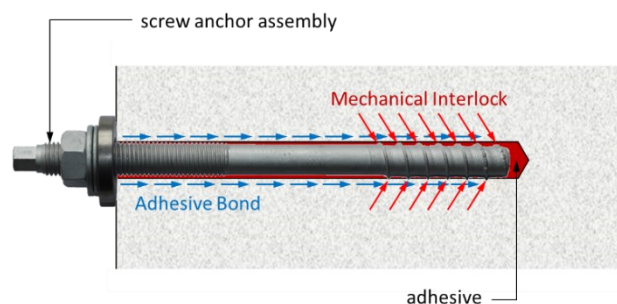


Figure 1. Würth RELAST bonded screw anchor and its load-transfer mechanism.

\* Corresponding author:

E-mail address: [jochen.buhler@wuerth.com](mailto:jochen.buhler@wuerth.com)

rules and rules for buildings” and in EN 1992-2 “Design of concrete structures – Part 2: Concrete bridges – Design and detailing rules” provide guidance for designing shear and punching shear using RELAST.

## 1.2 Scientific research, test and assessment, technical product specification

The components that make up RELAST are post-installed anchors which were successfully assessed and granted construction approval many years back in Europe. The European assessment covers the following aspects:

1. characteristic resistance to tension or shear,
2. sensitivity to different installation and service temperatures,
3. freeze/thaw conditions,
4. increased concrete crack width,
5. crack cycling under load,
6. repeated loads,
7. sustained loads,
8. various environmental exposure such as high alkalinity and sulphurous atmosphere,
9. the robustness of the anchor when installed in dry and water saturated concrete with different installation directions.

The mentioned approval, enabled the anchor to be designed and used in various structural anchoring applications successfully.

Since RELAST and its ‘retrofitting use’ do not fully align with post-installed anchoring models, additional tests and assessments were conducted to get construction approval for retrofitting applications. During a period of approximately

7 years, a number of large scale tests helped to investigate the real behaviour of the RELAST system.

Real-life retro-fitting on several bridges and buildings in Germany and Austria demonstrated the practicability of the system.

The additional large scale tests were conducted at the University of Innsbruck and at the Universität der Bundeswehr München (Fig. 2 and 3.).

### 1.2.1 Laboratory tests related to the shear capacity

Four-point bending tests on reinforced concrete beams with a span of 3.5m were setup to investigate the influence of screw anchor size/type, arrangements of bonded/unbonded installation, and anchoring depth (Fig 4.), to the shear performance of the beam.

Further 4-point tests on one-way slabs investigated the influence of the slab height.

Three pulsating load tests were conducted to evaluate the performance of retro-fitted beams under  $5 \times 10^6$  load cycles. The amplitude of the load applied, had a lower bound equal to one-third of the static ultimate load and the upper bound was two-thirds of the static ultimate load. No failure was identified.

The test setup and the results are described in detail by Lechner in [2]. The results of the test show that the retro-fitted beam achieved at least 100% shear capacity improvement compared to components without shear reinforcement.

Based on above tests, the characteristic values used for the design were derived and are detailed in the corresponding Technical Product Specifications Z-15.1-344, published in October 2019 [3].

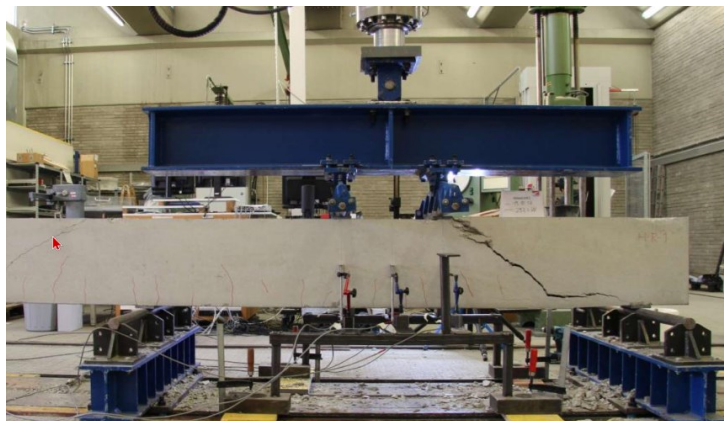


Figure 2. Large scale shear tests [1]



Figure 3. Large scale punching shear tests [1]

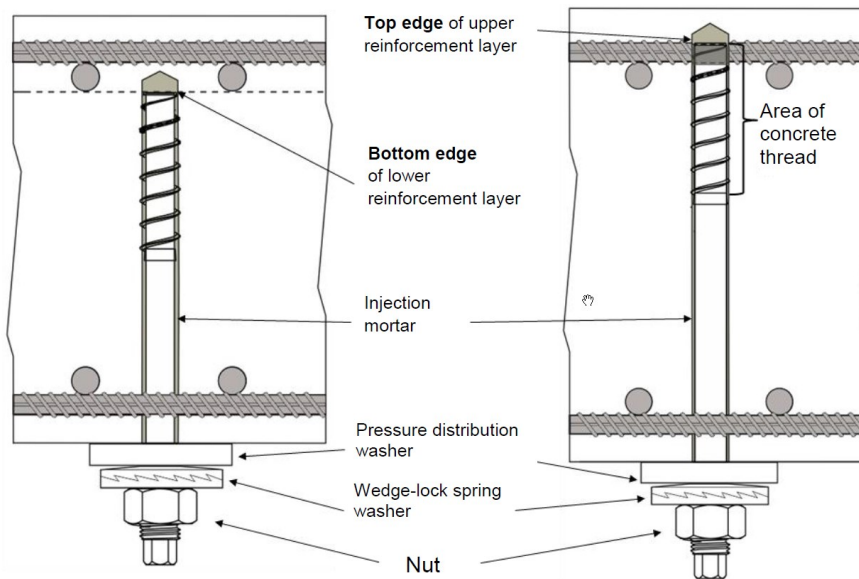


Figure 4. Optional installation conditions

### 1.2.2 Laboratory tests related to the punching shear capacity

The test rig of the very first punching shear tests is shown in Figure 5. In this test, 32 bonded concrete screw anchors in 8 radial rows of 4 were installed (Fig. 3).

Based on the results obtained from the tests described above, two research projects investigated the influence of screw anchor size/type, arrangements of bonded/unbonded installation, anchoring depth, and different ratios of the longitudinal reinforcement to the punching shear performance of the test specimen.

Pulsating loads on the retro-fitted slab with  $2 \times 10^6$  load cycles and a load amplitude calculated from a lower bound

equal to one-third of the static ultimate load and the upper bound equal to two-thirds of the static ultimate load, did not result in visual signs of damage. Residual static punching afterwards resulted in a failure load equivalent to the static ultimate load.

The test setup and the results are described in detail by Lechner in [2]. Summarily the retro-fitted components achieved up to 40% punching shear capacity improvement compared to components without punching shear reinforcement.

Based on the above tests, the characteristic values used for the design were derived and are detailed in the corresponding Technical Product Specifications Z-15.1-345, published in October 2019 [4].

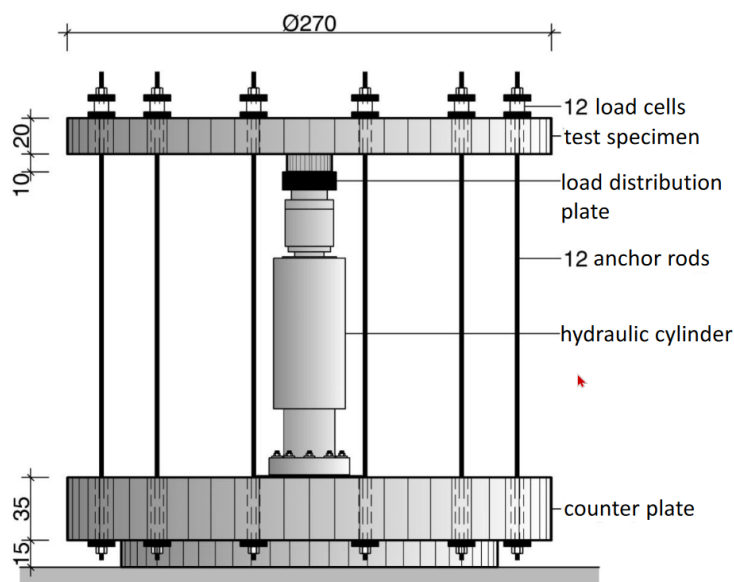


Figure 5. Test setup for the punching shear capacity tests [2]

### 1.3 Limitations on the use of the application

As previously mentioned, the punching shear and shear capacities are calculated using EN 1992-1 "Design of concrete structures – Part 1-1: General rules and rules for buildings" and in EN 1992-2 "Design of concrete structures – Part 2: Concrete bridges – Design and detailing rules". The European design standard and approval provide detailed guidance on the use of RELAST for retrofitting applications. Many local codes outside Europe, unfortunately, do not provide the same level of detail and guidance in the design of post-installed punching shear reinforcement. Still the said European approach may be implemented to a level that satisfies the respective country's performance requirements.

It is important to note as well that the approach detailed in this paper does not take existing punching shear or shear reinforcement into account.

The product also has minimum edge distance and spacing requirements which might not always be applicable to actual site conditions. As a consequence of a minimum embedment depth, there is a minimum concrete thickness of 200mm to observe. In the case of a punching shear retrofitting, the RELAST system is only applicable up to a maximum slab thickness of 1100mm.

The bonded concrete screw anchor can be used in corrosive environment classes C1 (minor) up to C5 (very strong) according to EN ISO 9223 and service temperature between -40°C to 80°C. The Technical Specification covers

concrete strength classes for C20/25 to C50/60 and allows the design under normal load cases with static, quasi-static, and fatigue loads.

## 2 Case study 1 - improving the shear capacity

### 2.1 Design parameters to use for retrofitting a single-span concrete slab bridge

In the rehabilitation of a single span concrete slab bridge (Fig. 6), the shear capacity is to be improved by only accessing the underside of the bridge.

The following design parameters are given for the design:

Span length:	$l = 15.00 \text{ m}$
Bridge width:	$w = 9.00 \text{ m}$
Slab thickness:	$h = 0.50 \text{ m}$
Effective depth of the cross-section:	$d = 0.46 \text{ m}$
Concrete strength class:	C 50/60
Maximum acting design shear load:	$V_{Ed,max,slab} = 712 \text{ kN/m}$

By calculating design shear resistance of the member without shear reinforcement, areas (Fig. 7) requiring design shear reinforcement and consequently retrofitting for shear were identified:

Acting design shear load Area I:	$V_{Ed,max,I} = 500 \text{ kN/m}$
Acting design shear load Area II:	$V_{Ed,max,II} = 300 \text{ kN/m}$



Figure 6. Single-span concrete slab bridge

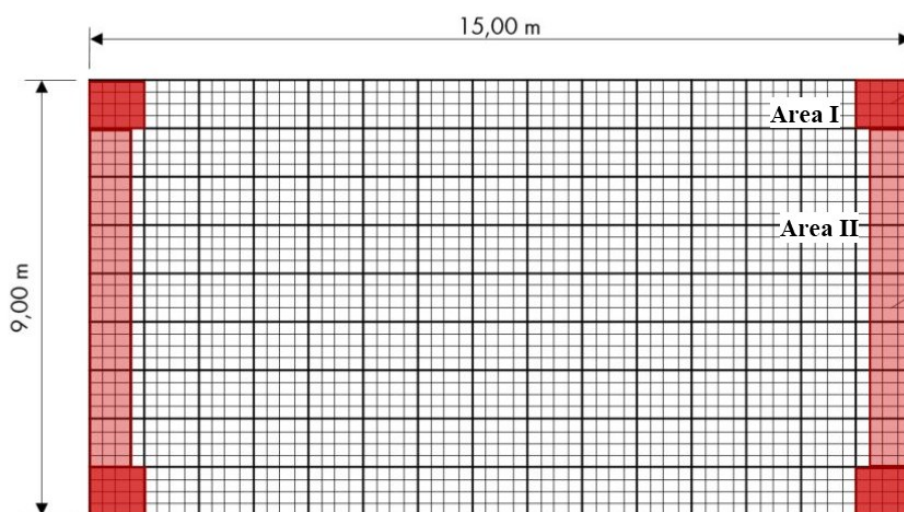


Figure 7. Various areas of the single-span concrete slab bridge

## 2.2 Design and detailing

The design of members with shear reinforcement is based on a truss model (Fig. 8), in which we take  $\alpha = 90^\circ$  and  $\theta = 45^\circ$  and as given, the inner lever arm with  $z = 0.9d = 0.414$  m and the minimum width of the compression chord  $b_w = 1$  m.

In this model, it is required to verify that both, the design resistance of the compression strut and of the tension tie is bigger than the acting design shear load in each area. The retrofitting bonded concrete screw anchor is taking on the task of the cast-in shear reinforcement.

### 2.2.1 Verification of the compression strut

The resistance of the compression strut [5] (6.9), [3]

$$V_{Rd,max} = \frac{1}{2} \cdot b_w \cdot z \cdot v_1 \cdot f_{cd} = \frac{1}{2} \cdot 1 \cdot 0.414 \cdot 0.75 \cdot 28.3 = 4394 \frac{kN}{m} \quad (1)$$

results in an utilisation level of the compression strut of

$$\frac{V_{Ed,max,slab}}{V_{Rd,max}} = 0.162. \quad (2)$$

In accordance with [3] and [5] the maximum permissible spacing from Table 1 must be taken into account

Table 1. Maximum permissible spacings [3]

Shear force ratio	max. longitudinal spacing $s_{l,max}$	max. longitudinal spacing $s_{l,max}$
$V_{Ed} \leq 0.3 \cdot V_{Rd,max}$	$0.7 \cdot h$	$h$
$0.3 \cdot V_{Rd,max} \leq V_{Ed} \leq 0.6 \cdot V_{Rd,max}$	$0.5 \cdot h$	$h$
$V_{Ed} > 0.6 \cdot V_{Rd,max}$	$0.25 \cdot h$	$h$

and are with the given member thickness  $s_{l,max} = 0.35$  m and  $s_{t,max} = 0.5$  m.

### 2.2.2 Verification of the tension tie

The resistance of the tension tie is calculated with [5] (6.8), [3]

$$V_{Rd,s} = a_{sw} \cdot z \cdot f_{ywd,ef} \quad (3)$$

where the effective design yield strength of the bonded concrete screw anchor is

$$f_{ywd,ef} = c_1 \cdot \frac{f_{ywk}}{\gamma_s} + c_2 \cdot \frac{v_1}{\rho_{sw}} \cdot f_{cd} \leq \frac{f_{ywk}}{\gamma_s} \quad (4)$$

The introduction of the effective yield strength takes into account that the concrete screw cannot be utilised to their full yield capacity. The parameters  $c_1$  and  $c_2$  are derived from tests and incorporate diameter and embedment depth of the concrete screws. While  $c_1$  represents the ratio of the concrete screw's resistance of the total shear resistance,  $c_2$  is the portion of the concrete depending resistances.

The ratio of cross section  $a_{sw}$  for improving the shear capacity is calculated with

$$a_{sw} = \frac{A_{sw,sc}}{s_l \cdot s_t} \quad (5)$$

For further verification we chose the RELAST system 22 with a diameter M20. The selected longitudinal spacing  $s_l = 0.30$  m and transverse spacing  $s_t = 0.30$  m are below their respective maximum allowed values.

The material parameter are given in Table 2 [3].

With the cross section of the screw anchor

$$A_{sw,sc} = \left(\frac{d_{k,1}}{2}\right)^2 \cdot \pi = 3.3cm^2 \quad (6)$$

we calculate  $a_{sw} = 36.67cm^2/m^2$  or the relative ratio to  $\rho_{sw} = 0.36\%$ .

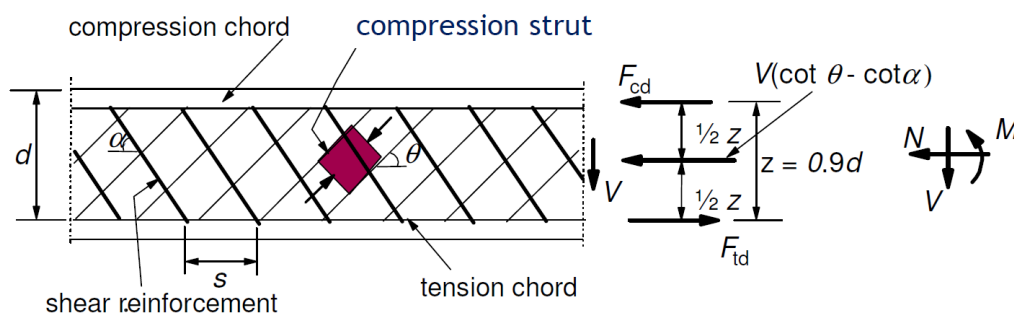


Figure 8. Truss model [5]

Table 2. Dimensions and material of the concrete screw anchor [3]

Bonded screw anchor	Connecting thread	External diameter	Core diameter	Core diameter	Yield strength
		$d_s$	$d_{k,1}$	$d_{k,2}$	$f_{ykw}$
		mm	mm	mm	N/mm <sup>2</sup>
<b>Würth RELAST 22</b>	M20	24.3	20.5	16.93	500

With the second load factor  $c_2 = 0.046$  and the first load factor  $c_1 = 0.2384$  according to table 5 in [3] for the installation condition below the upper reinforcement layer (Fig. 4 left), the effective design yield strength of the bonded concrete screw anchor is calculated to  $f_{ywd,ef} = 369.91 \text{ N/mm}^2 \leq 434.78 \text{ N/mm}^2$ .

The required cross section of the screws to verify successfully the tension tie in area I is

$$a_{sw.req} = \frac{V_{Ed,max,I}}{z \cdot f_{ywd,ef}} = \frac{5000 \text{ cm}^2}{0.414 \cdot 369.91 \text{ m}^2} = 32.65 \frac{\text{cm}^2}{\text{m}^2} \leq 36.67 \frac{\text{cm}^2}{\text{m}^2} \quad (7)$$

and to verify successfully the tension tie in area II

$$a_{sw.req} = \frac{V_{Ed,max,I}}{z \cdot f_{ywd,ef}} = \frac{3000 \text{ cm}^2}{0.414 \cdot 369.91 \text{ m}^2} = 19.59 \frac{\text{cm}^2}{\text{m}^2} \leq 36.67 \frac{\text{cm}^2}{\text{m}^2} \quad (8)$$

The installation plan of Figure 9 shows the screw with the respective selected longitudinal spacing  $s_l = 0.30 \text{ m}$  and transverse spacing  $s_t = 0.30 \text{ m}$  for area I and II, and an edge distance of  $c = 0.15 \text{ m}$  where it applies.

Each bonded concrete screw anchor is installed with an embedment depth of  $h_{nom} = 210 \text{ mm}$  and provides a minimum for the projected thread length of  $t_{ub} \geq 52 \text{ mm}$  to accommodate the big washer, the wedge-lock spring washer and the nut.

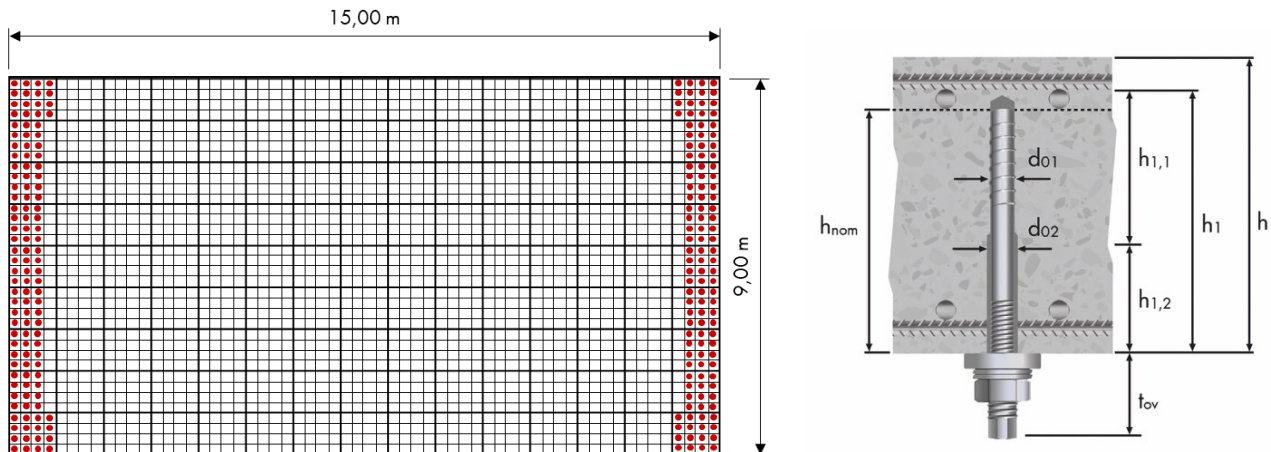


Figure 9. Installation plan and installed bonded concrete screw anchor

### 3 Case study 2 - improving the punching shear capacity

Several documented structural collapses in different parts of the world show that insufficient resistance to punching shear is the main reason for the collapse. Punching shear failure is particularly dangerous because of its, relatively, brittle behaviour. Some examples of documented failures related to punching shear are the Sampoong Department Store (Seoul, South Korea) and The Piper's Row Carpark, (Wolverhampton, GB). A common feature between these structures is the use of flat slabs.

Punching shear capacity is primarily influenced by the concrete strength, flexural reinforcements, geometry and dimension of columns, and the size effect. Punching failure can potentially result from design/planning errors, construction mistakes, changes in the type of occupancy of the building, and changes in the building codes. The punching capacity of new concrete structures can readily be addressed by following the provisions of new codes and standards. Extra punching shear reinforcements can be built-in to the design, and pre-installed before concrete is poured. For existing concrete structures however, a post-installed approach is more desirable. There are a number of different punching shear retrofitting approaches, but this paper focuses on a proprietary post-installed retrofitting system that is designed to significantly improve punching shear capacity, in a relatively quicker time, while the structure remains operational.

#### 3.1 Design parameters to use for retrofitting a flat concrete slab

In the rehabilitation of an office building, the punching shear capacity of the flat concrete slab is to be verified and improved when necessary. A representative area of the slab is shown in Figure 10.

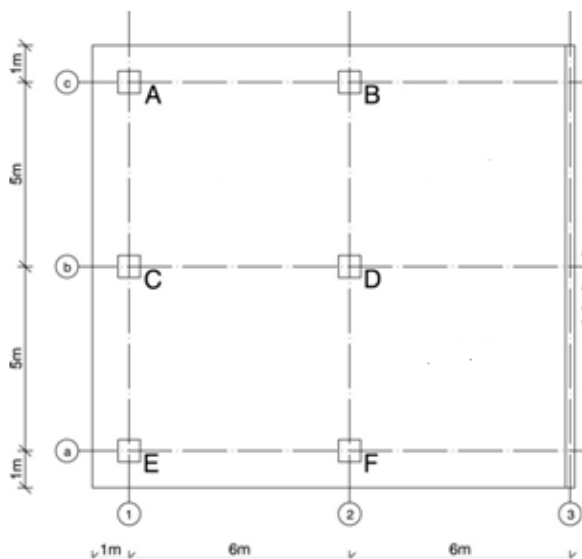


Figure 10. Representative area of the flat concrete slab

The following design parameters were given for the design:

Concrete strength class:	C 25/30
Span length	$l_x = 6.00$ m
Span length	$l_y = 5.00$ m
Cantilever length	$l_{pr} = 1.00$ m
Slab thickness:	$h = 0.25$ m
Concrete cover:	$c_{nom} = 20$ mm
Effective depth of the cross-section:	$d = 0.22$ m
Cross section of all columns:	$a \times a = 0.30$ m x 0.30 m
Acting design punching shear load – column A:	$V_{Ed,A} = 159.09$ kN
Acting design punching shear load – column B:	$V_{Ed,B} = 339.96$ kN
Acting design punching shear load – column C:	$V_{Ed,C} = 308.01$ kN
Acting design punching shear load – column D:	$V_{Ed,D} = 608.19$ kN

In order to establish the punching shear resistance above the column, a minimum flexural reinforcement is provided.

### 3.2 Design and detailing

The design procedure for punching shear is based on checks at the face of the column  $u_0$  and at the basic control perimeter  $u_1$ . If shear reinforcement is required a further perimeter  $u_{out,ef}$  should be calculated where shear reinforcement is no longer required.

#### 3.2.1 Verification at the face of the column

At the column perimeter  $u_0$ , or the perimeter of the loaded area, the maximum punching shear resistance should not exceed [5]

$$V_{Ed} \leq \frac{V_{Rd,max}}{\beta} = \frac{0.4 \cdot v \cdot f_{cd} \cdot u_0 \cdot d}{\beta} \quad (9)$$

where  $v = 0.54$  represents a strength reduction factor for concrete cracked in shear,  $f_{cd} = 16.67$  N/mm<sup>2</sup> the design concrete strength and  $u_0 = 4a = 1.2$  m the perimeter of the column. For structures where the lateral stability does not depend on frame action between the slabs and the columns,

and where the adjacent spans do not differ in length by more than 25%, approximate values for  $\beta$  may be used [4]:

Inner column D:	$\beta = 1.10$
Edge columns B and C:	$\beta = 1.40$
Edge Column A:	$\beta = 1.50$

With above assumptions, we have the following verifications:

Column A:	$159$ kN $\leq$ $633$ kN
Column B:	$340$ kN $\leq$ $678$ kN
Column C:	$308$ kN $\leq$ $678$ kN
Column D:	$608$ kN $\leq$ $863$ kN

#### 3.2.2 Verification at the basic control perimeter

The basic control perimeter  $u_1$  may be taken to be at a distance  $2.0d$  from the loaded area and should be constructed so as to minimise its length. The length for each column is shown in Figure 11. Note that the following calculations are only conducted for column D. Only column D requires additional improvement for punching shear capacity.

Punching shear reinforcement is not necessary, if

$$v_{Ed} \leq v_{Rd,c} \quad (10)$$

The maximum shear stress should be calculated with

$$v_{Ed} \leq \beta \frac{V_{Ed}}{u_{1,D} \cdot d} \quad (11)$$

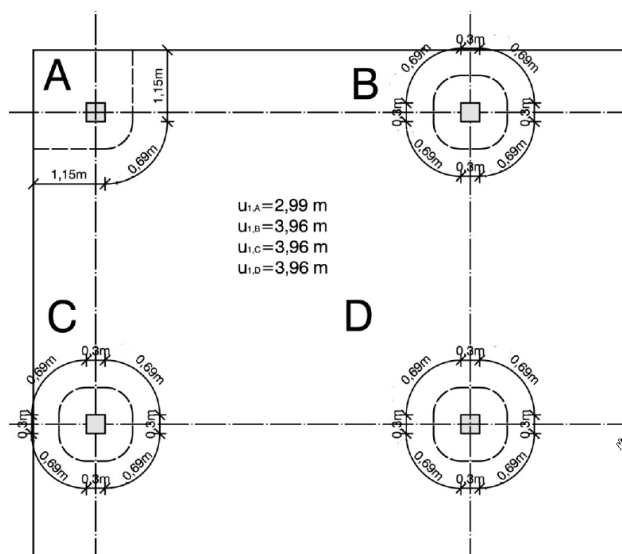


Figure 11 Length of the basic control perimeter

and the punching shear resistance of the slab without shear reinforcement in accordance with

$$v_{Rd,c} = C_{Rd,c} \cdot k \cdot (100 \cdot \rho_l \cdot f_{ck})^{\frac{1}{3}} + k_1 \cdot \sigma_{cp} \geq v_{min} + k_1 \cdot \sigma_{cp} \quad (12)$$

where  $C_{Rd,c} = 0.12$  for flat slabs in general, the scale factor  $k = 1.95$ , the mean reinforcement ratio  $\rho_l$  in x and y direction equals 0.0052 for column D and the coefficient for inclusion of normal stresses  $k_1 = 0.1$ . The design value of the mean normal concrete stresses  $\sigma_{cp}$  inside the basic control perimeter are zero. The Technical Product Specifications

Z-15.1-345 [4] calculates for the minimum value of the shear resistance

$$v_{min} = 0.035 \cdot (k)^{\frac{3}{2}} \cdot \sqrt{f_{ck}} \quad (13)$$

as  $d$  is smaller than 600mm. Other values apply for different effective depths.

For column D the verification  $v_{Ed} \leq v_{Rd,c}$  is not successful as shown in Eq. (14) and Eq. (15).

$$v_{Ed} = 1.1 \frac{608}{3.96 \cdot 0.22} = 0.767 N/mm^2 \quad (14)$$

$$v_{Rd,c} = 0.12 \cdot 1.95 \cdot (100 \cdot 0.0052 \cdot 25)^{\frac{1}{3}} = 0.550 N/mm^2 \quad (15)$$

Punching shear reinforcement needs to be provided.

The required number of bonded concrete screw anchors in a defined area around the column is resulting from the following two conditions

$$v_{ed} = \beta \frac{V_{ed}}{u_{1,D} \cdot d} \leq \begin{cases} v_{Rd,cs} \\ k_{max} \cdot v_{Rd,c} \end{cases} \quad (16)$$

The concrete screw anchors acting as punching shear reinforcement elements improve the punching shear capacity by up to 40%. With  $k_{max} = 1.4$ , the second condition is met, and the RELAST system can be used. RELAST system 16 with a diameter M18 is chosen and the following product parameter and limitations apply (Fig. 12):

1. first row of the bonded screw anchors shall be located between  $0.3d = 6.6\text{cm}$  and  $0.5d = 11\text{cm}$ ,
2. the spacing between the outer row of the bonded screw anchors and the control perimeter  $u_{out,ef}$  shall not exceed  $1.5d = 33\text{cm}$ ,
3. the radial spacing of the screw rows shall not be larger than  $0.75d = 16.5\text{cm}$ ,
4. the spacing of the screw in the peripheral direction shall not be larger than  $1.5d = 33\text{cm}$  in an area inside the basic control perimeter  $u_1$ , outside not larger than  $2d = 44\text{cm}$ ,
5. the minimum spacing is  $100\text{mm}$ ,
6. the core diameter  $d_{k,1} = 14.8\text{mm}$
7. the yield strength of the concrete screw anchor  $f_{ywd} = 434\text{N/mm}^2$ .

The punching shear resistance with punching shear reinforcement  $v_{Rd,cs}$  is calculated with

$$v_{Rd,cs} = 0.75 \cdot v_{Rd,c} + 1.5 \cdot \frac{d}{s_r} \cdot A_{SW} \cdot f_{ywd,ef} \cdot \frac{1}{u_1 d} \quad (17)$$

where the allowable cross-section area of the punching shear reinforcement in one row around the column is the minimum of

$$A_{SW} = \min \left\{ \begin{array}{l} A_{SW,i} \\ \frac{A_{SW,1.5d}}{1.5 \cdot d} \cdot s_r \end{array} \right. \quad (18)$$

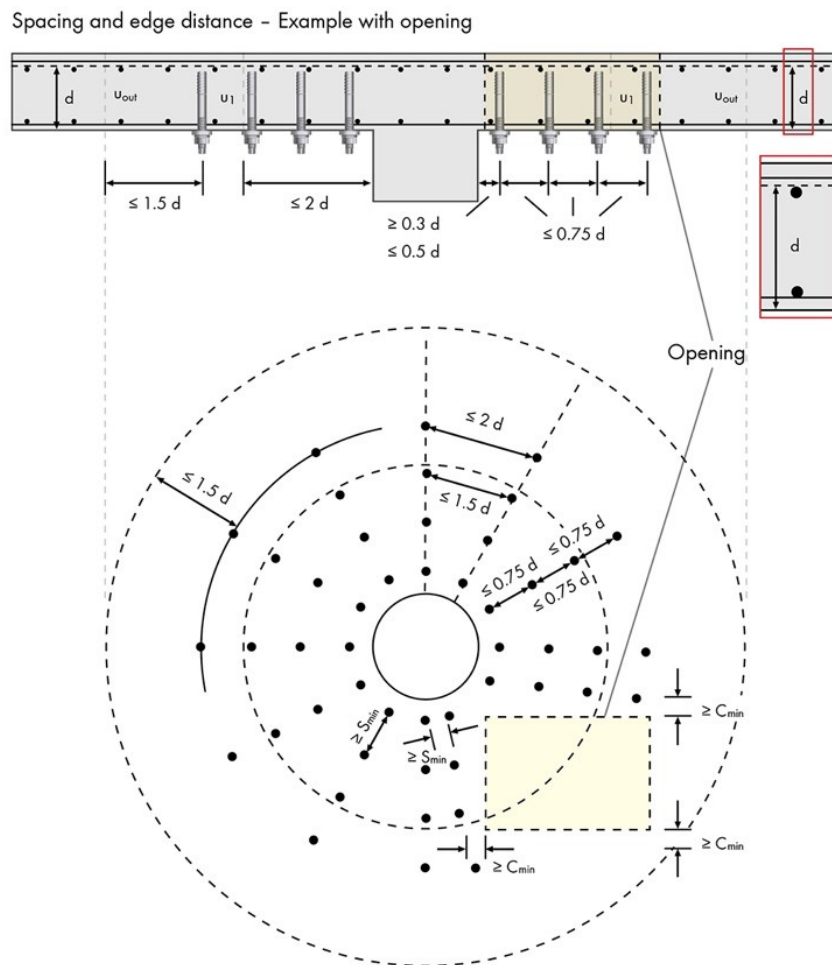


Figure 12. Geometrical limitations

For the verification we chose 5 rows with a radial spacing of  $s_r = 15$  cm and 12 anchors per row. The spacing of the first row to the column equals 10 cm. The cross section area in any row around the column is  $A_{sw,i} = 20.64$  cm<sup>2</sup>. The entire cross sectional area between  $0.3d = 6.6$  cm and  $1.5d = 33$  cm calculates from the cross section of 3 rows  $A_{sw,1.5d} = 61.92$  cm<sup>2</sup> and  $A_{sw} = 20.64$  cm<sup>2</sup>.

The design value of the active stress in the punching shear reinforcement is calculated with

$$f_{ywd,ef} = 5.5 \cdot \frac{k_{max}}{\gamma_s} \cdot \frac{d}{d_{k,1}} = 5.5 \cdot \frac{1.4}{1.15} \cdot \frac{22}{1.48} = 99.53 \text{ N/mm}^2 \leq 217 \text{ N/mm}^2 \quad (19)$$

The punching shear resistance with punching shear reinforcement equals  $v_{Rd,cs} = 0.93$  N/mm<sup>2</sup> and successfully verified as it is greater than the acting shear of  $v_{Ed} = 0.77$  N/mm<sup>2</sup>.

The perimeter  $u_{out,ef}$ , where shear reinforcement is no longer required is calculated with

$$u_{out,ef} = \beta \frac{V_{ed}}{v_{Rd,c} \cdot d} = \frac{1.1 \cdot 608}{550 \cdot 0.22} = 5.52 \text{ m} \quad (20)$$

which equals an outer radius  $r_{out,ef} = 88$  cm.

For the above calculated 60 bonded concrete screw anchors of the RELAST system 16 with a metric thread M18, the rules for the geometrical composition are successfully checked.

1. the first row of the bonded screw anchors is located at 10cm from the column which is between the required  $0.3d = 6.6$  cm and  $0.5d = 11$  cm. The respective radius  $r_a$  equals 25cm,
2. the perimeter of the first row equals 157 cm which makes with 12 screw anchors a spacing of 130.9 mm which is greater than the required minimum spacing of 100 mm.
3. the radial spacing of 15 cm is less than the required  $0.75d = 16.5$  cm,
4. the length of the basic control perimeter equals 339cm and is filled with 12 anchors at spacings of 28.25 cm in the peripheral direction which is less than  $1.5d = 33$  cm, the last row of the 5 radial rows has a radius  $r_{out} = 85$  cm and gives a spacing of 3 cm to  $r_{out,ef} = 88$ cm, which does not exceed required maximum spacing of  $1.5d = 33$  cm
5. the perimeter length of the last row equals 534 cm and is filled with 12 anchors at spacings of 44.0 cm in the peripheral direction which is lesser than  $2d = 44$  cm.

Each bonded concrete screw anchor is installed with a embedment depth of  $h_{nom} = 160$  mm and provides a minimum for the projected thread length of  $t_{ub} \geq 47$  mm to accommodate the big washer, the wedge-lock spring washer and the nut.

## 4 Summary

The two design examples show that the RELAST system improves the shear or punching shear capacity with a practicable number of bonded concrete screw anchors. The number of screws is not much different from the number of cast-in shear or punching shear reinforcement which would have been provided for a new structure. Thus, the provided solution is economically feasible and provides additional benefits from having to access only the soffit of the structure for installing the system. In many cases, occupancy could continue in the area above where RELAST installation is being done.

The design approach utilizes existing formulas of an established European Code, and provides modification parameters as necessary. As the design does not take existing shear and punching shear reinforcement into account, the described approach can be used when codes do not provide the same level of detail and guidance in the design.

## References

- [1] Feix, Jürgen and Lechner, Johannes, "RELAST. Betonschrauben zur nachträglichen Bauwerksverstärkung", Würth Internal Presentation citing from various papers, 2019.
- [2] Feix, Jürgen and Lechner, Johannes, "Das neue Bauaufsichtlich zugelassene System RELAST zur nachträglichen Bauwerksverstärkung; Von der Grundidee über wissenschaftliche Forschung zur Zulassung. [engl. The new technically approved RELAST system for post-installed structural reinforcement; from the basic idea to scientific research for approval]", *qlz8 - Das Planermagazin für Ingenieure, Architekten und Planer*. No. 19, Issue 14, March 2020.
- [3] Deutsches Institut für Bautechnik (DIBt), "Würth RELAST bonded screw anchor with a diameter of 16mm and 22mm for use as post-installed shear reinforcement.", National technical approval Z-15.1-344, October 2019.
- [4] Deutsches Institut für Bautechnik (DIBt), "Würth RELAST bonded screw anchor with a diameter of 16mm and 22mm for use as post-installed punching shear reinforcement.", National technical approval Z-15.1-345, October 2019.
- [5] Deutsches Institut für Normung e. V. (DIN), "Eurocode 2: Design of concrete structures – Part 1-1: General rules and rules for buildings; German version EN 1992-1-1:2004 + AC:2010", German National Code, January 2011.

## INSTRUCTIONS FOR AUTHORS

### Acceptance and types of contributions

The Building Materials and Structures journal will publish unpublished papers, articles and conference reports with modifications in the field of Civil Engineering and similar areas (Geodesy and Architecture). The following types of contributions will be published: original scientific papers, preliminary reports, review papers, professional papers, objects describe / presentations and experiences (case studies), as well as discussions on published papers.

Original scientific paper is the primary source of scientific information and new ideas and insights as a result of original research using appropriate scientific methods. The achieved results are presented briefly, but in a way to enable proficient readers to assess the results of experimental or theoretical numerical analyses, so that the research can be repeated and yield with the same or results within the limits of tolerable deviations, as stated in the paper.

Preliminary report contains the first short notifications on the results of research but without detailed explanation, i.e. it is shorter than the original scientific paper.

Review paper is a scientific work that presents the state of science in a particular area as a result of analysis, review and comments, and conclusions of published papers, on which the necessary data are presented clearly and critically, including the own papers. Any reference units used in the analysis of the topic are indicated, as well as papers that may contribute to the results of further research. If the reference data are methodically systematized, but not analyzed and discussed, such review papers are classified as technical papers.

Technical paper is a useful contribution which outlines the known insights that contribute to the dissemination of knowledge and adaptation of the results of original research to the needs of theory and practice.

Other contributions are presentations of objects, i.e. their structures and experiences (examples) in the construction and application of various materials (case studies).

In order to speed up the acceptance of papers for publication, authors need to take into account the Instructions for the preparation of papers which can be found in the text below.

### Instructions for writing manuscripts

The manuscript should be typed one-sided on A-4 sheets with margins of 31 mm (top and bottom) and 20 mm (left and right) in Word, font Arial 12 pt. The entire paper should be submitted also in electronic format to e-mail address provided here, or on CD. The author is obliged to keep one copy of the manuscript.

As of issue 1/2010, in line with the decision of the Management Board of the Society and the Board of Editors, papers with positive reviews, accepted for publication, will be published in Serbian and English, and in English for foreign authors (except for authors coming from the Serbian and Croatian speaking area).

Each page should be numbered, and the optimal length of the paper in one language is about 16 pages (30.000 characters) including pictures, images, tables and references. Larger scale works require the approval of the Board of Editors.

The title should describe the content of the paper using a few words (preferably eight, and up to eleven). Ab-

brevisions and formulas should be omitted in the title. The name and surname of the author should be provided after the title of the paper, while authors' title and position, as well as affiliation in the footnote. The author should provide his/her phone number, e-mail address and mailing address.

The abstract (summary) of about 150-250 words in Serbian and English should be followed by key words (up to seven). This is a concise presentation of the entire article and provides the readers with insight into the essential elements of the paper.

The manuscript is divided into chapters and sub-chapters, which are hierarchically numbered with Arabic numerals. The paper consists of introduction and content with results, analysis and conclusions. The paper ends with the list of references. All dimensional units must be presented in international SI measurement units. The formulas and equations should be written carefully taking into account the indexes and exponents. Symbols in formulas should be defined in the order they appear, or alternatively, symbols may be explained in a specific list in the appendix. Illustrations (tables, charts, diagrams and photos) should be in black and white, in a format that enables them to remain clear and legible when downscaled for printing: one to two columns (8 cm or 16.5 cm) in height, and maximum of 24.5 cm high, i.e. the size of the letters and numbers should be at least 1.5 mm. Original drawings should be of high quality and fully prepared for copying. They also can be high-quality, sharp and contrasting photo-copies. Photos should be in black and white, on quality paper with sharp contours, which enable clear reproduction.

The list of references provided at the end of the paper should contain only papers mentioned in the text. The cited papers should be presented in alphabetical order of the authors' first name. References in the text should be numbered with Arabic numerals in square brackets, as provided in the list of references, e.g. [1]. Each citation in the text must be contained in the list of references and vice versa, each entry from the list of references must be cited in the text.

Entries in the list of references contain the author's last name and initials of his first name, followed by the full title of the cited article, the name of the journal, year of publication and the initial and final pages cited (from - to). If the doi code exists it is necessary to enter it in the references. For books, the title should be followed by the name of the editor (if any), the number of issue, the first and last pages of the book's chapter or part, the name of the publisher and the place of publication, if there are several cities, only the first in the order should be provided. When the cited information is not taken from the original work, but found in some other source, the citation should be added, "cited after ..."

Authors are responsible for the content presented and must themselves provide any necessary consent for specific information and illustrations used in the work to be published.

If the manuscript is accepted for publication, the authors shall implement all the corrections and improvements to the text and illustrations as instructed by the Editor.

Writings and illustrations contained in published papers will not be returned. All explanations and instructions can be obtained from the Board of Editors.

Contributions can be submitted to the following e-mails: [sneska@imk.grf.bg.ac.rs](mailto:sneska@imk.grf.bg.ac.rs) or [miram@uns.ac.rs](mailto:miram@uns.ac.rs)  
Website of the Society and the journal: [www.dimk.rs](http://www.dimk.rs)

Financial support



**MINISTRY OF EDUCATION, SCIENCE AND  
TECHNOLOGICAL DEVELOPMENT OF  
REPUBLIC OF SERBIA**



**UNIVERSITY OF BELGRADE FACULTY OF  
CIVIL ENGINEERING**



**INSTITUTE FOR TESTING OF MATERIALS-  
IMS INSTITUTE, BELGRADE**

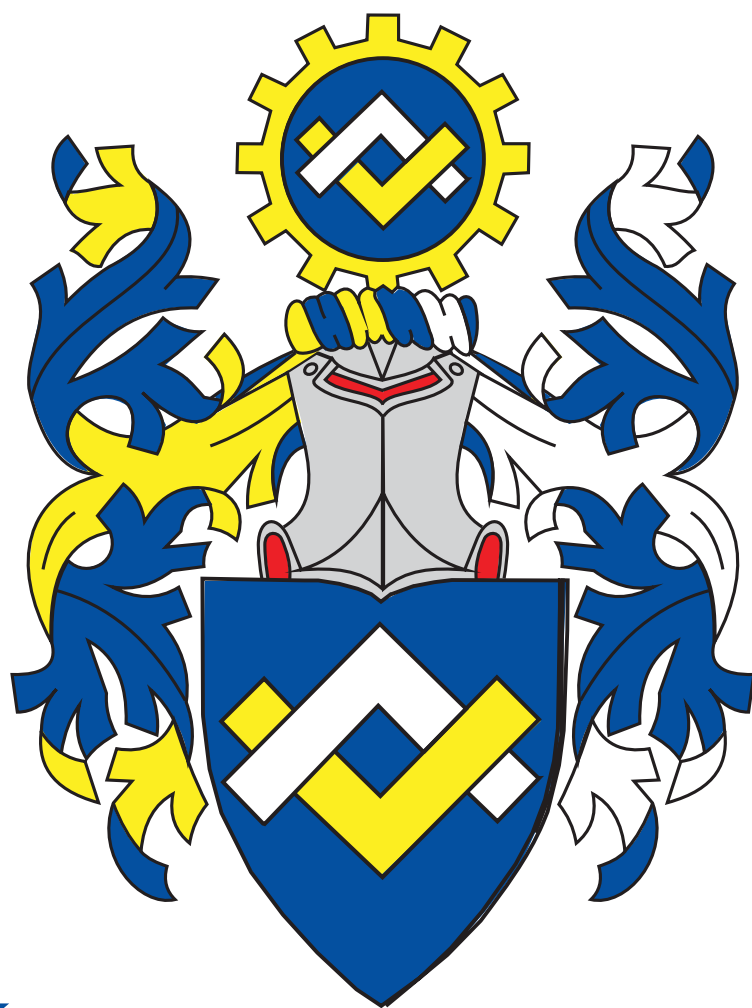


**FACULTY OF TECHNICAL SCIENCES,  
UNIVERSITY OF NOVI SAD, DEPARTMENT  
OF CIVIL ENGINEERING**



**ИНЖЕЊЕРСКА  
КОМОРА  
СРБИЈЕ**

**SERBIAN CHAMBER OF ENGINEERS**



**INŽENJERSKA  
KOMORA  
SRBIJE**

## Visokokvalitetni sistemi građevinske hemije



## Napredna sistemska rešenja za trajne betonske konstrukcije



PREDSTAVLJAMO NAPREDNU TEHNOLOGIJU

# PENETRON ADMIX® TRACER

Nevidljiva Tehnologija Kristalizacije Postaje Vidljiva



**PENETRON ADMIX®**, kristališući aditiv treće generacije, sada se isporučuje sa dodatkom zelenog pigmenta. Zelena boja signalizira da je u beton zamešan originalni **PENETRON ADMIX®**.

Posetite nas:  
[www.penetron.gr](http://www.penetron.gr)  
[www.nivo381.rs](http://www.nivo381.rs)

Kontaktirajte nas:  
[m.jovanovic@penetron.gr](mailto:m.jovanovic@penetron.gr)  
[r.tesla@nivo381.rs](mailto:r.tesla@nivo381.rs)

Pratite nas na:  
 **PenetronHellas**





**doka**

Oplatna tehnika.

## Pravi partner za sve vaše građevinske poduhvate.

**Doka** je jedan od svetskih lidera na polju razvoja, proizvodnje i distribucije oplatnih sistema za sve oblasti građevinarstva. Uz bogatu ponudu **Doka** inovativnih i visokokvalitetnih proizvoda i usluga, efikasnu globalnu distributivnu mrežu, gradite brže, bezbednije i ekonomičnije. **Doka** uvek ima pravo rešenje za svaki vaš projekat - onda kada treba podneti velika opterećenja, postići velike visine, savladati velike raspone, ali i kada se traži fleksibilnost, lakoća rukovanja i brzina.

**Doka Serb d.o.o.** | Svetogorska 4, 22310 Šimanovci, Srbija  
T +381 (0)22 400 100 | serb@doka.com | [www.doka.com/rs](http://www.doka.com/rs)



Panelna oplata za ploču Dokadek 30



Ramovska oplata DokaXlight



Ramovska oplata Framini

**ADING**  
sastojak svake građevine



Objekat: Tuneli "Lipak" / "Železnik" (Obilaznica oko Beograda, R.Srbija); Korišćeni materijali: ADINGPOKS AKVA / ADINGPOKS AKVA 1B

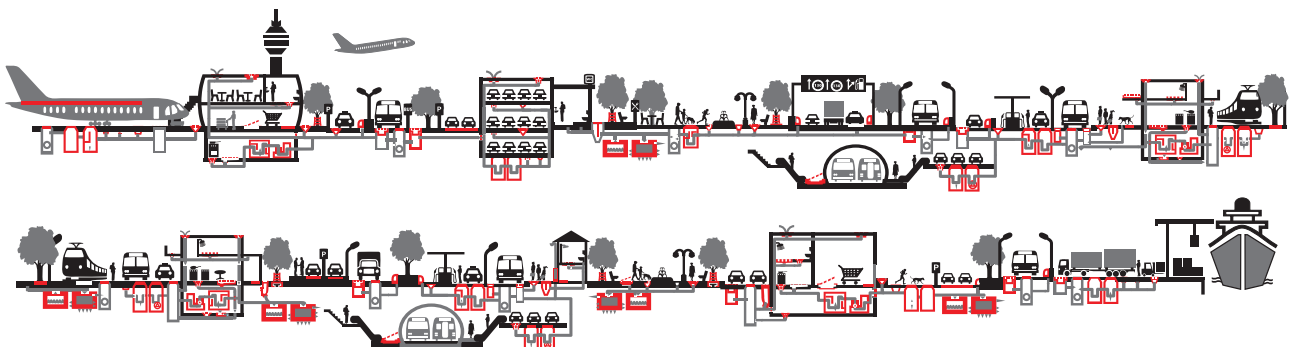


## ZAŠTITNI PREMAZI

[www.ading.rs](http://www.ading.rs)

Adresa: Nehruova 82, 11070 Novi Beograd, Tel/Fax: + 381 11 616 05 76 ; email: [ading@ading.rs](mailto:ading@ading.rs)

# ACO. The future of drainage.



aco.rs

**CENTAR ZA PUTEVE I GEOTEHNIKU**

U okviru centra posluju odeljenja za geotehniku, nadzor i terenska ispitivanja, projektovanje saobraćajnica, laboratorija za puteve i geotehniku. Značajna aktivnost centra usmerena je ka terenskim i laboratorijskim geološko - geotehničkim istraživanjima i ispitivanjima terena za potrebe izrade projektno - tehničke dokumentacije, za različite faze i nivoe projektovanja objekata visokogradnje, niskogradnje, saobraćaja i hidrogradnje, kao i za potrebe prostornog planiranja i zaštite životne sredine. Stručni nadzor, kontrola kvaliteta tokom građenja, rekonstrukcije i sanacije objekata različite namene, izrada studija, ekspertiza, konsultantske usluge, kompletan konsalting u oblasti geotehničkog inženjeringa, neke su od delatnosti centra.



**Ispitivanje šipova**

- **SLT metoda (Static load test)**
- **DLT metoda (Dynamic load test)**
- **PDA metoda (Pile driving analysis)**
- **PIT (SIT) metoda (Pile (Sonic) integrity testing)**
- **CSL - Crosshole Sonic Logging**



- **Ispitivanje šipova**
  - **Geotehnička istraživanja i ispitivanja - in situ**
    - **Laboratorija za puteve i geotehniku**
      - **Projektovanje puteva i sanacija klizišta**
        - **Nadzor**

# Najlepši krov u komšiluku



Continental Plus Natura je premium crep u natur segmentu! Dobro poznatog oblika, trajan i veoma otporan, a povrh svega pristupačan, naprosto oduzima dah svima. Čak i vašim komšijama!

Continental Plus Natura crep potražite kod ovlašćenih Tondach partnera.

## PUT INŽENJERING



Put inženjering d.o.o punih 25 godina radi kao specijalizovano preduzeće za izgradnju infrastrukture u niskogradnji i visokogradnji, kao i proizvodnjom kamenog agregata i betona. Preduzeće se bavi i transportom, uslugama građevinske mehanizacije i specijalne opreme.

Koristeći inovativne tehnike i kvalitetan građevinski materijal iz sopstvenih resursa, spremni smo da odgovorimo na mnoge zahteve naših klijenata iz oblasti niskogradnje.



Osnovna prednost prefabrikovane konstrukcije jeste brzina kojom konstrukcija može biti projektovana, proizvedena, transportovana i namontirana.



Izvodimo hidrograđevinske radove u izgradnji kanalizacionih mreža za odvođenje atmosferskih, otpadnih i upotrebljenih voda, izvođenjem hidrograđevinskih radova u okviru regulacije rečnih tokova, kao i izvođenjem hidrotehničkih objekata.



Površinski kop udaljen je 35 km od Niša. Savremene drobilice, postrojenje za separaciju i sejalice efikasno usitnjavaju i razdvajaju kamene agregate po veličinama. Tehnički kapacitet trenutne primarne drobilice je 300 t/h.



Za spravljanje betona koristimo drobljeni krečnjački agregat sa našeg kamenoloma, deklariranih frakcija, kontrolisane vlažnosti. Kompletan proces proizvodnje i kontrole kvaliteta vršimo prema važećim standardima.



Obradu armature vršimo brzo, stručno i kvalitetno, sa kompjuterskom preciznošću i dimenzijama po projektu.



Naša kompanija u oblasti visokogradnje primenjuje sistem prefabrikovanih betonskih elemenata koji u odnosu na klasičnu gradnju ima brojne prednosti.



Prednapregnute šuplje ploče su konstruktivni elementi visokog kvaliteta, proizvedeni u fabrički kontrolisanim uslovima.



Izrađujemo betonske "New Jersey profile" koji se u svetu koriste za preusmeravanje saobraćaja i zaštitu pešaka u toku izgradnje puta, kao i Betonblock sistem betonskih blokova.



Uslugu transporta vršimo automikserima, kapaciteta bubnja od 7 m<sup>3</sup> do 10 m<sup>3</sup> betonske mase. Za ugradnju betona posedujemo auto-pumpu za beton, radnog učinka 150 m<sup>3</sup>/h, sa dužinom strele od 36 m.



Kao generalni izvođač radova, vršimo koordinaciju svih učesnika na projektu, planiranje, praćenje i nabavku materijala, kontrolu kvaliteta izvedenih radova, poštujući zadate vremenske rokove i finansijski okvir investitora.



Osnovi princip našeg poslovanja zasniva se na individualnom pristupu svakom klijentu i pronalaženje najoptimalnijeg rešenja za njegove transportne i logističke potrebe.



Usluge građevinske mehanizacije vršimo tehnički ispravnim mašinama, sa potrebnim sertifikatima kako za rukovoce građevinskim mašinama tako i za same mašine.



Raspoložemo opremom i mašinama za sve zemljane radove, kipere i dampere za rad u teškim terenskim uslovima, automiksere i pumpe za beton, autodizalice, podizne platforme.



Sakupljanje i privremeno skladištenje otpada vršimo našim specijalizovanim vozilima i deponujemo na našu lokaciju sa odgovarajućom dozvolom. Kapacitet mašine je 250 t/h građevinskog neopasnog otpada.



### NIŠ

Krnjaževačka bb, 18000 Niš - Srbija  
+381 18 215 355  
office@putinzenjering.com

### BEOGRAD

Jugoslovenska 2a, 11250 Beograd - Železnik  
+381 11 25 81 111  
beograd@putinzenjering.com





## MATEST "IT TECH" KONTROLNA JEDINICA



### JEDNA TEHNOLOGIJA MNOGO REŠENJA

IT Touch Technology je Matestov najnoviji koncept koji ima za cilj da ponudi inovativna i user-friendly tehnologiju za kontrolu i upravljanje najmodernijom opremom u domenu testiranja građevinskih materijala

Ova tehnologija je srž Matestove kontrolne jedinice, software baziran na Windows platformi i touch screen sistem koji je modularan, fleksibilan i obavlja mnoge opcije

- IT TECH pokriva | INOVATIVNOST
- | INTERNET KONEKCIJA
- | INTERFEJS SA IKONICAMA
- | INDUSTRIJALNA TEHNOLOGIJA

### SISTEM JEDNOG RAZMIŠLJANJA

### JEDNOM SHVATIŠ - SVE TESTIRAŠ



#### NAPREDNA TEHNOLOGIJA ISPITIVANJA ASFALTA

- | GYROTRONIC - Gyrotory Compactor
- | ARC - Electromechanical Asphalt Roller Compactor
- | ASC - Asphalt Shear Box Compactor
- | SMARTTRACKER™ - Multiwheels Hamburg Wheel Tracker, DRY + WET test environment
- | SOFTMATIC - Automatic Digital Ring & Ball Apparatus
- | Ductilometers with data acquisition system

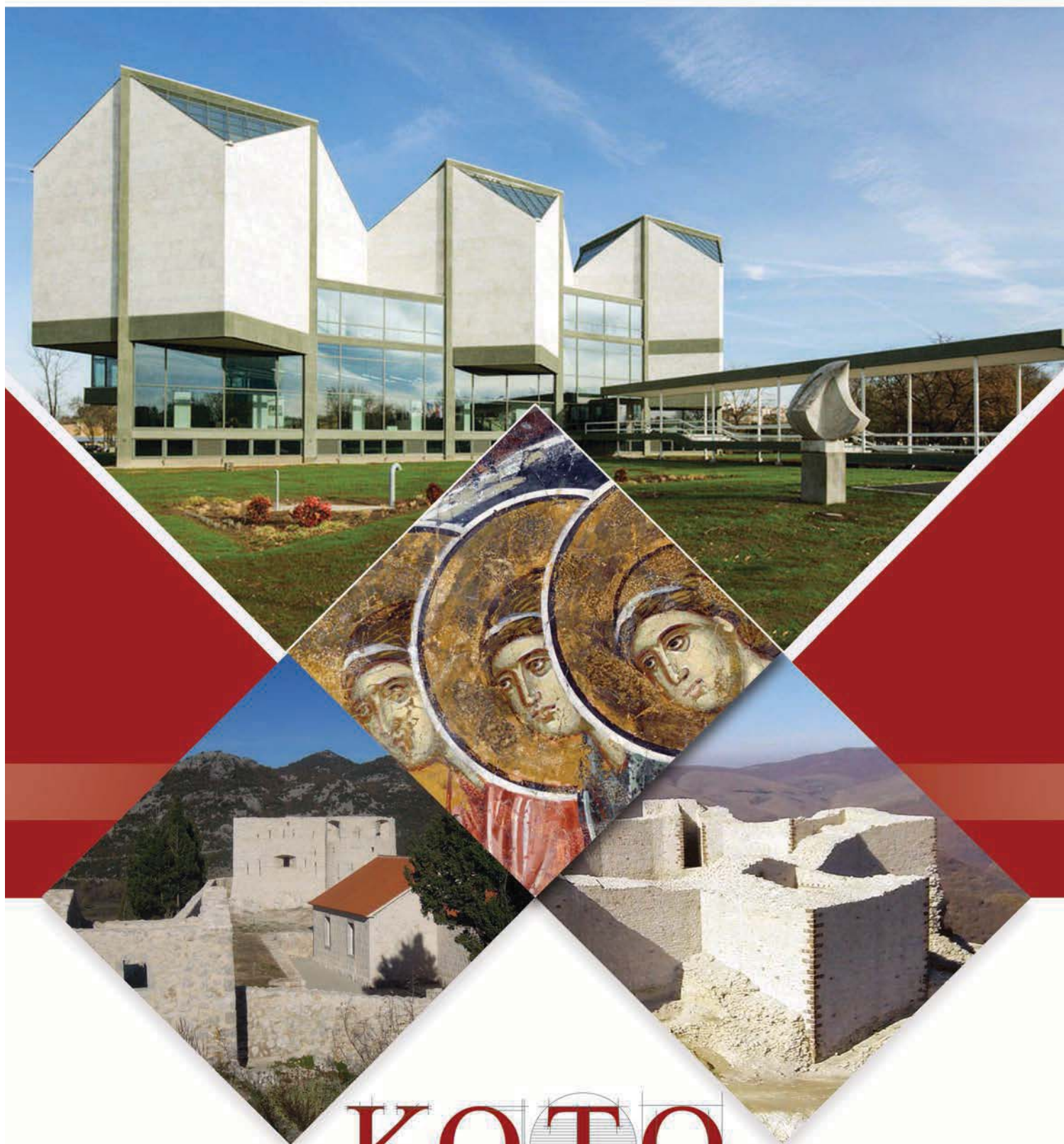
#### MULTIFUNKCIONALNI RAMOVI ZA TESTIRANJE

- | CBR/Marshall digital machines
- | Universal multispeed load frames
- | UNITRONIC 50kN or 200kN Universal multipurpose compression/flexural and tensile frames

#### OPREMA ZA GEOMEHANIČKO ISPITIVANJE

- | EDOTRONIC - Automatic Consolidation Apparatus
- | SHEARLAB - AUTOSHEARLAB - SHEARTRONIC
- Direct / Residual shear testing systems
- | Triaxial Load Frame 50kN

**MIXMATIC** - Automatic Programmable Mortar Mixer



# KOTO

[www.koto.rs](http://www.koto.rs) | [office@koto.rs](mailto:office@koto.rs) | 011 309 7410 | Vojvode Stepe br. 466, Beograd